Final Report:

Estimating Nutrient Loads to Falls Lake from Streambank Erosion

Project Funding Provided by:
N.C. Collaboratory

Project Period: October 2022 – October 2023

Principal Investigator:
Barbara A. Doll, PhD, PE, Extension Associate Professor, NC State University, NC Sea Grant & Biological and Agricultural Engineering Department, Box 7625, NC State University, Raleigh, NC 27695-7625, bdoll@ncsu.edu, 919-515-5287.

Co- Investigator:
Daniel Line, Extension Specialist, Biological & Agricultural Engineering Department, Box 7625, NC State University, Raleigh, NC 27695-7625, dline@ncsu.edu

Jack Kurki-Fox, PhD, PE, Research Scholar, Biological & Agricultural Engineering Department, Box 7625, NC State University, Raleigh, NC 27695-7625, jjkurkif@ncsu.edu

Student Researcher:
Layla El-Khoury, PhD Student, Biological & Agricultural Engineering Department, Box 7625, NC State University, Raleigh, NC 27695-7625, lcelkhou@ncsu.edu

Table of Contents

Executive Summary

In 2016, the NC Policy Collaboratory was funded by the NC General Assembly to analyze water quality and investigate nutrient management strategies for Falls Lake. In 2022, NC State University (NCSU), Biological & Agricultural Engineering (BAE) Department was invited to evaluate the potential nutrient inputs that could be arriving to the Lake from streambank erosion to complement the work and findings of the existing funded projects.

Streambanks were assessed at 111 locations throughout the watershed including a range of streambank conditions from stable to severely eroding. Erosion rates were monitored for 7 to 9 months at 28 locations exhibiting active erosion using repeat cross-section surveys. Soil samples were collected from the streambanks at all cross-sections and analyzed for nutrient content and bulk density. For a period of one year, NCSU also measured flow, turbidity, total suspended solids (TSS) and total phosphorus (TP) at five subwatersheds to generate TSS and TP loads. Strong relationships between turbidity and TSS and TP were observed. The loadings were also used to estimate the total proportion of streambank erosion loads to total TSS and TP loads, which also include land-based sources of sediment for the five subwatersheds. Long-term water quality data measured by USGS at three of the flow gauging stations was used to develop total loads for TSS and nutrients for comparison.

Field-based assessments of streambank condition and erosion rates were combined with detailed geospatial mapping and modeling of land use and landforms to develop three models to 1) estimate potential locations where erosion was occurring, 2) the height of the streambank and 3) the rate of streambank erosion at 100 feet increments for all the streams in the Falls Lake watershed. Results of all models were combined with measured soil densities to generate a range of predicted sediment loading for each catchment in the watershed. Delivery ratios obtained from the Upper Neuse River Basin Association (UNRBA) watershed trapping analysis of phosphorus were used to estimate the amount of sediment that would be delivered to Falls Lake. Soil TN and TP concentrations were also used to generate predictions of nutrients for streambank erosion. Average, upper and lower estimates of TSS and nutrient loads were estimated for five study watersheds as well as for the entire Falls Lake watershed.

Out of the 111 reaches assessed, on average 45% of the banks were stable, 30% had minor erosion and 25% were severely eroding. Twenty-five of the 28 cross-sections monitored had measurable erosion with five of them eroding on both sides of the stream. The rate of average bank retreat for eroding banks ranged from 0.1-1.7 ft/yr with the maximum erosion rate reaching a little more than double the average rate.

Our modeled TSS load range for Falls Lake was substantially larger than the US Geological Survey SPAtially Referenced Regression on Watershed (SPARROW) estimates for streambed erosion and UNRBA estimates for streambank erosion. Our lower and upper limits were almost 10 to nearly 40 times greater than the SPARROW estimate. Our model loads were also much higher than the UNRBA delivered load, with our lower limit almost 4 times the UNRBA estimate. Our overestimation of TSS incremental and delivered load was likely due to several factors: double the length of channels identified in the model, a bias towards selecting the most

severely eroding cross-sections for monitoring, an overprediction of eroding banks from the erosion classification model and high delivery ratios that overlook the loss of sediment within channels. Despite our much larger TSS loading estimate, the UNRBA model prediction of TP from streambanks was about 1 to 3 times our TP estimates for the lower and upper limits, respectively. Our TN delivered estimate was 8 times larger than the UNRBA load.

The SPARROW TP loads for streambed erosion for Ellerbe, Eno and Falls Lake fell within the range of our model estimates for streambank erosion. SPARROW does not include an estimate of TN from streambed or streambank erosion. When comparing the proportion of sediment and nutrient loads that are from streambank erosion for the five study subwatersheds, our estimates for Ellerbe and Eno were closer to UNRBA and SPARROW. However, our estimates for Horse, Mountain and New Light were substantially larger, with UNRBA tending to estimate nearly 0 for the sediment and nutrient loads. Total TSS loads based on NCSU water quality monitoring and estimated by SPARROW and UNRBA models were in the low range of the annual loads calculated from past USGS monitoring at Ellerbe, Eno and Mountain creeks. Total TP loads were also on the low range based on past USGS monitoring for NCSU and SPARROW estimates, but UNRBA estimates were similar to the range of loads calculated based on past USGS monitoring for Eno and Ellerbe but were low for Mountain Creek. The NCSU water quality monitoring loads were likely on the low end of the range due to no very large storm events occurring during the monitoring period of our study.

UNRBA and SPARROW both estimate approximately 30% of all sediments delivered to the lake come from unstable stream reaches and that these streams contribute between 14.5 to 16% of the total TP load but only 0.8% of the TN load (UNRBA only). Our models and field-based work indicated that there may be larger amounts of sediment being eroded, but greater in-channel losses may be occurring. Despite much larger estimates of sediment volume, our nutrient loads were close to SPARROW and UNRBA, which indicates that the SPARROW and UNRBA may overestimate the soil nutrient concentrations. Further, by leveraging terrain data, our models provide desktop procedures for indicating locations where potential stream restoration and enhancement activities could be implemented to target reductions in turbidity, TSS and associated nutrients. Most of the catchments with the highest loads are closer to the outlet of the watershed and in higher developed areas. Maps indicating areas of predicted higher sediment and nutrient loading included in this report could be used to target areas for stream restoration and stabilization efforts.

Background and Site Selection

Excess sediment negatively impacts downstream waters by degrading instream habitats, reducing reservoir capacity, and increasing costs for drinking water treatment facilities, among others impacts (DWER, 2000; USEPA, 2017). Soil erosion including channel instability and streambank erosion introduces sediment bound nutrients to surface waters, which in dissolved forms can lead to downstream water quality degradation. While some species of nitrogen are found sorbed to soil, most attention is focused on dissolved inorganic fractions of nitrogen. Phosphorus, however, is the main focus of sediment loss prevention, as phosphorus is readily sorbed to soils high in metal hydroxides (Hesterberg, 2010).

In order to effectively reduce nutrient loading to Falls Lake, it is critical to first determine which sources of nutrients are most significant and secondly to evaluate the feasibility of reducing the loadings of nutrients from each source. The USGS (2018) developed a SPARROW model specific to North Carolina in order to estimate long-term average values of sediment and nutrients that are delivered to the river. The model links water quality monitoring data with information on watershed characteristics and contaminant sources. Data layers based on land surface forms (i.e. positive openness and slope area index) were used to estimate the occurrence of streambank incision and scour for the model. The model estimated that 54% of the total suspended sediments are from stream channel incision, erosion and scour compared to 46% from development, agriculture and land disturbance.

The Upper Neuse River Basin Association (UNRBA) also developed a watershed and lake model for Falls Lake. This model was used to examine specific sources of nutrient loading in order to propose alternate nutrient management plans (Upper Neuse River Basin Association, 2019). The UNRBA model (2019) estimates about 14% of the total phosphorus load for the basin comes from streambank erosion while the SPARROW model (USGS, 2018) estimated 18% of the total phosphorus comes from streambed erosion. The SPARROW model does not account for any phosphorus or nitrogen loading from streambank erosion. Field studies were not conducted to verify the presence of erosion or incision for either model. In addition, only limited sampling and laboratory analysis of streambank and streambed soils has been conducted to establish the nutrient contributions for streambank and streambed sediments.

This study combines geospatial analysis, inventory of streambank condition, assessment of streambank erosion rates and analysis of nutrient levels in streambank soils to validate the SPARROW and UNRBA model estimated potential nutrient loads from eroding streambanks upstream of Falls Lake.

Streambank conditions were assessed at 111 locations throughout the watershed covering a range of streambank conditions from stable to severely eroding. The location of the assessment reach was geospatially located by phone or by an RTK type GPS receiver. Twenty-eight sites exhibiting active streambank erosion were selected for permanent cross-sections to measure bank erosion rates and nutrient levels in streambank soils. Five study subwatersheds were selected within the basin to measure sediment and phosphorus loads. Three stations were located at USGS flow gauging stations. Flow monitoring was established at the remaining two locations.

The locations visited, cross section monitoring locations and the five study subwatersheds are identified in Figure 1.

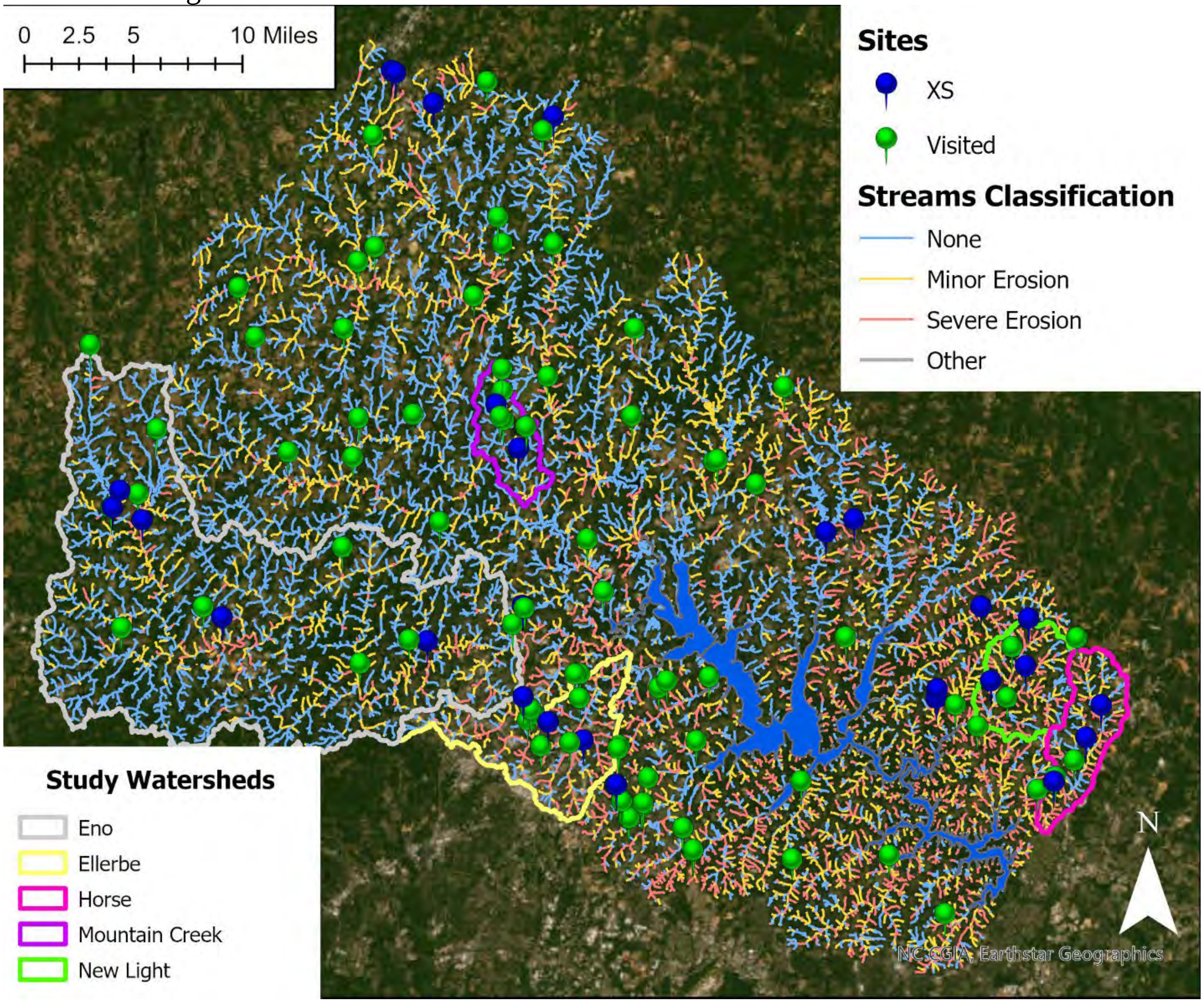

Figure 1. Project site locations and study watersheds.

Key Questions

The data collected during this study was used to answer the following questions:

- Is streambank erosion a significant source of nitrogen and phosphorus loads to Falls Lake?
- Can streambank erosion hotspots be identified throughout the watershed?
- Are the estimates from the UNRBA model and USGS NC SPARROW model reasonable for total suspended solids (TSS), total nitrogen (TN) and total phosphorus (TP) loads from streambank erosion?

Methods

Field Methods

The relationship between positive openness (PO) and erosion categories developed for Mine Creek in Raleigh by El-Khoury (2022) was used to classify every 100 ft segment of stream channel as either stable, minor erosion or severe erosion. PO is a visualization of a DEM that identifies the location of concave surfaces based on the average measure of the eight zenith angles like the one developed by USGS for North Carolina (Rowley et al., 2018). Over 100 potential sites that were spatially distributed across the Falls Lake watershed and, including a range of erosion categories and stream orders were selected for assessment. In total 111 sites were assessed. Both sides of the stream were visually assessed to classify the type of bank erosion for each selected 100 ft reach. A representative bank height and top of bank (TOB) width were measured and recorded at each reach.

Erosion rates were monitored at 28 locations exhibiting active erosion using repeat cross-section surveys. Cross-sections were established and surveyed between October and December 2022 and resurveyed in June 2023 (Table 6).

Undisturbed soil samples were collected at each eroding bank at every cross-section. One sample was taken for each distinct soil layer. The soil samples were analyzed for Total Nitrogen (TN), Total Phosphorus (TP) and bulk density at the BAE Environmental Analysis Laboratory. These results were used to estimate nutrient loading to Falls Lake from streambank erosion.

Automated samplers with integrated flowmeters were installed at five monitoring sites (Ellerbe Creek, Eno River, Horse Creek, Mountain Creek and New Light Creek) as shown in Figure 40 in Appendix B. Water quality monitoring was conducted at each station to evaluate turbidity levels and concentrations of total suspended sediment (TSS) and total phosphorus (TP). Turbidity was measured for all samples and a subset of samples were also used to measure TP and TSS concentrations. Each sampler included 24 1,000-ml bottles. Five of the bottles collected baseflow (nonstorm) samples while the remaining 19 collected during stormflow. Nonstorm and storm discharge were delineated using the stage of the stream. Samplers were programmed to collect a 400-ml sample every 48 hours during nonstorm flows and every 4-6 hours during storm flows. More frequent sampling during storms was required to characterize the variability of total suspended solids (TSS) since previous research showed greater variability of TSS concentrations during storm flows.

Monitoring stations were visited approximately every two weeks to perform maintenance and retrieve samples. An aliquot of sample was withdrawn from each sampler bottle and placed in a glass vial and then in a turbidimeter for analysis. Turbidity levels were recorded on a field sheet. Between 180 and 270 samples were collected from each monitoring station and analyzed for turbidity. Due to limited resources, only 20-30 of the samples from each station were analyzed for TSS and TP. The resulting water quality data were then used to develop relationships between turbidity and TSS and TP and the data were combined with flow data to estimate total annual loads of TSS and TP for each study subwatershed.

GIS Analysis

Terrain

Available terrain data layers were used and several new layers were generated to aid in identifying landforms, stream paths and potential locations of streambank erosion. Light Detection and Ranging (LiDAR) data from the 2015 NC statewide LiDAR DEM (OCM Partners, 2023) were used to generate several visualizations of digital elevation models (DEM). A 3 ft resolution was used for the LiDAR data. Bridges and road crossings were burned into the DEM to allow the creation of a detailed stream network. The resulting streams network used for this study has double the length compared to the National Hydrography Dataset (NHD) stream layer. The Relief Visualization Toolbox (RVT) was used to generate a positive openness raster from the DEM based on guidance provided by Hopkins (2022). Positive openness represents depressions where the angles are less than 90°. Openness is best at representing concave surfaces, "superficially resemble[ing] digital images of shaded relief" (Yokoyama, 2002). Further details are provided in Appendix D – GIS Analysis. A land slope raster was generated in ArcGIS Pro using the Slope (3D Spatial Analyst) tool from the DEM. A relative elevation model (REM), also known as height above river (HAR) rasters, was created following the tutorial developed by Coe (2019) and modified by Ersi (*Relative Elevation Model in ArcGIS Pro*, 2022) for ArcGIS Pro. REM visualizations are helpful for discerning river channels and nearby features such as meander scars, oxbow lakes and terraces.

Land Use

The change in land use and land cover over the past ten years (2011-2021) were examined for the entire Falls Lake watershed and five study watersheds. The yearly USGS land change monitoring assessment and projection dataset was used (USGS, 2021). Land use percentage in 2021 was defined for the watershed of each of the 111 sites through steps performed in ArcGIS Pro and RStudio.

Quantifying Streambank Retreat

Cross sections were established and surveyed using a robotic total station at 28 locations experiencing active erosion in October and December of 2022. All cross sections were resurveyed in June of 2023. Streambank retreat was computed following the methods outlined by El-Khoury (2022).

Developing Models to Predict Sediment and Nutrient Loads

Three separate statistical models were developed to estimate the total volume of eroded sediment for one side of the bank along each 100 ft stream segment. The first model classified each streambank segment as either eroding or not. The second model predicted the bank height, and the last model predicted the annual bank retreat. Each side of the bank was separately examined since erosion sometimes only effects one side of the stream such as in a meander bend. No field measured values were used in the final models to allow these models to be applied to the entire stream network in a watershed. ArcGIS Pro was used to develop the GIS data used in the models. Figure 2 shows the process followed to develop the three models. All models were developed in RStudio (R version 4.2.2). Leave-one-out cross-validation (LOOCV) was used to train and test all models because this is the most rigorous type of cross-validation and best to use on small datasets.

A confusion matrix was created to examine the accuracy and kappa values based on each LOOCV run for the classification model. The kappa value is the accuracy corrected for chance. The best regression model was selected by choosing the one with the highest R^2, r^2 and adjusted r^2, and lowest RSME, MAE, AIC and BIC.

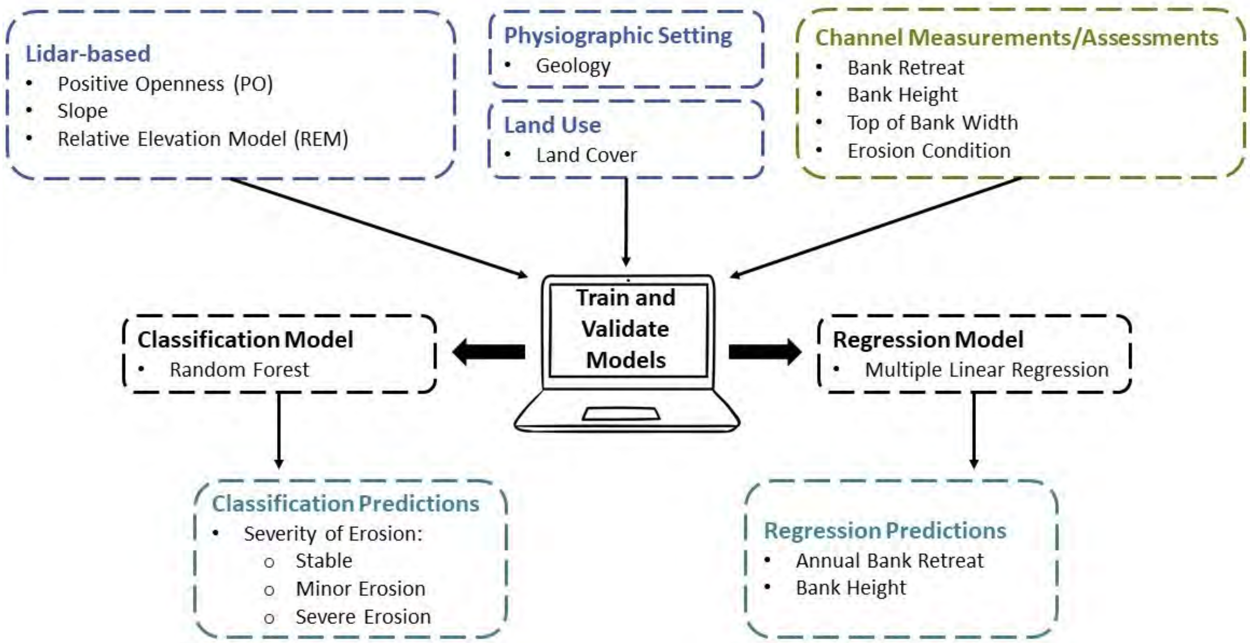

Figure 2. Outline of model development to predict amount of eroded sediment from streambanks across the watershed.

Predicting Sediment and Nutrient Loads

Long-term Load Estimates

Annual sediment and nutrient loads were estimated using regression methods developed by the USGS. For the Eno River and Ellerbe Creek, the LOAD ESTimator (LOADEST) program (Runkel et al., 2004) was employed to estimate annual TSS, TP and TN loads using the grab samples collected by the UNRBA from 2014-2018 and daily average streamflow from the USGS. For Mountain Creek, which had a longer record of water quality samples (1996-2014), Weighted Regression on Time, Discharge, and Season with a Kalman filter (WRTDS-K) (Zhang and Hirsch, 2019) was applied to estimate annual TN and TP loads using grab sample results and daily mean flow from the USGS. TSS results were not available for Mountain Creek.

Turbidity Monitoring Predictions

Regression equations were developed to estimate TSS and TP based on field measured turbidity and corresponding lab analyzed samples for TSS and TP concentrations for each of the five study watersheds. These predictions of TSS and TP represent the total amount from all watershed sources not just streambank erosion (see Appendix for more details).

Model Predictions

The three developed models were used in conjunction to estimate the total amount of sediment eroded from streambanks. First the erosion classification model was applied to determine which banks were eroding. Only the eroding banks were run through the bank height and bank retreat models. The volume of eroded sediment was calculated as shown in Equation 1. The sediment load was calculated by multiplying the volume by the bulk density. The median measured bulk density for each geologic region was used. The TN and TP loads were estimated by multiplying the sediment load by the median measured TN/TP per geologic region. The delivered load was estimated by multiplying the sediment load by the delivery fraction used in the NC SPARROW model.

Equation 1. Volume of eroded sediment.

$$Volume\ of\ Eroded\ Sediment\ \left({ft^3}/_{yr}\right) = Bank\ Height\ (ft) * Bank\ Retreat\ \left({ft}/_{yr}\right) * Length\ of\ Stream\ Segment\ (ft)$$

Originally, the sediment loads were calculated using the estimated load produced from both sides of the bank. This appeared to significantly overestimate sediment loads compared to estimates from the turbidity regression equations for the five study watersheds. Due to this, first order streams were excluded and an average load from both sides of the banks was estimated for each segment. Even though the LiDAR was collected during winter months (1/10/2015 to 3/22/2015) with minimal tree canopy cover and leafy vegetation, the majority of the watershed is forested. Since LiDAR is less accurate in forested areas, first order streams were excluded from the model results as was similarly done in a study by Wolter et al. (2021). In addition, the omission of first order streams is reasonable given the stream layer generated for this project from DEM data doubled the length of the stream network over the NHD. Only one load was estimated for each segment instead of two separate loads for the right and left bank. The estimated load was the average of the right and left bank loads. One of the few studies to account for both sides of the streams was Wolter et al. (2021), which doubled their prediction of eroded sediment.

Comparing Modeled Loads to Measured Loads and Other Models

The NCSU modeled loads (TSS, TN and TP) from streambanks were compared to NC SPARROW incremental loads and UNRBA delivered loads (Table 1 and Table 2). Delivered loads could not be extracted from the SPARROW model so only incremental loads were compared. The NCSU delivered load was estimated by multiplying the incremental load by a phosphorus delivery percentage estimated by the UNRBA initial watershed trapping analysis (Matos, 2014). The sediment delivery percentage was assumed to be equivalent to the phosphorus delivered since phosphorus is mainly sorbed to sediment. The NCSU turbidity monitoring estimates for the delivered sediment and nutrient loads from all sources were compared to the long-term load estimates (LOADEST) and UNRBA model. The SPARROW incremental estimates were extracted from the model results (USGS, 2018) by identifying each subcatchment associated with our study watersheds. UNRBA shared the results of their model for each of our subwatersheds. All results were converted to Mg/km^2/yr for sediment and kg/km^2/yr for nutrients loads to enable comparison. To calculate the percentage of streambank erosion relative to the total sediment load for 5 study watersheds, the delivered model loads were divided by total loads determined from the turbidity monitoring.

Table 1. Models that provided delivered load estimates from streambank erosion.

Watershed	TSS			TP			TN		
	NCSU	SPARROW	UNRBA	NCSU	SPARROW *	UNRBA	NCSU	SPARROW	UNRBA
Falls Lake	✓	×	✓	✓	×	✓	✓	×	✓
Ellerbe	✓	×	✓	✓	×	✓	✓	×	✓
Eno	✓	×	✓	✓	×	✓	✓	×	✓
Horse	✓	×	✓	✓	×	✓	✓	×	✓
Mountain Creek	✓	×	✓	✓	×	✓	✓	×	✓
New Light	✓	×	✓	✓	×	✓	✓	×	✓

*SPARROW only has estimates from streambed for TP, not streambank erosion.

Table 2. Models that provided delivered load estimates from all sources.

Watershed	TSS				TP				TN			
	NCSU Turbidity	LOADEST	SPARROW	UNRBA	NCSU Turbidity	LOADEST	SPARROW	UNRBA	NCSU Turbidity	LOADEST	SPARROW	UNRBA
Falls Lake	×	×	×	✓	×	×	×	✓	×	×	×	✓
Ellerbe	✓	✓	×	✓	✓	✓	×	✓	✓	✓	×	✓
Eno	✓	✓	×	✓	✓	✓	×	✓	✓	✓	×	✓
Horse	✓	×	×	✓	✓	×	×	✓	✓	×	×	✓
Mountain Creek	✓	×	×	✓	✓	×	×	✓	✓	×	×	✓
New Light	✓	×	×	✓	✓	×	×	✓	✓	×	×	✓

Results & Discussion

Land Use Change

Figure 3 illustrates the percentage of land cover in 2021 for the entire Falls Lake watershed and the five study watersheds within Falls Lake. Ellerbe, located in Durham County, is the most urbanized (72%) while the remaining watersheds have less than 20% developed land. The Eno watershed has a similar makeup of land use to Falls Lake with the 66% and 63% forested, respectively. Horse and Mountain Creek watersheds have the largest percentage of cropland (35% and 34%, respectively). Overall, there was minimal change in developed land cover in most subwatersheds within the past ten years (2011-2021), with the greatest annual change of around 2%.

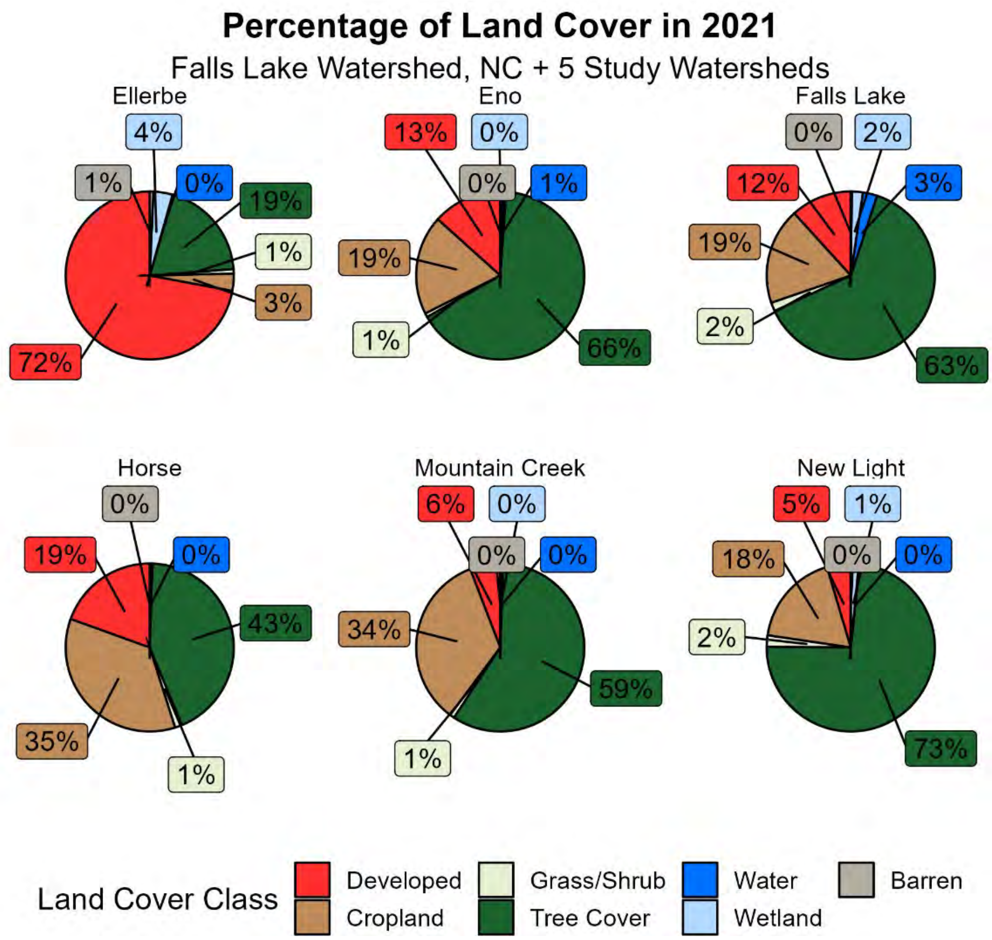

Figure 3. Percentage of land cover in 2021 for the Falls Lake watershed and five study watersheds.

Water Quality Monitoring

The median baseflow turbidity was similar for each station with the highest recorded median value at the Eno River station (25 NTU) and the lowest at Ellerbe Creek (14 NTU) (Figure 4). Flow-weighted storm turbidities were two to five times greater than the corresponding baseflow turbidities with greatest median recorded for Horse Creek (75 NTU) and the lowest for the Eno River (46 NTU) (Figure 5). Stormflow turbidity had a greater variability seen by the larger interquartile ranges. It should be noted that the ranges for Eno River and Ellerbe Creek would likely be higher if storm samples had been successfully collected during high discharges that occurred on 4/7-4/8/23 and 4/14/23.

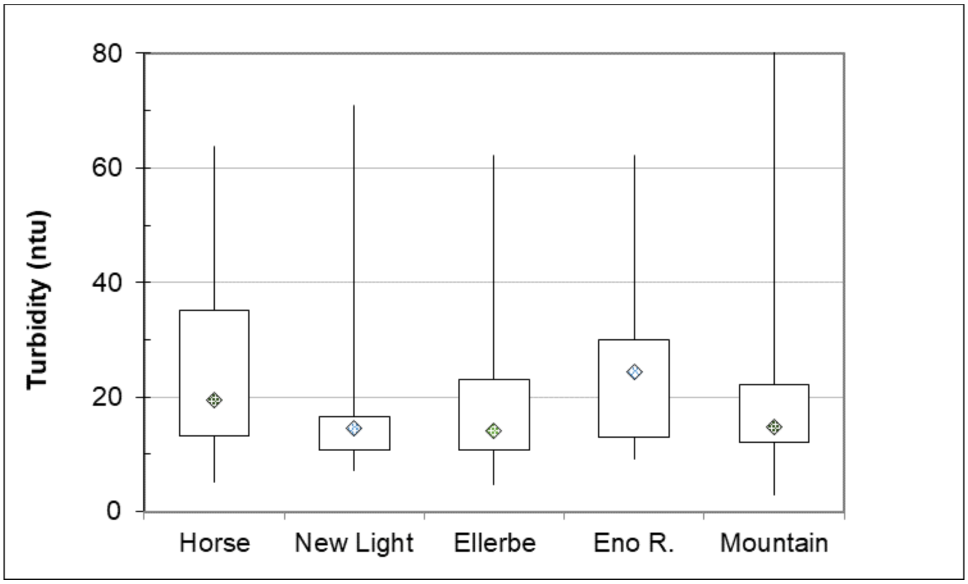

Figure 4. Turbidity of two-week baseflow samples for the five monitoring stations.

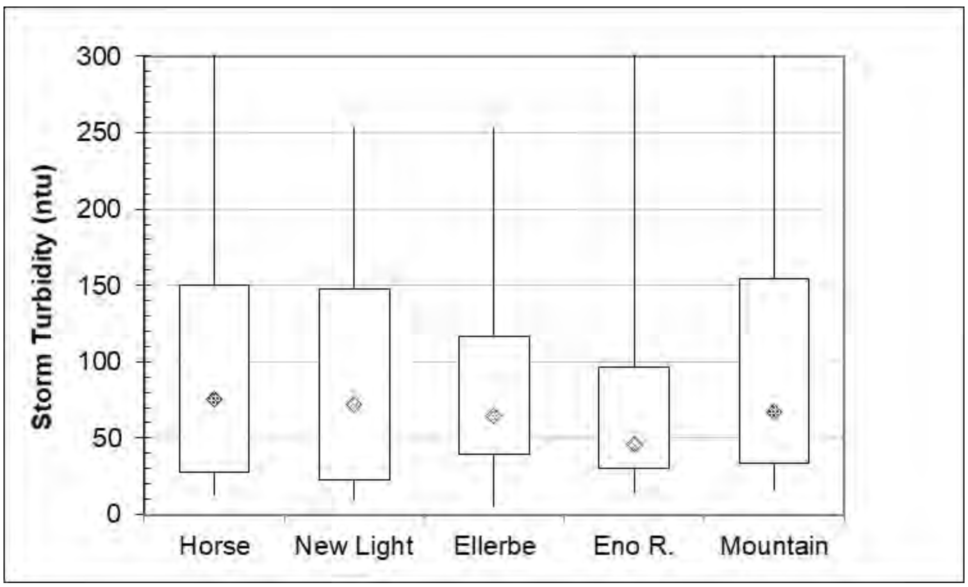

Figure 5. Turbidity of two-week storm flow-weighted turbidity for the five monitoring stations.

For loads, often one or two large storm events can cause the majority of the total TSS or TP loading for an entire year or for several years. This is illustrated by the loads for Horse Creek (Figure 6). In Figure 7, date shown is the beginning date of the 2-week period between visits when samples were retrieved; therefore, the bars indicate the nonstorm and storm event load for the 2-week period. The storms on 4/7 and 4/14 (included in the orange bar labelled 4/3/23) and 7/14 (included in bar labelled 7/11/23) resulted in 76% and 81% of the total TP and TSS load for the 0.96-year duration of monitoring. These large storms (4.0 and 2.0 inches on 4/7 and 4/14) with their very high discharge often cause severe land and streambank erosion, which are major contributors to TSS and TP loading in surface waters. While not shown, the distribution of TP and TSS loads over time for the other four streams also had one or two high load events over the duration of the monitoring.

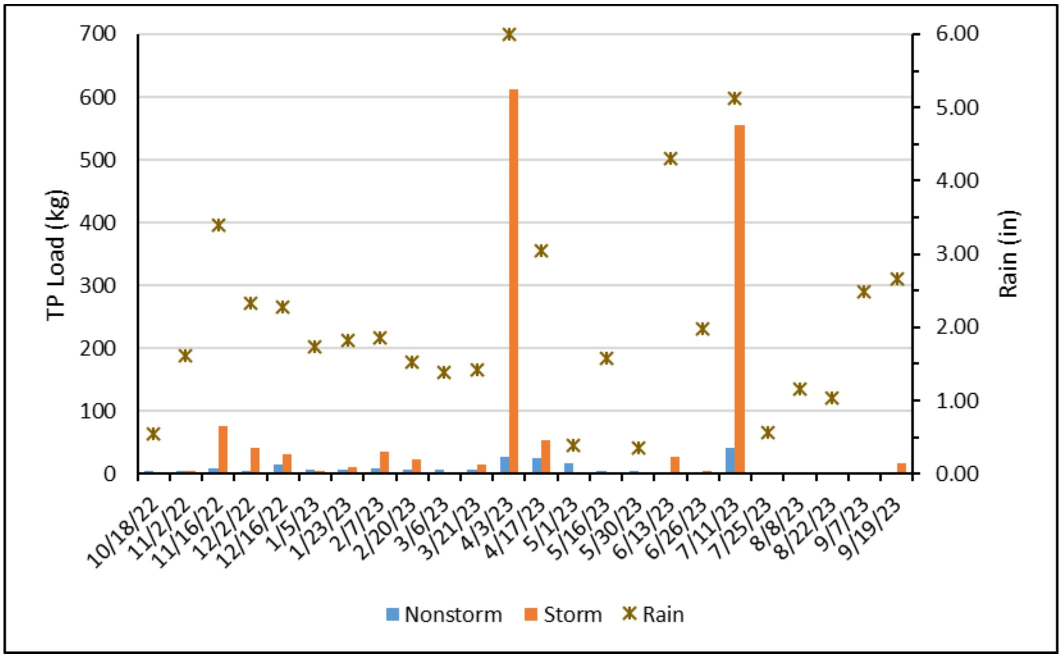

Figure 6. Bi-weekly TP loads for Horse Creek.

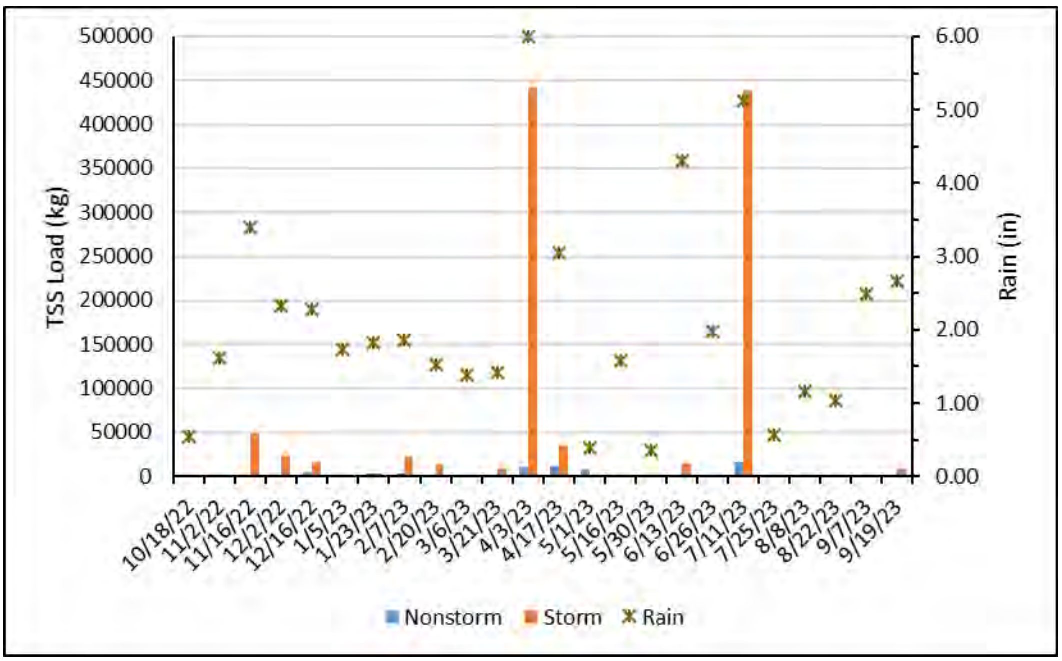

Figure 7. Bi-weekly TSS load for Horse Creek.

Streambank Assessment and Bank Retreat Monitoring

Out of the 111 reaches assessed, on average 45% of the banks were stable, 30% had minor erosion and 25% were severely eroding (e.g., Figure 8). The distribution of erosion within each reach varied where some reaches ranging from 0-100% minor erosion and stable banks and 0-75% severe erosion. From the 28 cross-sections, only 25 had measurable erosion with five of them eroding on both sides of the stream. Most cross-sections were on 4th order streams (Figure

9). The rate of average bank retreat for eroding banks ranged from 0.1-1.7 ft/yr with the maximum erosion rate reaching a little more than double the average rate (Table 3).

Figure 8. Example of erosion classification along Falls Lake reaches.

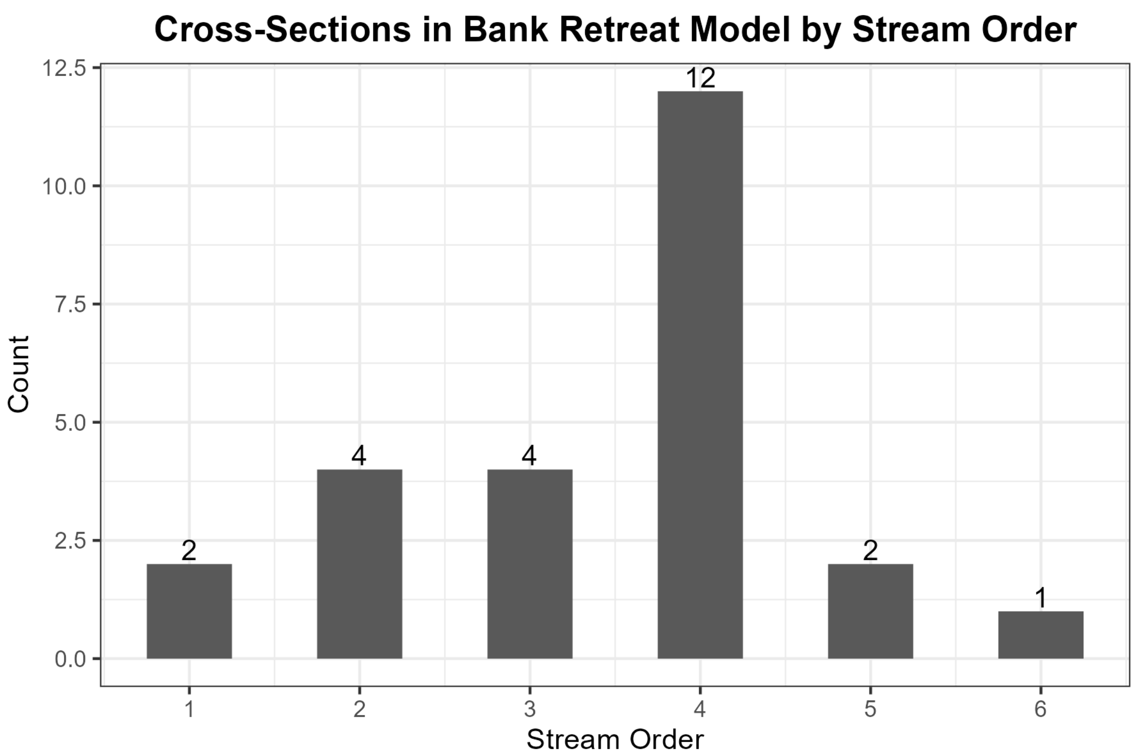

Figure 9. Number of coss-sections per stream order used in bank retreat model.

During the period between surveys, there were few large storm events. Most of the watersheds experienced no to only a couple of bankfull events. Only Ellerbe experienced storm events larger than bankfull with two 2-year storms. After completing the second resurvey, a large storm occurred over the eastern part of the Falls Lake watershed (near Horse and New Light watersheds). The road near site FL53 was overtopped, prompting a follow-up visit to several sites in this area. As illustrated in Figure 10, a single large storm event can have a greater impact on the rate of erosion than multiple combined storm events over the course of an entire year. The frequency and intensity of storms combined with antecedent soil conditions dictate the amount of erosion that will occur due to unstable undercutting and mass wasting (Daly et al., 2015; Zhao et al., 2022), therefore these types of erosion are more episodic in nature when compared to surface scour or hoof shear erosion and will vary more from year to year. Mass wasting is more likely to occur after events that have fully saturated the bank decreasing the matrix suction of the bank (Daly et al., 2015; Midgley et al., 2012). If the conditions that drive bank failure were not met or met as frequently during the time period that the data were collected, bank failure will be underrepresented and potentially underestimated in the model. A major limitation of this study was the short time frame allowed to monitor streambank retreat. Long-term monitoring of cross-sections would capture a greater range of precipitation events including both dry and wet years. This would provide a truer average annual bank retreat that could be used to improve the bank retreat model.

Table 3. Summary of average and maximum bank retreat for eroding banks.

Metric	Average Bank Retreat (ft/yr)	Maximum Bank Retreat (ft/yr)
# of eroding banks	30	36
Minimum	0.1	0.2
Average	0.5	1.4
Maximum	1.7	3.8

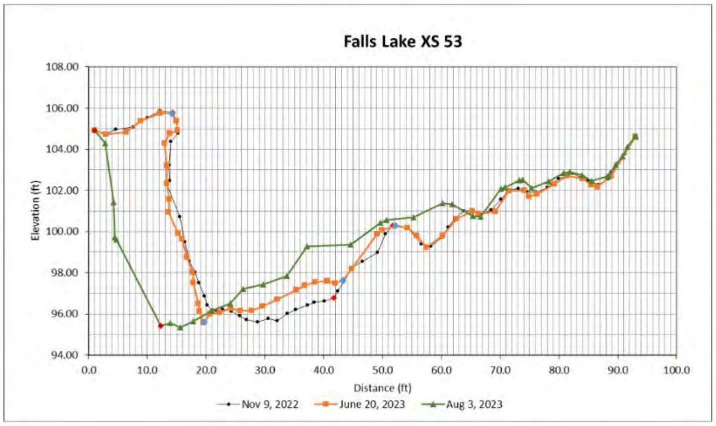

Bank Retreat	Nov 22 - June 23		June 23 - Aug 23	
	(ft)	**(ft/yr)**	**(ft)**	**(ft/yr)**
Avg	0.7	1.2	9.8	81.1
Min	0	0	7.5	62.3
Max	2.1	3.4	13.9	115.4

Figure 10. Example of cross-section at FL53.

Statistical Model Results

Table 4 contains a summary of the final models developed to estimate the eroded sediment volume from streambank erosion. All of the models have test metrics above 50% for accuracy or 0.5 for adjusted r^2 which is generally accepted as satisfactory for environmental watershed model like SWAT (D. N. Moriasi et al., 2007). Many of the models contain similar predictors like PO, land cover and geologic factors.

Table 4. Summary of final statistical models.

Model	Type	Model Predictors	Fit of Test Data	Fit of Final Model
Erosion Classification	Random Forest	90th percentile PO, max slope, cropland land cover %, barren land cover %, tree land cover %, 75th percentile REM, geologic belt and developed land cover %	Accuracy of 57% and kappa value of 0.4	Accuracy of 60% and kappa value of 0.4.
Bank Height Model	Multiple Linear Regression	$Transformed\ Bank\ Height\ (ft) = 0.00182 * Developed - 0.0134 * PO + 0.00820 * Slope + 0.00970 * REM + 0.0880 * Dbfk$	Adjusted r^2: 0.53 RMSE: 0.09 ft	Adjusted r^2: 0.58
Bank Retreat Model	Multiple Linear Regression	$Bank\ Retreat\ (ft/yr) = -0.012 * Abkf + 0.027 * WTOB + 0.047 * PO - 0.0037 * Developed - 0.0603 * GrassShrub + 0.122 * Barren + 0.36 * RaleighBelt - 0.224 * IntrusiveRock$	Adjusted r^2: 0.55 RMSE: 0.15 ft/yr	Adjusted r^2: 0.77

Dbkf = bankfull height (ft); Slope = 90^{th} slope percentile; REM = median REM percentile; Abkf = bankfull area (ft); WTOB = TOB width (ft); PO = minimum PO (Bank Height)/median PO (Bank Retreat) ; Developed = % of developed land in watershed; GrassShrub = % of grass/shrub land in watershed; Barren = % of barren land in watershed; RaleighBelt = 0 not in Raleigh Belt, 1 in Raleigh Belt; Intrusive Rock = 0 not made of intrusive rock, 1 made of intrusive rock

Sediment Loads

NCSU Model Loads

The final resulting sediment loads produced by the three NCSU models for presence of erosion, bank height and bank retreat are provided below in Table 5. Most of the load was estimated to come from stream orders 2-4 (Figure 11).

Table 5. Delivered sediment load from NCSU model estimates, excluding all first order streams, including only severely eroding banks and using an average load per stream segment.

Watershed	Prediction	Lower Limit	Upper Limit	Prediction	Lower Limit	Upper Limit
	(Mg/yr)			(Mg/km^2/yr)		
Falls Lake	128184	72084	205478	64	36	103
Ellerbe	6577	2833	12221	116	50	216
Eno	17666	9894	28321	48	27	78
Horse	6023	3848	8840	195	125	287
Mountain Creek	486	263	784	23	13	38
New Light	6118	4104	8581	192	129	270

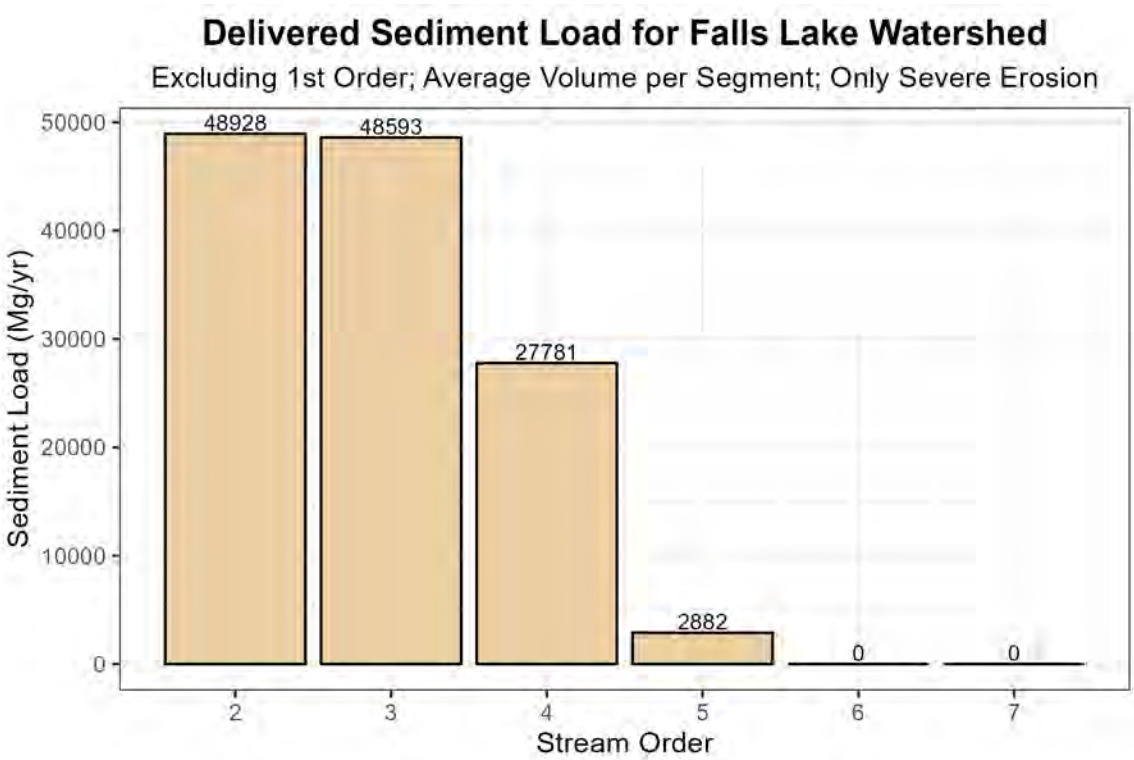

Figure 11. Delivered sediment load to Falls Lake segregated by stream order.

Comparison of Sediment Loads

Estimates from the NCSU model ranged from 10 to 40 times the amount of streambank erosion estimated by SPARROW for Falls Lake (Figure 12). The NCSU model loads were also much higher than the UNRBA delivered load, with our lower limit almost 4 times the UNRBA estimate for Falls Lake. (Figure 13). For the five study watersheds, the model streambank sediment estimates were all far greater than the turbidity-based TSS estimates, which include all sources of sediment (Figure 16). The model estimates were higher for Ellerbe and Eno than the other watersheds for the UNRBA model. In contrast, UNRBA could be underestimating the contribution of sediment from streambank erosion for the remaining three watersheds.

This confirms that our model overestimates the sediment from streambank erosion. There are several possible reasons for the high estimates. First, our model could overestimate sediment load from streambank erosion because the length of channels delineated in our model (excluding first order) was about two times the length used in SPARROW. Studies have shown that a substantial volume of sediment comes from streambank erosion in headwaters, making up 58% of the total streambank sediment flux (Hopkins et al., 2023). Excluding smaller headwater streams from the model could significantly alter the loads affecting watershed management decisions.

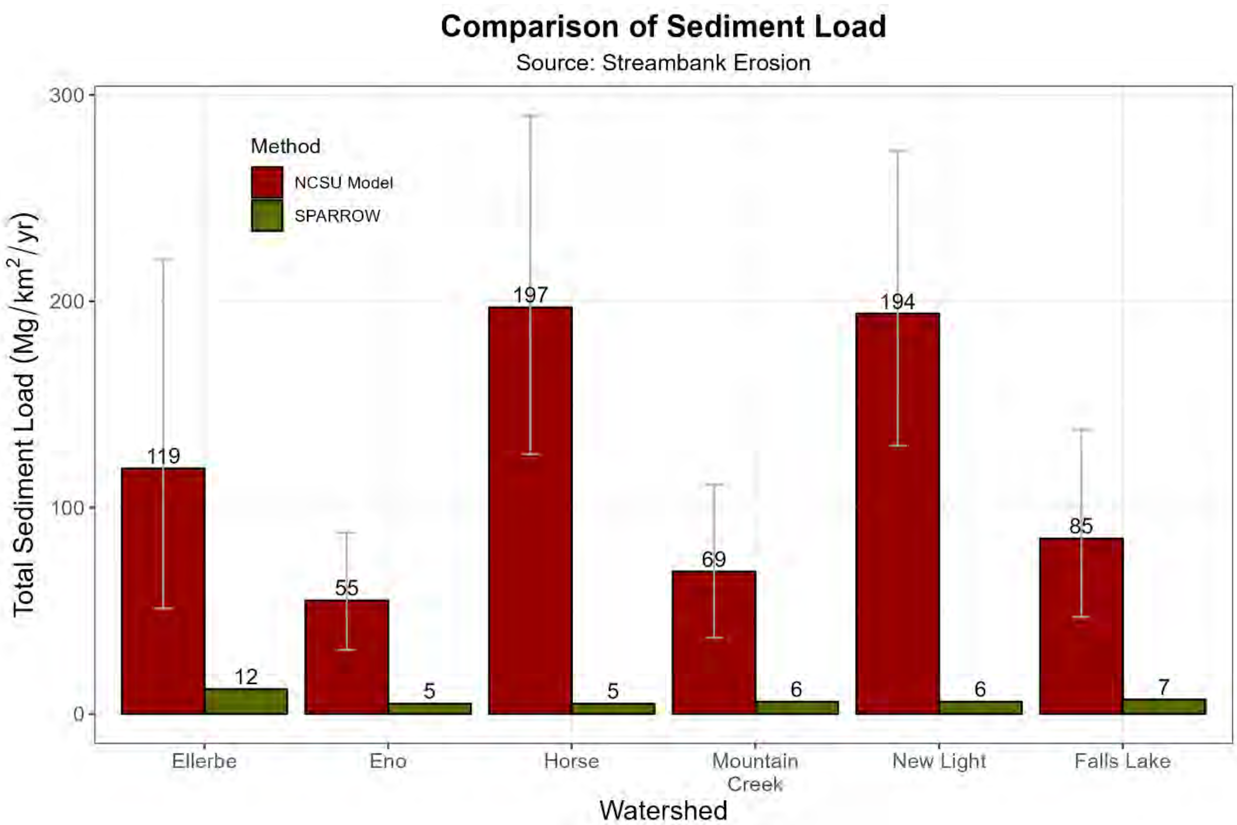

Figure 12. Comparing sediment loads from streambank erosion for Falls Lake watershed and 5 subwatersheds. Error bars are used to show the range of lower and upper predictions from the NCSU model.

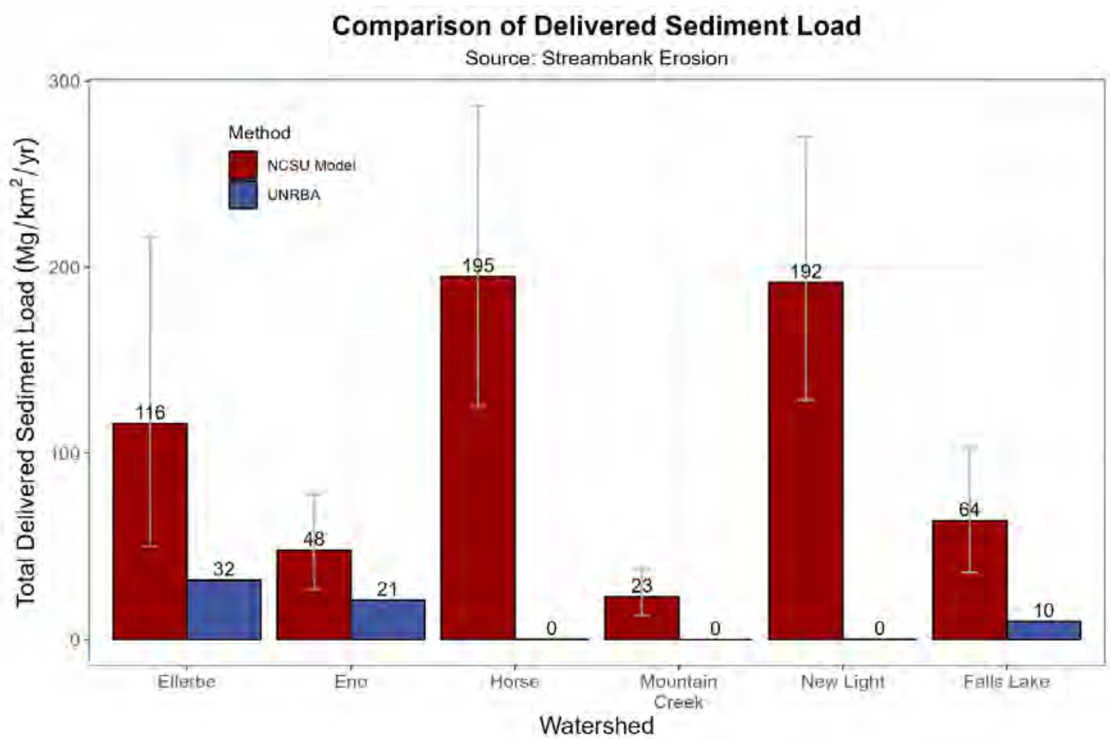

Figure 13. Comparing delivered sediment loads from streambank erosion for Falls Lake watershed and 5 subwatersheds. Error bars are used to show the range of lower and upper predictions from the NCSU model.

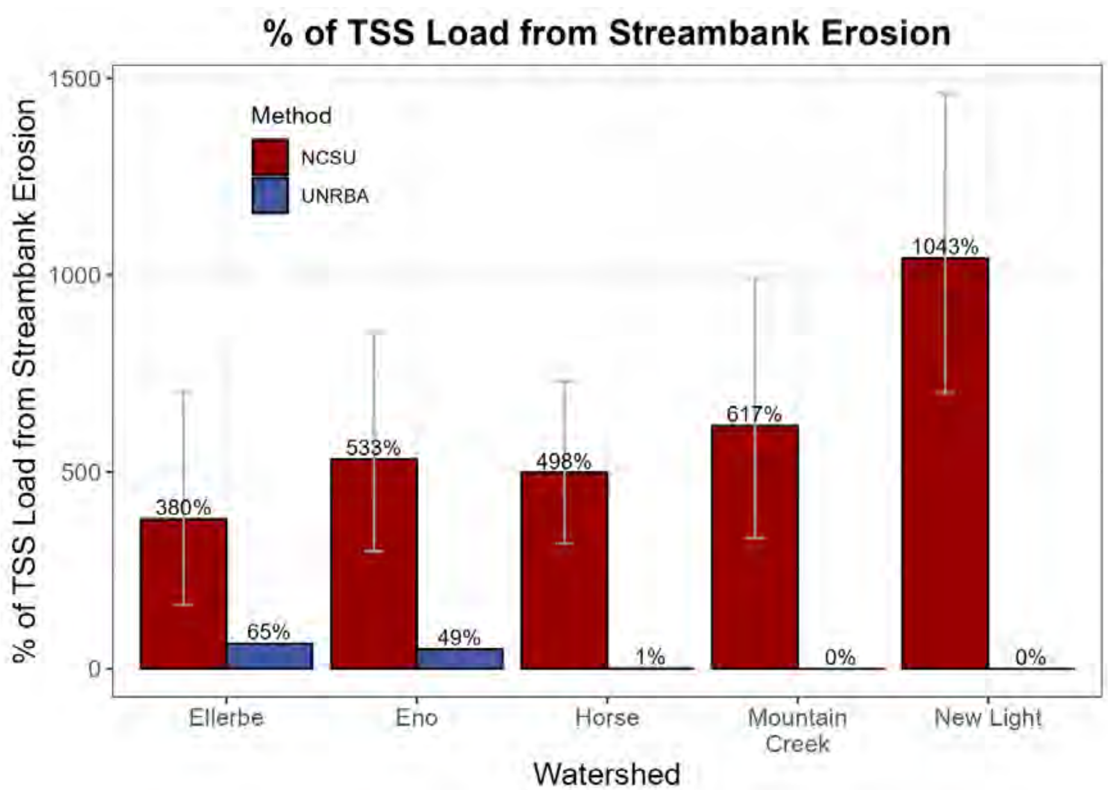

Figure 14. Percentage of streambank erosion out of total sediment load for 5 study watersheds. The NCSU percentage was calculated by dividing the NCSU model results by the NCSU turbidity results.

Another reason the NCSU model could overestimate sediment was the bias towards more severe erosion. The cross-sections were targeted towards sites that exhibited active and the most severe erosion to capture measurable streambank retreat in less than a year. Even with this selection, three cross-sections showed no measurable erosion. Figure 15 displays the difference between the measured and predicted bank retreat. The model successfully captures the wide variation but predicts a higher median for both minor and severe erosion. A higher median is expected for severe compared to minor erosion, but the model showed similar values. The predicted medians for both erosion conditions were higher than what was observed, which is the nature of a linear regression model. Future work should monitor streambank retreat over longer terms and include more minor erosion. The inclusion of additional variables, such as precipitation, could also increase the accuracy of the model.

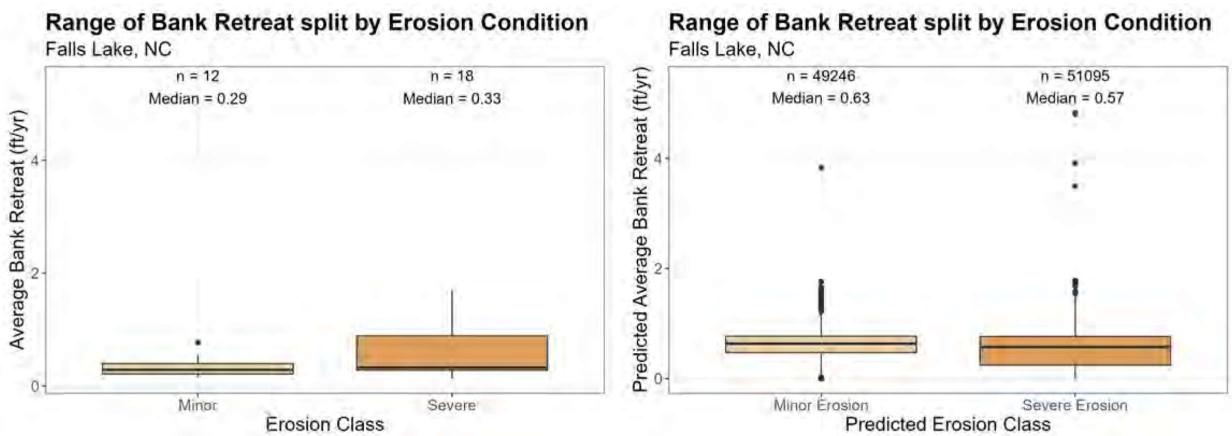

Figure 15. Boxplot of measured and predicted bank retreat split by erosion condition.

The delivery ratio used, based on phosphorus, essentially estimated no net loss from in-channel processes (Matos, 2014). Ratios used ranged from 10 to 100% with a median value of 96% and a mean of 70%. Therefore, the majority of the sediment from most stream segments was delivered to Falls Lake. However, based on reach assessments, deposition was prevalent in the watershed, recorded along 61% of the surveyed reaches (Figure 16). The grain size distribution of bank material also plays a role in the amount of sediment transported with silt and clay traveling much further than sand. Assessments of eroding banks at cross-sections revealed 22 of 30 had some sand content with scores of 2 (low sand content) up to 10 (pure sand). There were few to no events that overtopped banks during our monitoring period, so the majority of sediment lost during transport would be due to channel losses and not floodplain deposits. Future work should delve further into delivery ratios and sediment transport to more accurately represent sediment transport processes occurring within the Falls Lake watershed.

Figure 16. Example of deposition in Falls Lake.

In the case of total TSS loads for the five study subwatersheds, which includes all sources of sediment, the load derived from NCSU water quality monitoring and UNRBA were in the low range when compared to the range of annual loads calculated from past USGS monitoring at Ellerbe, Eno and Mountain creeks (Figure 13). This may be due to no large storm events occurring during the monitoring period for our study.

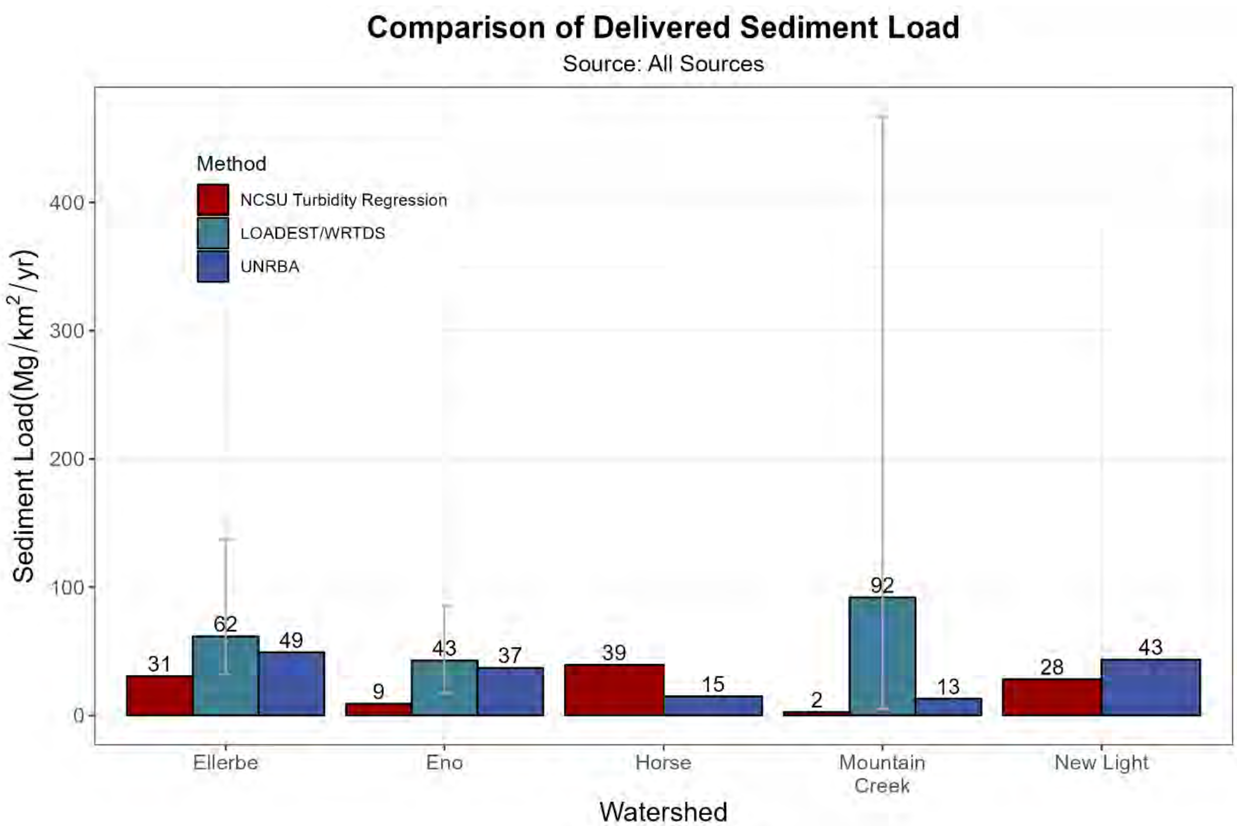

Figure 17. Comparing sediment loads from all sources for the 5 subwatersheds. Error bars are used to show the range of lower and upper ranges from the LOADEST estimates. Loads for Mountain Creek are Suspended Sediment Concentration rather than for TSS.

It is possible that the erosion classification model was overpredicting the number of eroding banks in the watershed since this was our poorest performing model. While our team observed erosion throughout the watershed, it was more difficult than anticipated to find locations for cross-section monitoring. In addition, we were unable to field validate the model results due to time constraints. The model predicts that a majority of streambanks were stable for Eno, Horse and New Light watersheds (Figure 18). Despite only having 34% eroding streambanks, the model overestimated the delivered sediment load for New Light by a factor of 10 when compared to the turbidity regression estimate. Most of the severely eroding streams were located on the main reach of New Light, which is a 5th order stream that contributed a larger volume of eroded sediment compared to lower order streams (see Figure 19). Recent construction and urbanization over the past few years have likely accelerated streambank erosion. Mountain Creek had the lowest frequency of observed streambanks with severe erosion, matching the model results which categorized only 17% of streambanks as severely eroding and 61% experiencing minor erosion such as surface scour. In all of Falls Lake, 46% of streambanks were predicted to be eroding (Figure 42). Similarly, (Wolter et al., 2021) also used LiDAR to quantify the extent of streambank erosion across a large watershed in Iowa and found about 41% of all third through sixth order streams were severely eroding. This also mirrors the percentage of banks eroding from our 111 assessment reaches, where 55% were eroding (30% minor erosion and 25% severe erosion).

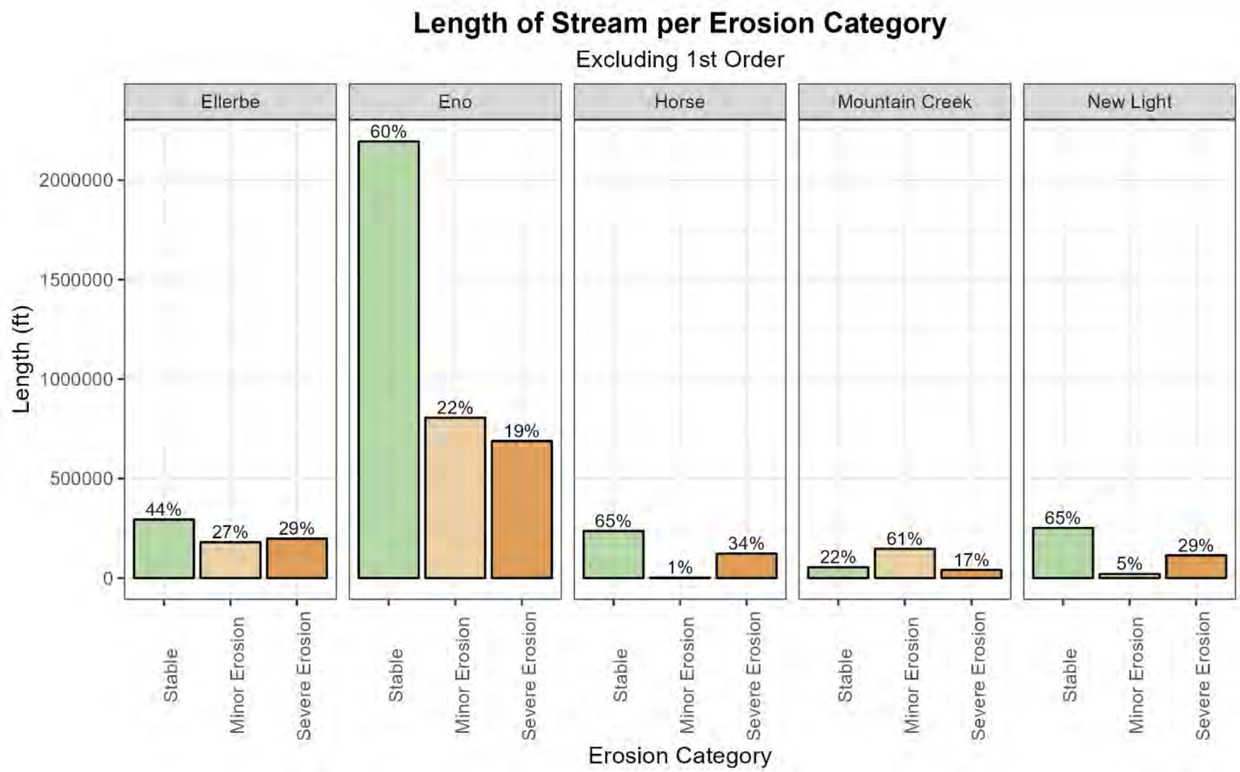

Figure 18. Length streambank per erosion category for 5 study watersheds.

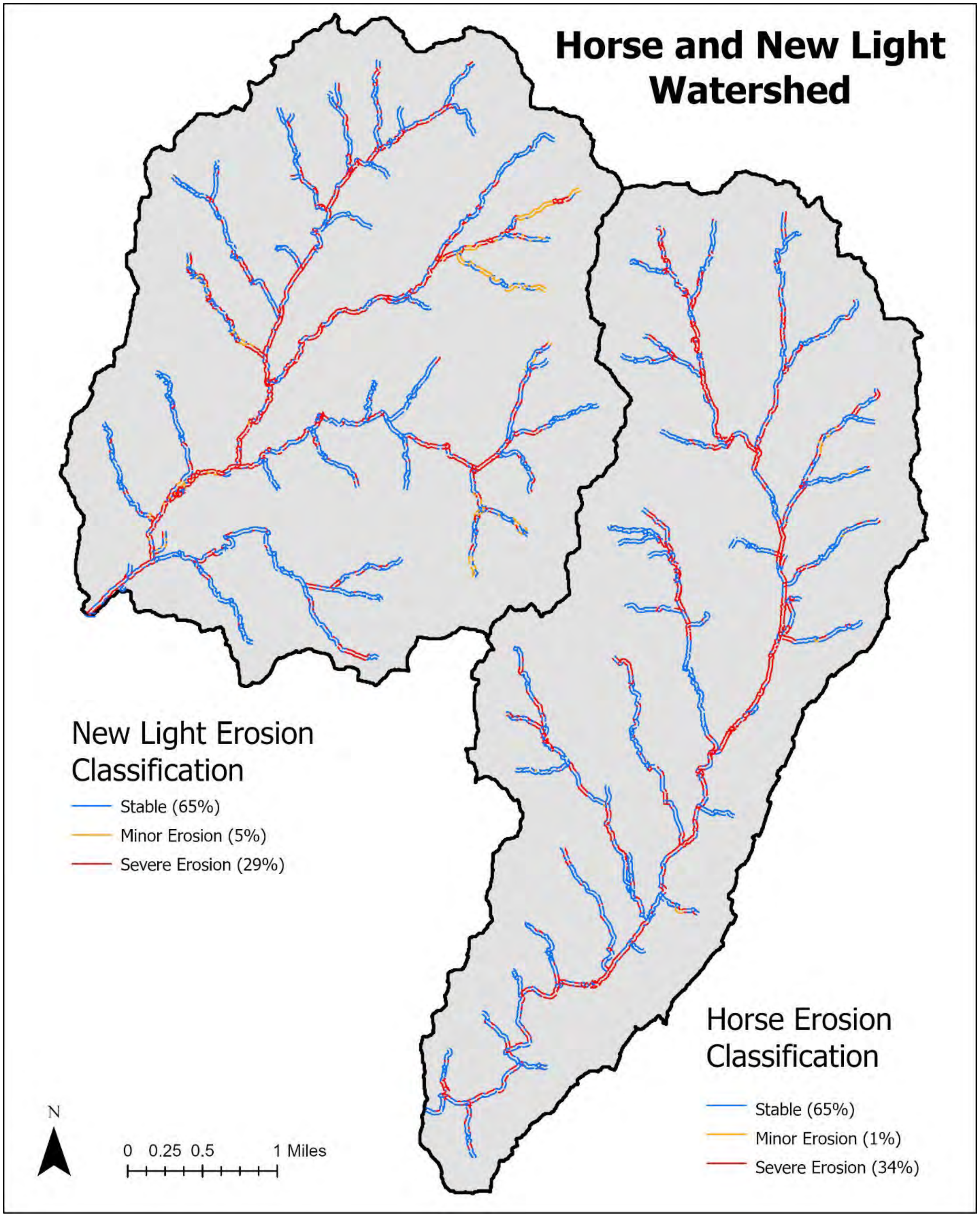

Figure 19. Model prediction of erosion classification for Horse and New Light watershed.

Nutrient Loads

Despite the NCSU models significantly overestimating TSS, the NCSU TP loads fall within or near the range of TP estimated by SPARROW and UNRBA (Figure 20 and Figure 21). This was because the TP concentrations from streambank erosion used in the NCSU models, which was based on laboratory analysis of our collected soil samples, was lower. Our measured Falls Lake TP concentrations were on the lower end of the spectrum when compared to other measured values from North Carolina and Virginia (Figure 60 in Appendix H).

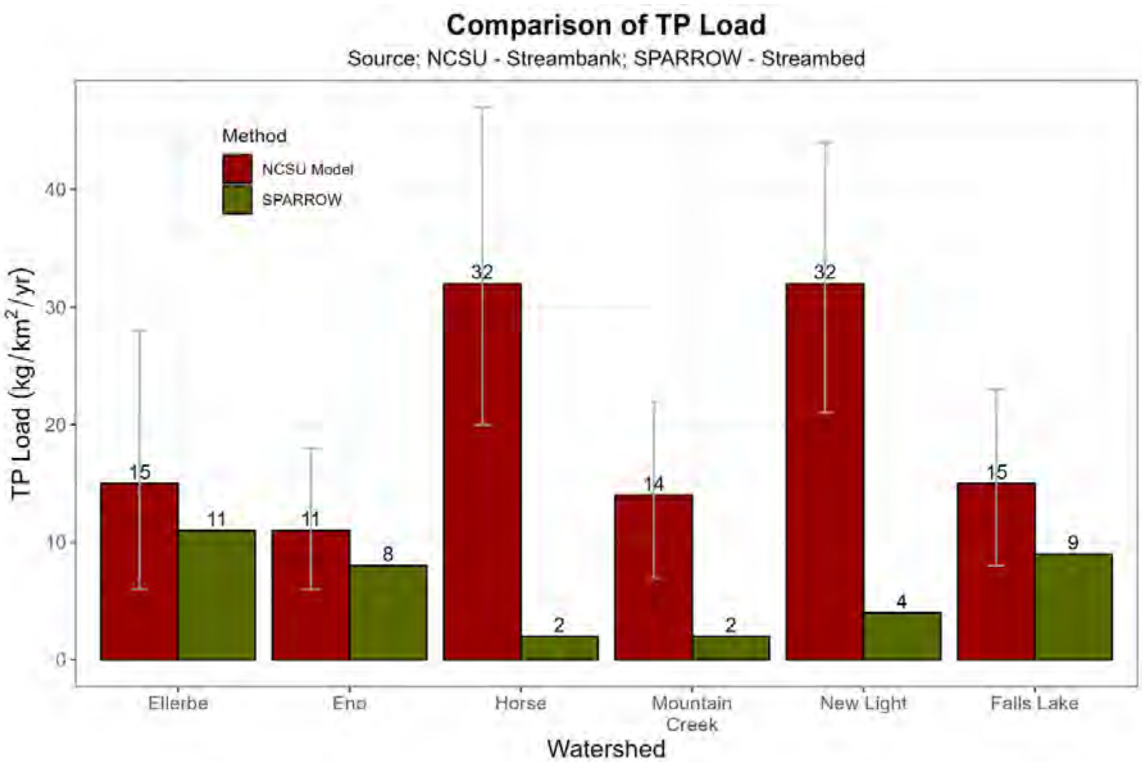

Figure 20. Comparing incremental TP loads from streambank erosion for Falls Lake and subwatersheds.

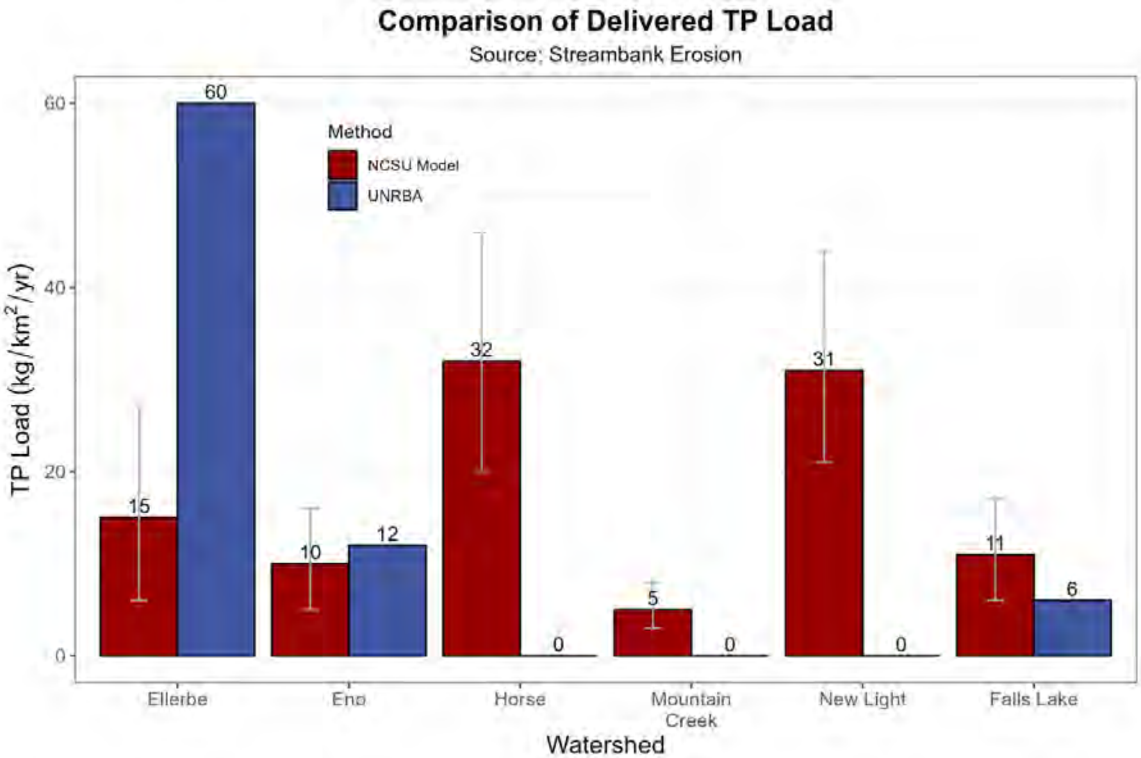

Figure 21. Comparing delivered TP loads from streambank erosion for Falls Lake and subwatersheds.

Floodplain deposition was found to have a far greater contribution to nutrient loads despite a relatively small contribution to total sediment loads (Noe et al., 2022). It would be important to consider the impacts of floodplain deposition on both sediment and nutrient transport to represent delivered loads more accurately. Ellerbe Creek had the highest TN and TP loading rates for UNRBA from streambank erosion, and the highest TP load from all sources estimated from all four methods. However, there is a large wastewater treatment plant upstream of the sampling location. Mountain Creek showed the greatest variability for LOADEST/WRTDS method, but this was likely the result of a longer period of record that ranged from 1996 to 2014. Ellerbe and Eno only had five years of data for the LOADEST method but this was longer than the one year monitoring period for our project. In Figure 22, the estimate from the turbidity regressions fell along the lower limit from the LOADEST/WRTDS method indicating the conditions during our year of monitoring were similar to the drier years in the LOADEST/WRTDS model. From the figures in Appendix B, we can see there were no large storm events during the monitoring period. The turbidity monitoring appears to be predicating reasonable values for TP from streambank erosion for Horse and New Light creeks (Figure 22). The rest of the NCSU turbidity monitoring appears to underestimate TP due to lower flows than other years.

The percentage of TP load from streambank erosion was closest between NCSU and UNRBA for Ellerbe and Eno (Figure 23). Similar percentages of phosphorus and nitrogen from streambank erosion were reported for a modeled study in Chesapeake Bay at 21% and 5% respectively.

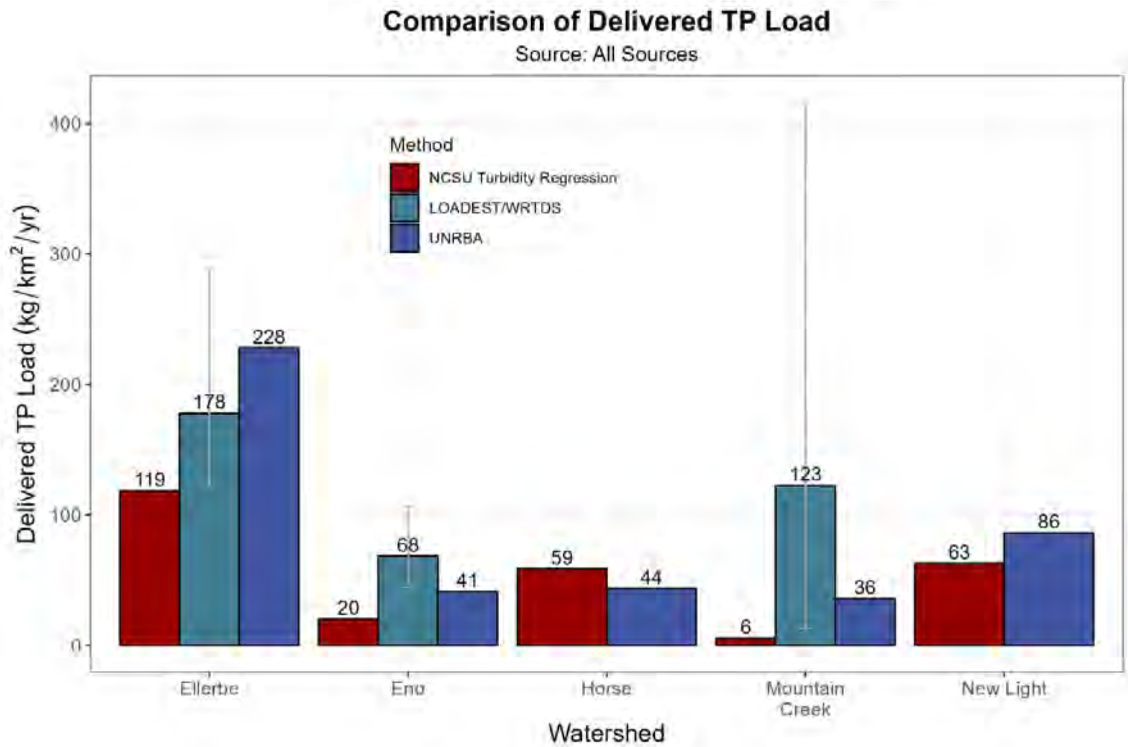

Figure 22. Comparing TP loads from all sources for Falls Lake and 5 subwatersheds.

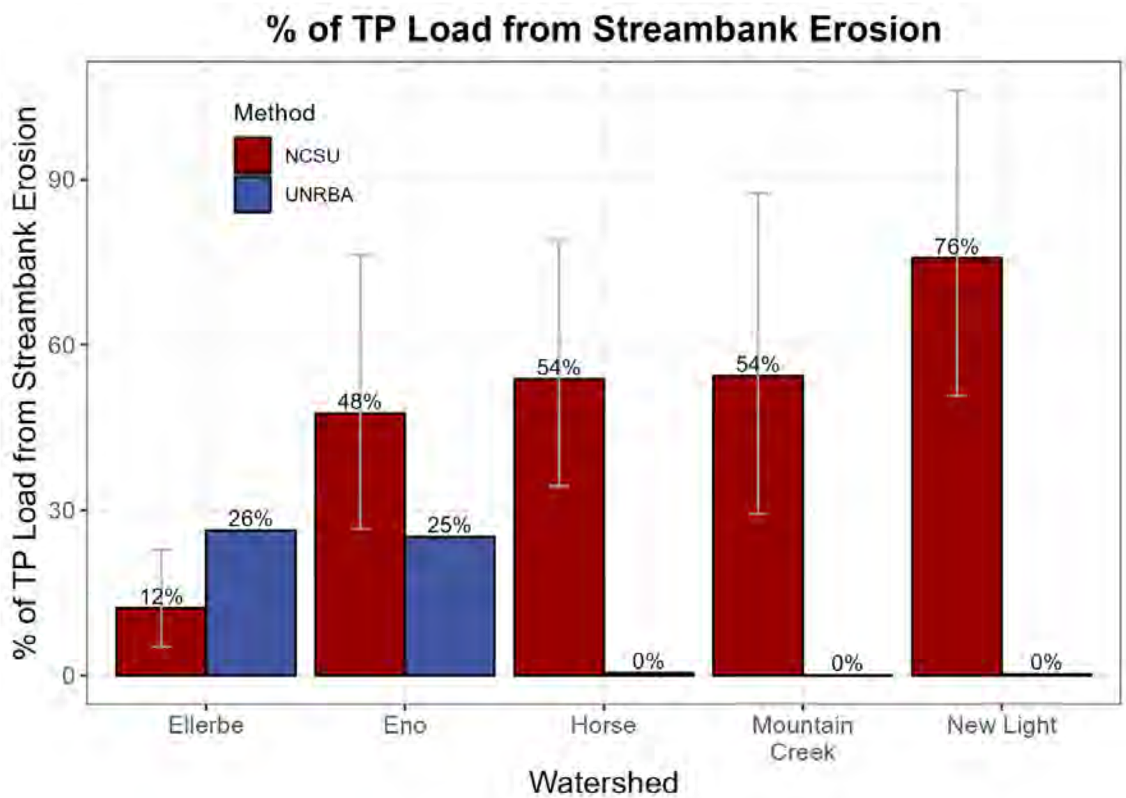

Figure 23. The percentage of TP from streambank erosion for five study watersheds. The NCSU percentage was calculated by dividing the NCSU model results by the NCSU turbidity results.

For Falls Lake, the UNRBA estimate for TN from streambank erosion was much lower than the NCSU model result due to our model's overestimation of sediment load (Figure 24). UNRBA results showed streambank erosion only contributed 0.8% of the TN load. Using the UNRBA TN load from all sources, the NCSU model still only estimated 6% of the load came from streambank erosion (Figure 25). Subsequently, we can conclude that streambank erosion was not a significant source of TN. However, the NCSU model predicted a significantly higher amount of TN for three of the five study watersheds: Horse, Mountain Creek and New Light. The UNRBA TN estimates do not fall within the NCSU model limits for any of the watersheds. This could be in part of how the measured TN concentration from soil samples were applied across the watershed to estimate NCSU model TN load.

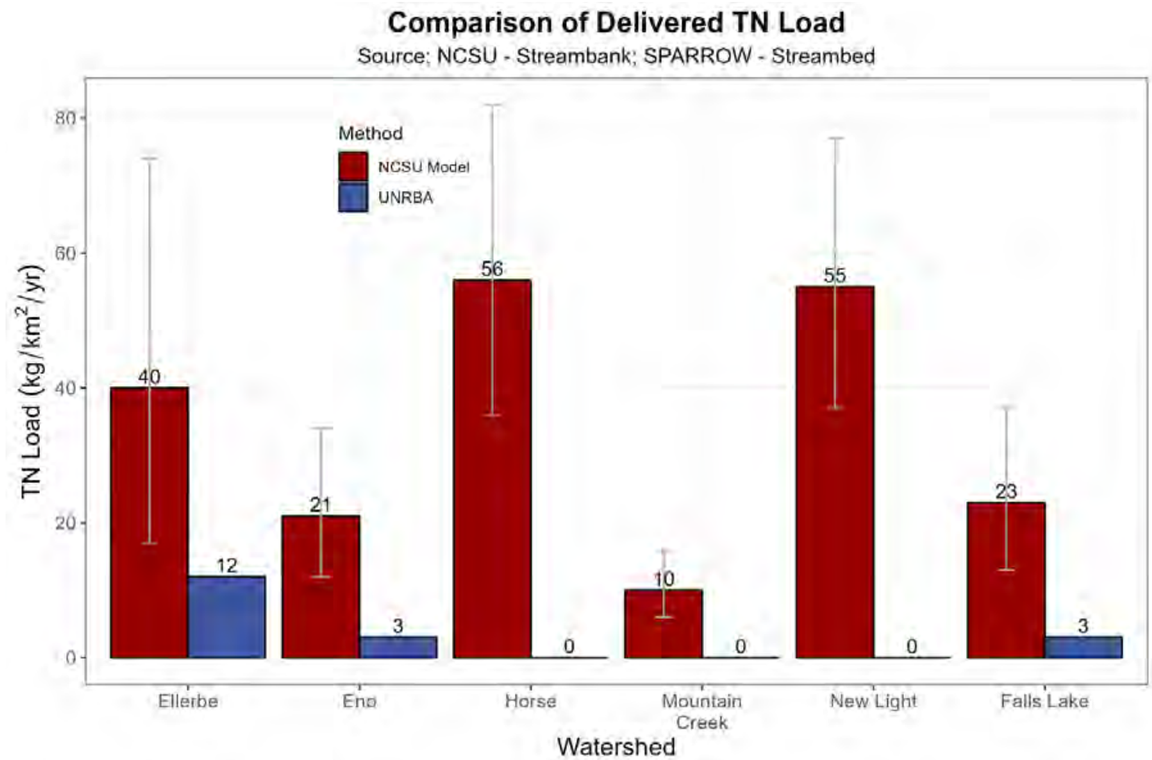

Figure 24. TN load estimates from streambank erosion for Falls Lake watershed and subwatersheds.

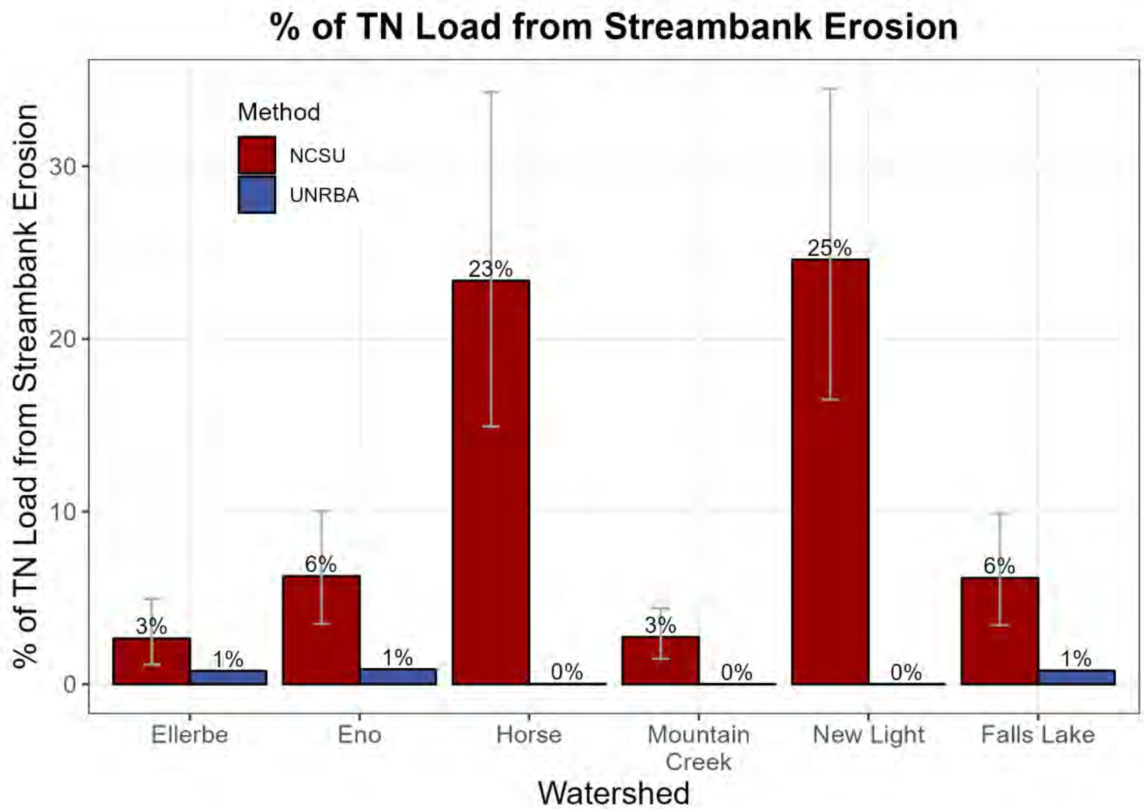

Figure 25. Percentage of TN from streambank erosion for five study watersheds. The NCSU percentage was calculated by dividing the NCSU model results by the UNRBA TN load from all sources.

The UNRBA model estimates for TN from all sources fell within the lower and upper limits for Ellerbe and Mountain Creek watersheds with LOADEST/WRTDS estimates (Figure 26). Despite the UNRBA model simulating the period as LOADEST (2014-2018), the UNRBA model appeared to overestimate TN from the Eno watershed.

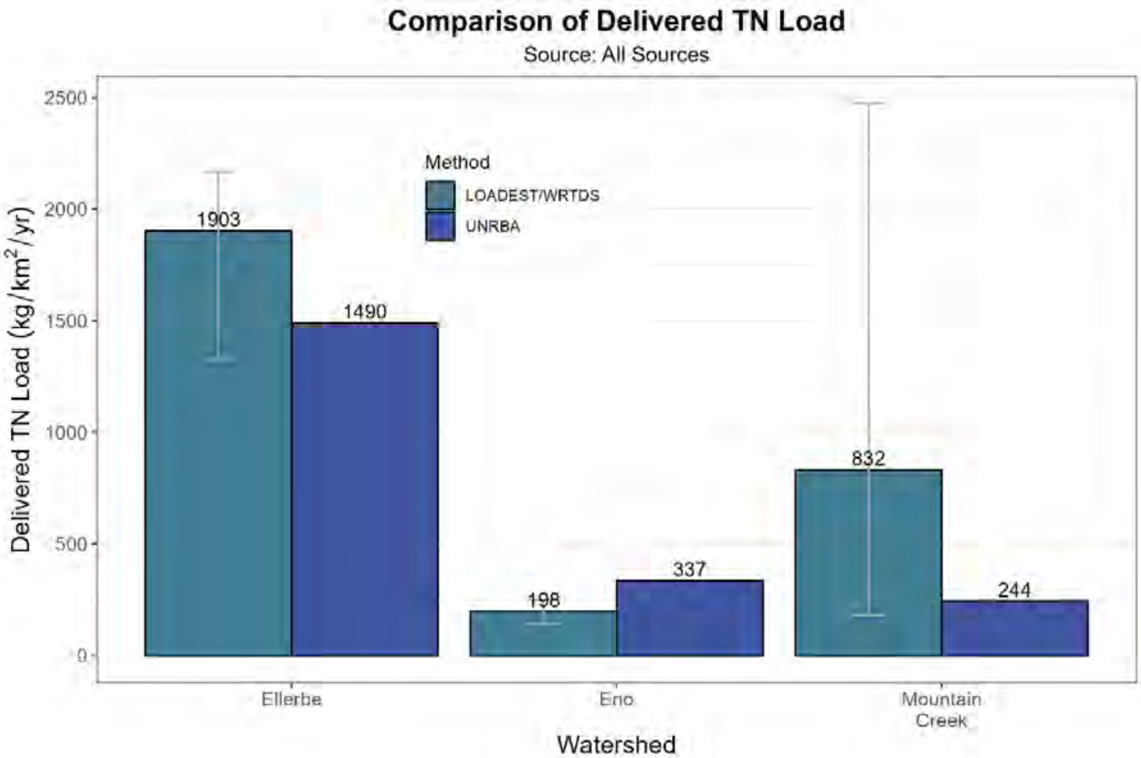

Figure 26. TN load estimates from all sources for three subwatersheds.

Conclusions & Recommendations

Geospatial analyses, inventory of streambank condition, assessment of streambank erosion rates, analysis of nutrient levels in streambank soils, field-based water quality monitoring and extensive statistical analyses were conducted to estimate the potential nutrient loads from eroding streambanks upstream of Falls Lake. Locations of expected erosion were mapped (Figure 27) and predicted rates of erosion and streambank height were used to estimate total sediment and nutrient loads for five study subwatersheds and for Falls Lake. Modeled loads were then compared to estimates of sediment and nutrient loading from the USGS NC SPARROW and UNRBA models.

For a period of one year, five study watersheds were monitored for flow and water quality. Strong correlation between turbidity and TSS and TP were observed. Pollutant loads of TSS and TP were developed from this sampling campaign. The loadings were used to estimate the total proportion of predicted streambank erosion loads to observed TSS and TP loads, which also included land-based sources of sediment. Loads were also compared to SPARROW and UNRBA total loads and to long-term loads calculated based on past USGS water quality monitoring at three gauged locations.

Our model-predicted range of sediment loads were substantially larger than the SPARROW predictions for streambed erosion and UNRBA predictions for streambank erosion. Our lower and upper limits were almost 10 to nearly 40 times greater than the SPARROW estimate. The NCSU model loads were also higher than the UNRBA delivered load, with our lower limit almost 4 times the UNRBA estimate for Falls Lake. Despite our overestimate of TSS load from streambanks, The SPARROW TP load for Ellerbe, Eno and Falls Lake fell within the NCSU range. UNRBA TP from streambanks for all of Falls Lake was about the same to 3 times smaller than our TP estimates for the lower and upper limits, respectively. Our TN delivered estimate was 8 times larger than the UNRBA load. SPARROW does not include an estimate of TN from streambed/bank erosion. When comparing the proportion of sediment and nutrient loads from streambank erosion for the five study subwatersheds, our estimates for Ellerbe and Eno were closer to UNRBA and SPARROW. However, our estimates for Horse, Mountain and New Light were substantially larger with UNRBA, which estimated nearly 0 for the sediment and nutrient loads.

Examining TSS from all sources, NCSU turbidity and UNRBA estimates were similar to the longer-term estimates from LOADEST/WRTDS for Ellerbe and Eno. The NCSU TP loads from all sources were all on the lower end of the range of TP estimated from the long-term USGS data (LOADEST/WRTDS). UNRBA estimates of TN from all sources fell on the lower range of values from the LOADEST/WRDTS estimate for Ellerbe and Mountain Creek while UNRBA overestimated TN in the Eno watershed.

UNRBA and SPARROW both estimated approximately 30% of all sediments delivered to the lake comes from unstable stream reaches and that these streams contribute between 14.5 to 16% of the total TP load but only 0.8% of the TN load (UNRBA only). Streambank erosion is likely a significant source of sediment and TP loads and reducing streambank erosion could reduce TSS and TP loads to the lake. The maps below show our model estimated amount of sediment, TN and TP likely contributed from streambank erosion (figures 28-30). These results indicate that several catchments in the Horse and New Light subwatersheds located in the far eastern portion (Wake and Granville County) of the Falls Lake watershed are likely contributing higher volumes of sediment and nutrients to the lake than basins located further west and north. The areas with higher sediment loads also tended to be more developed like Wake and Durham County. Wake County is projected to nearly double the number of households from 2000 to 2025 (UNRBA, 2019). As seen in Figure 31, the streams in Wake and Granville County have bank heights at least 2 times higher than the bankfull height indicating incision and likely active erosion. These areas could be targeted for restoration and/or streambank repair and enhancement activities.

Restoration efforts have been shown to successfully improve bank stabilization and prevent sloughing and further incision of the channel (Selvakumar et al., 2010). Bank stabilization efforts focused on protecting the bank toe-region have been shown to reduce erosion by 90% (Simon et al., 2009). And simulations by Lammers and Bledsoe (2017) indicated that streambank stabilization could provide the greatest potential for the prevention/removal of TP (609 kg P/km/yr) over other restoration practices. These restoration activities could also afford other habitat and water quality related benefits. Detailed economic analysis is recommended to compare the cost of repairing these streams or their eroding streambanks against reducing other sources of sediment and associated phosphorus to optimize any investments targeted are reducing negative impacts to the water quality of Falls Lake. Future steps could be taken to field validate and improve the models developed by our study. The erosion classification model was the poorest performing model, likely due to the spatial distribution of the data used to build the model. As seen from the flow data, relatively few storms occurred during the monitoring period, and the NCSU sediment estimates were on the low end of the LOADEST estimates that spanned several years. Streambank erosion is highly variable and episodic in nature (Daly et al., 2015; Midgley et al., 2012; Zhao et al., 2022), therefore it could be years before a significant amount of the bank erodes. To fully capture the range of flow conditions (dry, wet and extreme events) long-term monitoring of erosion rates is required. Adding additional cross-sections, especially for minor erosion, will fill in the missing gaps in the current models. Further exploring delivery ratios could provide better insight into the sediment transport and dynamics within the watershed. To better understand the transport capacity of streams, sediment grain size analysis of bank material is recommended as sand is more likely to be deposited within the channel whereas fines (silt and clay) have a much higher chance of reaching Falls Lake.

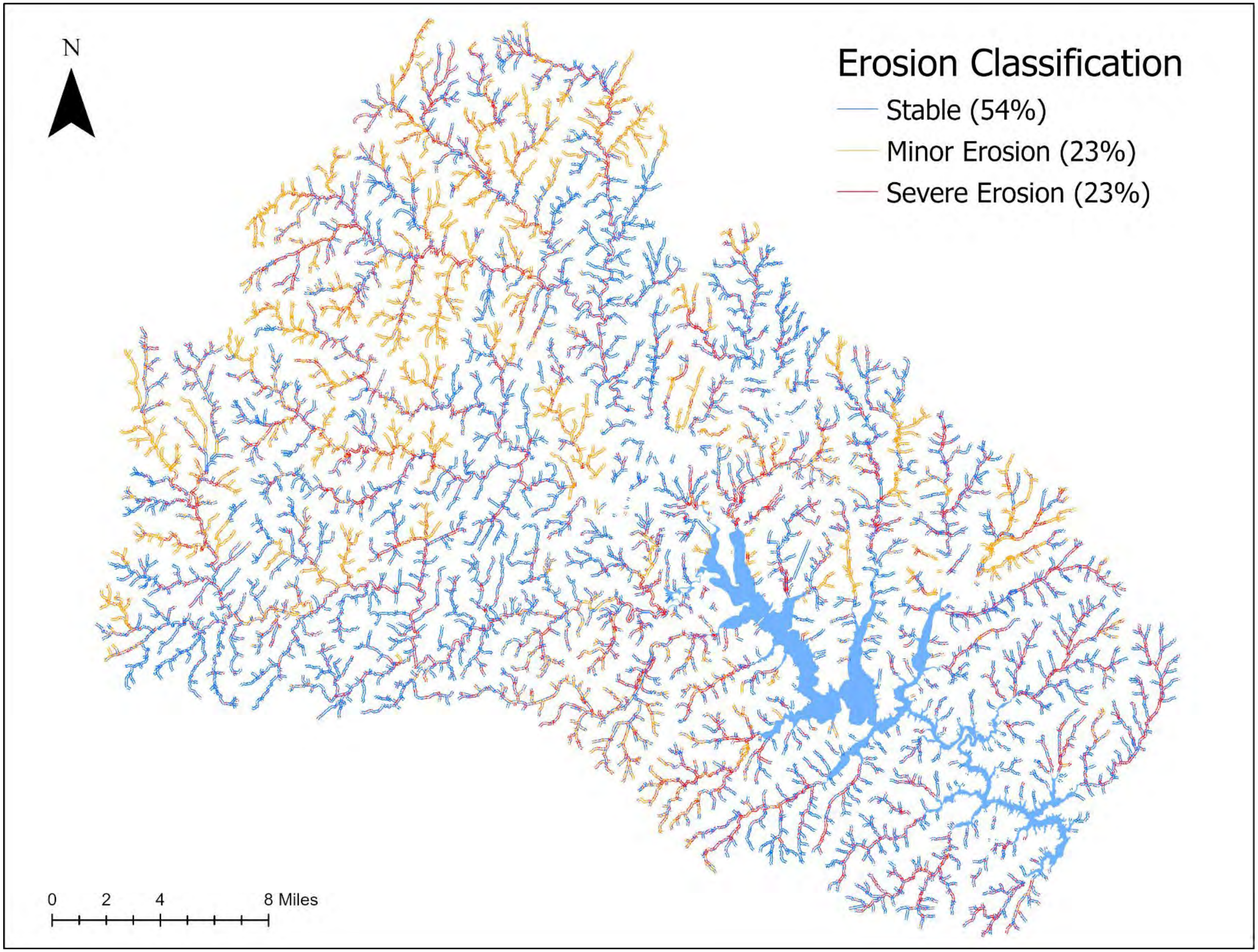

Figure 27. Map of severity of streambank erosion.

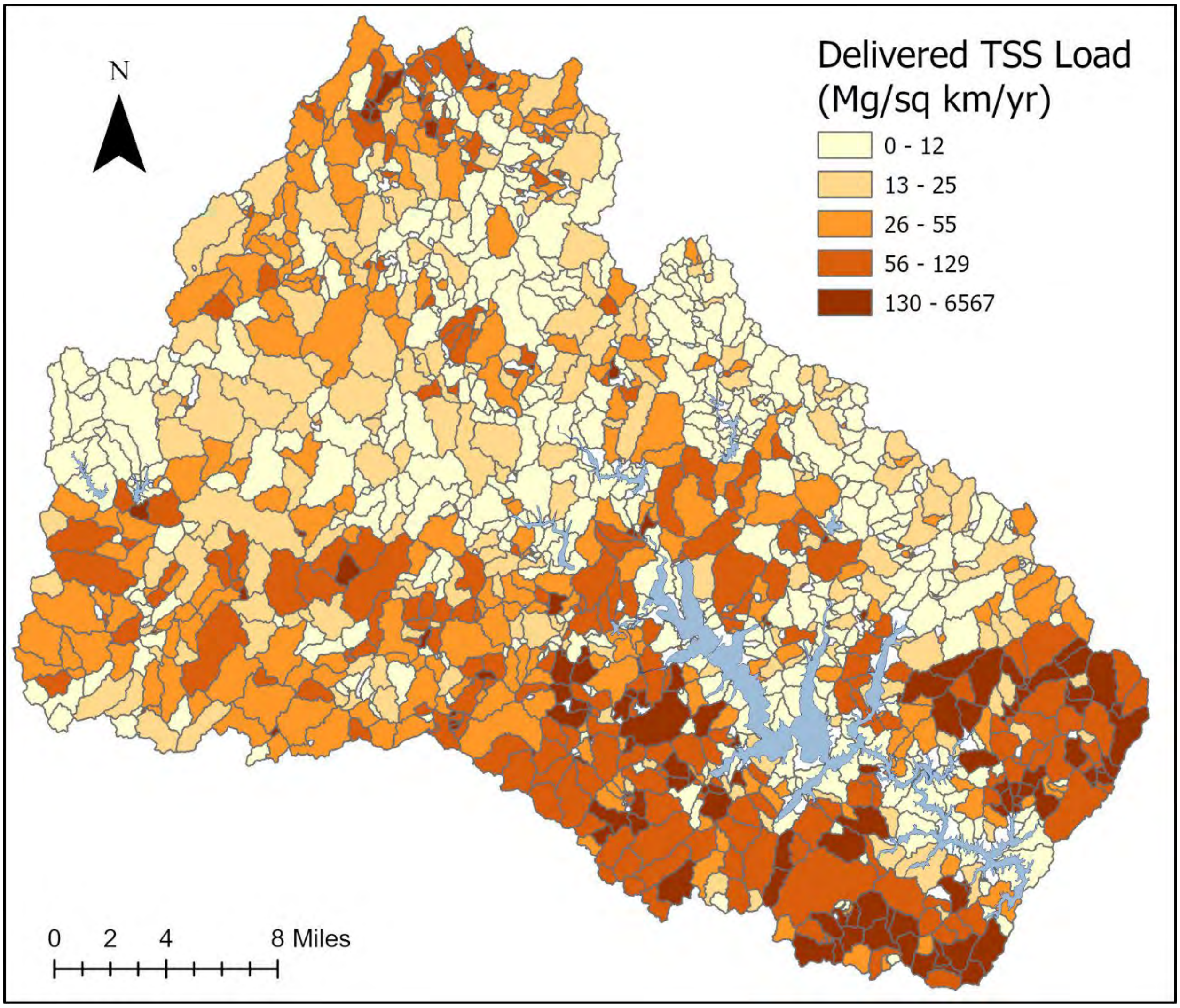

Figure 28. Delivered annual sediment load for each catchment estimated from NCSU model.

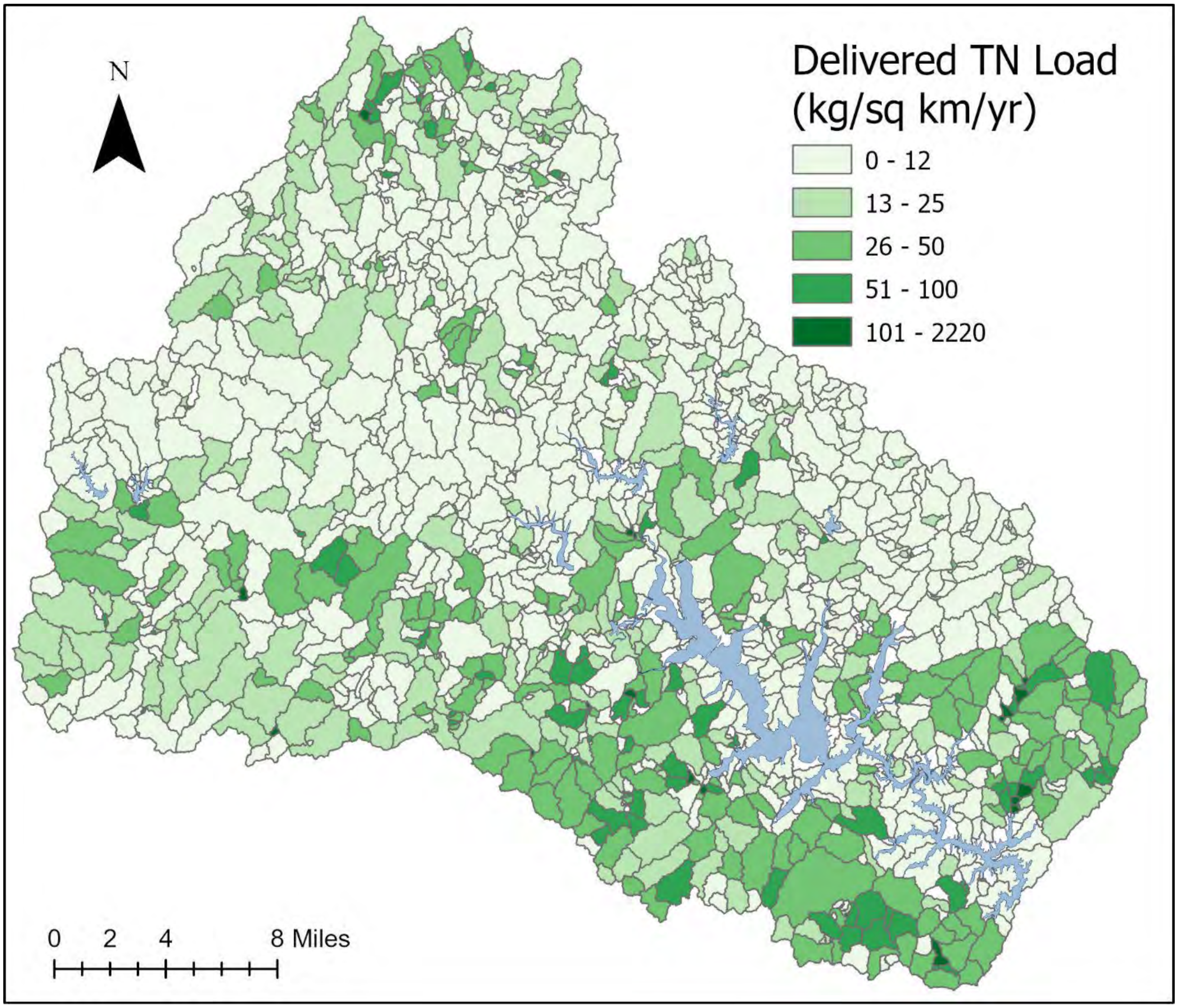

Figure 29. Delivered annual TN load for each catchment estimated from NCSU model.

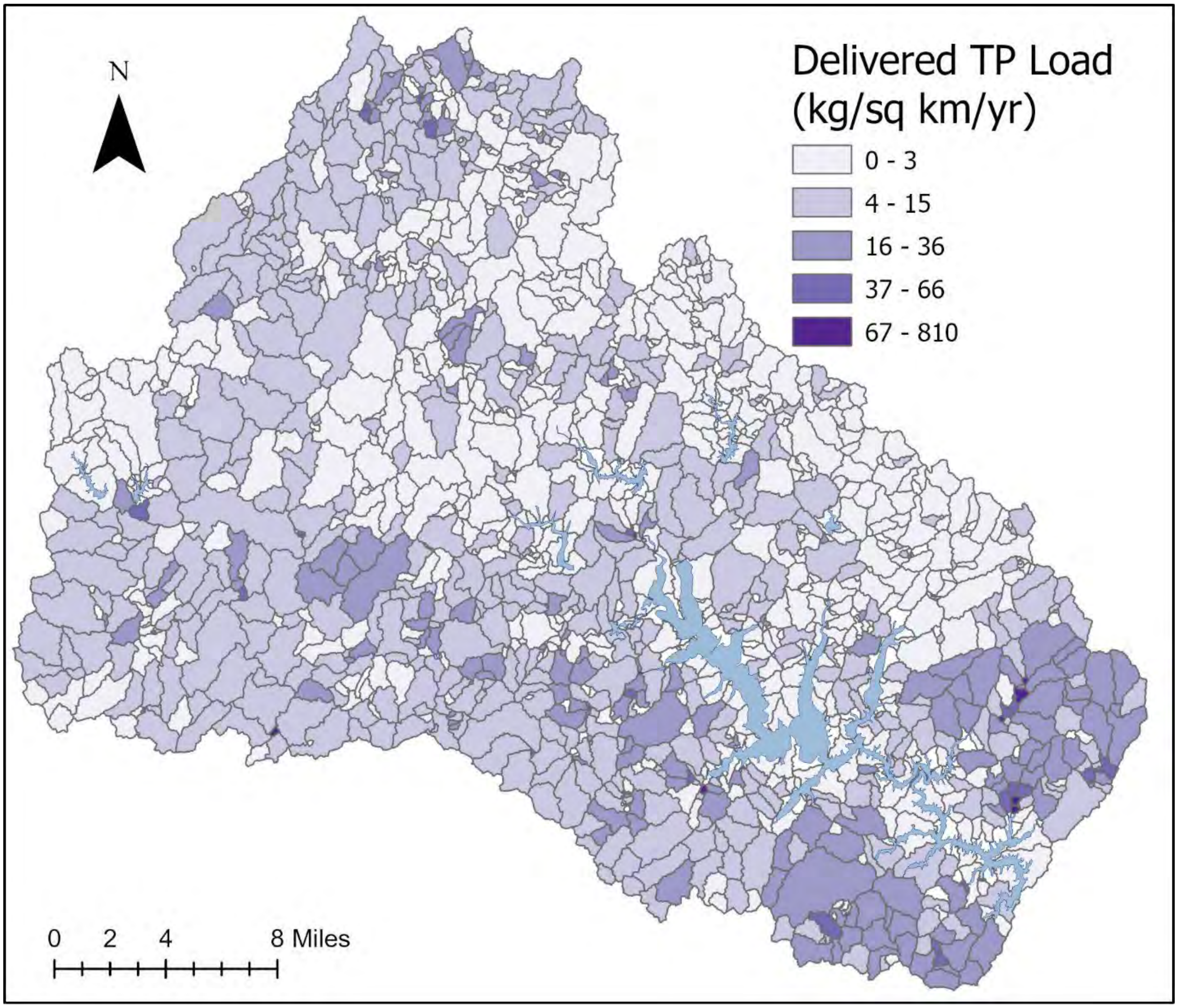

Figure 30. Delivered annual TP load for each catchment estimated from NCSU model.

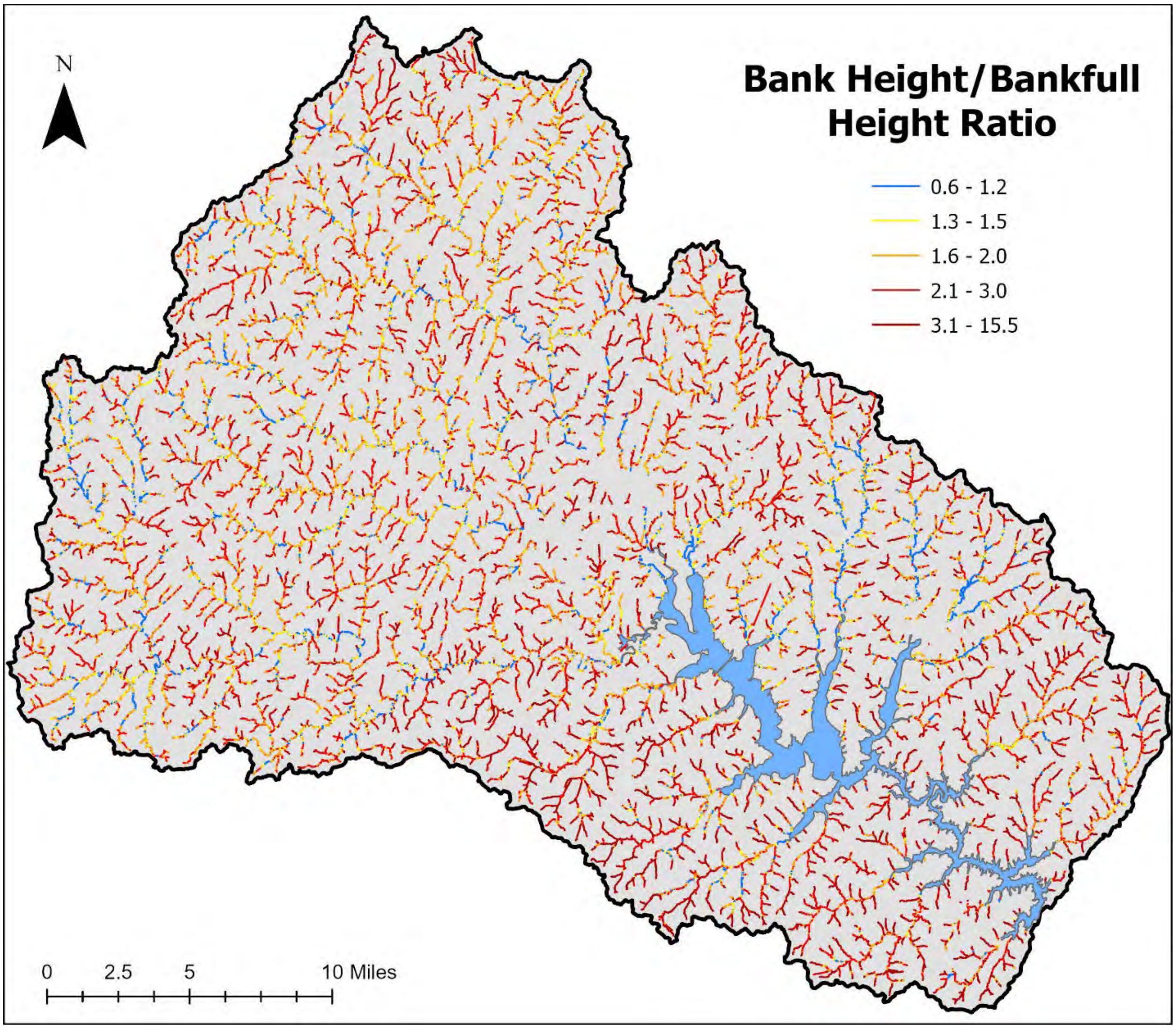

Figure 31. Map of predicted bank height to bankfull height ratio. The bankfull height was estiamted from the NC rural Piedmont curve.

References

Allmendinger, N. E., Pizzuto, J. E., Moglen, G. E., Lewicki, M. (2007). A Sediment Budget for an Urbanizing Watershed, 1951-1996, Montgomery County, Maryland, U.S.A.1: A Sediment Budget for an Urbanizing Watershed, 1951-1996, Montgomery Co., Maryland, U.S.A. *JAWRA Journal of the American Water Resources Association*, *43*(6), 1483–1498. https://doi.org/10.1111/j.1752-1688.2007.00122.x

Boothroyd, R. J., Williams, R. D., Hoey, T. B., Barrett, B., Prasojo, O. A. (2021). Applications of Google Earth Engine in fluvial geomorphology for detecting river channel change. *WIREs Water*, *8*(1). https://doi.org/10.1002/wat2.1496

Coe, D. (2019). Creating REMs in QGIS with the IDW Method. Retrieved from https://dancoecarto.com/creating-rems-in-qgis-the-idw-method

D. N. Moriasi, J. G. Arnold, M. W. Van Liew, R. L. Bingner, R. D. Harmel, T. L. Veith. (2007). Model Evaluation Guidelines for Systematic Quantification of Accuracy in Watershed Simulations. *Transactions of the ASABE*, *50*(3), 885–900. https://doi.org/10.13031/2013.23153

Daly, E. R., Miller, R. B., Fox, G. A. (2015). Modeling streambank erosion and failure along protected and unprotected composite streambanks. *Advances in Water Resources*, *81*, 114–127. https://doi.org/10.1016/j.advwatres.2015.01.004

Doll, B. A., Wise-Frederick, D. E., Buckner, C. M., Wilkerson, S. D., Harman, W. A., Smith, R. E., Spooner, J. (2002). HYDRAULIC GEOMETRY RELATIONSHIPS FOR URBAN STREAMS THROUGHOUT THE PIEDMONT OF NORTH CAROLINA. *Journal of the American Water Resources Association*, *38*(3), 641–651. https://doi.org/10.1111/j.1752-1688.2002.tb00986.x

DWER. (2000). Sediment in streams. Retrieved July 7, 2020, from https://www.water.wa.gov.au/water-topics/waterways/managing-our-waterways2/water-notes

El-Khoury, L. (2022, October 27). *Validating Positive Openness Raster Data for Indicating Locations of Streambed Incision and Streambank Erosion*. North Carolina State University. Retrieved from https://www.lib.ncsu.edu/resolver/1840.20/40156

Fine, J. M., Harned, D. A., Oblinger, C. J. (2013). *Water-Quality Characteristics, Trends, and Nutrient and Sediment Loads of Streams in the Treyburn Development Area, North Carolina, 1988–2009* (No. Scientific Investigations Report 2013-5062). Reston, VA: USGS.

Florsheim, J. L., Mount, J. F., Chin, A. (2008). Bank Erosion as a Desirable Attribute of Rivers. *BioScience*, *58*(6), 519–529. https://doi.org/10.1641/B580608

Fox, G. A., Purvis, R. A., Penn, C. J. (2016). Streambanks: A net source of sediment and phosphorus to streams and rivers. *Journal of Environmental Management*, *181*, 602–614. https://doi.org/10.1016/j.jenvman.2016.06.071

Gage, M. S., Spivak, A., Paradise, C. J. (2004). Effects of Land Use and Disturbance on Benthic Insects in Headwater Streams Draining Small Watersheds North of Charlotte, NC.

Southeastern Naturalist, *3*(2), 345–358. https://doi.org/10.1656/1528-7092(2004)003[0345:EOLUAD]2.0.CO;2

Gamble, R. S. (2021, June 12). *Evaluating Streambank Retreat Prediction Using the BANCS Model in the Valley and Ridge Physiographic Province* (Thesis). Virginia Tech. Retrieved from https://vtechworks.lib.vt.edu/bitstream/handle/10919/103819/Gamble_RS_T_2021.pdf?sequence=1&isAllowed=y

Gellis, A.C., Myers, M. K., Noe, G. B., Hupp, C. R., Schenk, E. R., Myers, L. (2017). Storms, channel changes, and a sediment budget for an urban-suburban stream, Difficult Run, Virginia, USA. *Geomorphology*, *278*, 128–148. https://doi.org/10.1016/j.geomorph.2016.10.031

Gellis, Allen C., Noe, G. B. (2013). Sediment source analysis in the Linganore Creek watershed, Maryland, USA, using the sediment fingerprinting approach: 2008 to 2010. *Journal of Soils and Sediments*, *13*(10), 1735–1753. https://doi.org/10.1007/s11368-013-0771-6

Haefner, J. W. (2005). *Modeling Biological Systems: Principles and Applications*. Boston, MA: Springer US. https://doi.org/10.1007/b106568

Hesterberg, D. (2010). Macroscale Chemical Properties and X-Ray Absorption Spectroscopy of Soil Phosphorus. In *Developments in Soil Science* (Vol. 34, pp. 313–356). Elsevier. https://doi.org/10.1016/S0166-2481(10)34011-6

Hohenthal, J., Alho, P., Hyyppä, J., Hyyppä, H. (2011). Laser scanning applications in fluvial studies. *Progress in Physical Geography: Earth and Environment*, *35*(6), 782–809. https://doi.org/10.1177/0309133311414605

Hopkins, K. G., Noe, G. B., Franco, F., Pindilli, E. J., Gordon, S., Metes, M. J., … Hogan, D. M. (2018). A method to quantify and value floodplain sediment and nutrient retention ecosystem services. *Journal of Environmental Management*, *220*, 65–76. https://doi.org/10.1016/j.jenvman.2018.05.013

Hopkins, K. G., Welles, J. S., Pindilli, E. J., Noe, G. B., Claggett, P. R., Ahmed, L., Metes, M. J. (2023). Societal benefits of floodplains in the Chesapeake Bay and Delaware River watersheds: Sediment, nutrient, and flood regulation ecosystem services. *Journal of Environmental Management*, *345*, 118747. https://doi.org/10.1016/j.jenvman.2023.118747

Hupp, C. R., Noe, G. B., Schenk, E. R., Benthem, A. J. (2013). Recent and historic sediment dynamics along Difficult Run, a suburban Virginia Piedmont stream. *Geomorphology*, *180–181*, 156–169. https://doi.org/10.1016/j.geomorph.2012.10.007

Inamdar, S., Sienkiewicz, N., Lutgen, A., Jiang, G., Kan, J. (2020). Streambank Legacy Sediments in Surface Waters: Phosphorus Sources or Sinks? *Soil Systems*, *4*(2), 30. https://doi.org/10.3390/soilsystems4020030

Kronvang, B., Audet, J., Baattrup-Pedersen, A., Jensen, H. S., Larsen, S. E. (2012). Phosphorus Load to Surface Water from Bank Erosion in a Danish Lowland River Basin. *Journal of Environmental Quality*, *41*(2), 304–313. https://doi.org/10.2134/jeq2010.0434

Lammers, R. W., Bledsoe, B. P. (2019). Quantifying pollutant loading from channel sources: Watershed-scale application of the River Erosion Model. *Journal of Environmental Management*, *234*, 104–114. https://doi.org/10.1016/j.jenvman.2018.12.074

Lenhart, C. F., Smith, D. J., Lewandowski, A., Belmont, P., Gunderson, L., Nieber, J. L. (2018). Assessment of Stream Restoration for Reduction of Sediment in a Large Agricultural Watershed. *Journal of Water Resources Planning and Management*, *144*(7), 04018032. https://doi.org/10.1061/(ASCE)WR.1943-5452.0000908

Line, D. E. (2013). Effect of development on water quality for seven streams in North Carolina. *Environmental Monitoring and Assessment*, *185*(8), 6277–6289. https://doi.org/10.1007/s10661-012-3024-z

Matos, A. (2014, December 15). UNRBA Nutrient Credits Project, Task 1.1, Watershed Trapping Analysis. Memorandum.

Midgley, T. L., Fox, G. A., Heeren, D. M. (2012). Evaluation of the bank stability and toe erosion model (BSTEM) for predicting lateral retreat on composite streambanks. *Geomorphology*, *145–146*, 107–114. https://doi.org/10.1016/j.geomorph.2011.12.044

Noe, G. B., Hopkins, K. G., Claggett, P. R., Schenk, E. R., Metes, M. J., Ahmed, L., … Hupp, C. R. (2022). Streambank and floodplain geomorphic change and contribution to watershed material budgets. *Environmental Research Letters*, *17*(6), 064015. https://doi.org/10.1088/1748-9326/ac6e47

OCM Partners. (2023). *North Carolina Statewide Lidar DEM 2015 Phase 3 from 2010-06-15 to 2010-08-15* [Data set]. NOAA National Centers for Environmental Information. Retrieved from https://www.fisheries.noaa.gov/inport/item/49413

Palmer, J. A., Schilling, K. E., Isenhart, T. M., Schultz, R. C., Tomer, M. D. (2014). Streambank erosion rates and loads within a single watershed: Bridging the gap between temporal and spatial scales. *Geomorphology*, *209*, 66–78. https://doi.org/10.1016/j.geomorph.2013.11.027

Purvis, R. A., Fox, G. A. (2016). Streambank sediment loading rates at the watershed scale and the benefit of riparian protection: Streambank Sediment Loading Rates at the Watershed Scale. *Earth Surface Processes and Landforms*, *41*(10), 1327–1336. https://doi.org/10.1002/esp.3901

Relative Elevation Model in ArcGIS Pro. (2022). [Video]. Ersi. Retrieved from https://mediaspace.esri.com/media/t/1_pn5ltf54

Rowley, T. H., Hopkins, K. G., Terziotti, S. (2018). *Geomorphological Features of North Carolina* [Data set]. U.S. Geological Survey. https://doi.org/10.5066/P9PRAVAQ

Runkel, R. L., Crawford, C. G., Cohn, T. A. (2004). *Load Estimator (LOADEST): A FORTRAN program for estimating constituent loads in streams and rivers* (Techniques and Methods No. No. 4-A5).

Schaffrath, K. R., Belmont, P., Wheaton, J. M. (2015). Landscape-scale geomorphic change detection: Quantifying spatially variable uncertainty and circumventing legacy data issues. *Geomorphology*, *250*, 334–348. https://doi.org/10.1016/j.geomorph.2015.09.020

Sekely, A. C., D.J. Mulla, Bauer, D. W. (2002). Streambank slumping and its contribution to the phosphorus and suspended sediment loads of the Blue Earth River, Minnesota. *Journal of Soil and Water Conservation*, *57*(5), 243–250.

Selvakumar, A., O'Connor, T. P., Struck, S. D. (2010). Role of Stream Restoration on Improving Benthic Macroinvertebrates and In-Stream Water Quality in an Urban Watershed: Case Study. *Journal of Environmental Engineering*, *136*(1), 127–139. https://doi.org/10.1061/(ASCE)EE.1943-7870.0000116

Simon, A., Pollen-Bankhead, N., Mahacek, V., Langendoen, E. (2009). Quantifying Reductions of Mass-Failure Frequency and Sediment Loadings From Streambanks Using Toe Protection and Other Means: Lake Tahoe, United States. *JAWRA Journal of the American Water Resources Association*, *45*(1), 170–186. https://doi.org/10.1111/j.1752-1688.2008.00268.x

Stott, T. (1997). A comparison of stream bank erosion processes on forested and moorland streams in the Balquhidder Catchments, central Scotland. *Earthh Surface Processes and Landforms*, *22*(4), 383–399.

Topcon. (2016). GT Series Robotic Total Station. Topcon Corporation. Retrieved from https://www.topconpositioning.com/sites/default/files/product_files/gt_series_broch_7010_2214_revb_sm.pdf

UNRBA. (2019). Upper Neuse River Basin Association. Retrieved from https://unrba.org/about-unrb

Upper Neuse River Basin Association. (2019). *Final UNRBA Monitoring Report for Supporting the Re-Examination of the Falls Lake Nutrient Management Strategy*. Retrieved from https://unrba.org/sites/default/files/UNRBA%202019%20Annual%20Report%20Final.pdf

U.S. EPA. (2017). *National Water Quality Inventory: Report to Congress* (No. 841- R-16– 011).

USEPA. (2017). *National Water Quality Inventory: Report to Congress (No. 841- R-16– 011)*.

USGS. (2018). NC Water-Quality Model Mapper. Retrieved from https://www2.usgs.gov/water/southatlantic/nc/projects/sparrow/

USGS. (2021). *USGS Land Change Monitoring, Assessment, and Projection Dataset* [Data set]. LCMAP Viewer. Retrieved from https://eros.usgs.gov/lcmap/viewer/index.html

USGS. (n.d.). StreamStats Streamflow Statistics and Spatial Analysis Tools for Water-Resources Applications.

Voli, M. T., Wegmann, K. W., Bohnenstiehl, D. R., Leithold, E., Osburn, C. L., Polyakov, V. (2013). Fingerprinting the sources of suspended sediment delivery to a large municipal drinking water reservoir: Falls Lake, Neuse River, North Carolina, USA. *Journal of Soils and Sediments*, *13*(10), 1692–1707. https://doi.org/10.1007/s11368-013-0758-3

Wallach, D., Makowski, D., Jones, J. W. (2006). *Working with dynamic crop models: evaluation, analysis, parameterization, and applications*. Amsterdam: Elsevier.

Walling, D. E., Collins, A. L. (2008). The catchment sediment budget as a management tool. *Environmental Science & Policy*, *11*(2), 136–143. https://doi.org/10.1016/j.envsci.2007.10.004

Wohl, E., Bledsoe, B. P., Jacobson, R. B., Poff, N. L., Rathburn, S. L., Walters, D. M., Wilcox, A. C. (2015). The Natural Sediment Regime in Rivers: Broadening the Foundation for Ecosystem Management. *BioScience*, *65*(4), 358–371. https://doi.org/10.1093/biosci/biv002

Wolter, C. F., Schilling, K. E., Palmer, J. A. (2021). Quantifying the Extent of Eroding Streambanks in Iowa. *JAWRA Journal of the American Water Resources Association*, *57*(3), 391–405. https://doi.org/10.1111/1752-1688.12902

Yen, K. S., Ravani, B., Lasky, T. A. (2011). *LiDAR for Data Efficiency* (No. WA-RD 778.1). University of Carlifornia at Davis.

Yokoyama, R. (2002). Visualizing Topography by Openness:A New Application of Image Processing to Digital Elevation Models. *PHOTOGRAMMETRIC ENGINEERING*, *68*(3), 9.

Zhang, Q., Hirsch, R. M. (2019). River Water-Quality Concentration and Flux Estimation Can be Improved by Accounting for Serial Correlation Through an Autoregressive Model. *Water Resources Research*, *55*(11), 9705–9723. https://doi.org/10.1029/2019WR025338

Zhao, K., Coco, G., Gong, Z., Darby, S. E., Lanzoni, S., Xu, F., … Townend, I. (2022). A Review on Bank Retreat: Mechanisms, Observations, and Modeling. *Reviews of Geophysics*, *60*(s), 51.

Appendices

Appendix A - Literature Review

Sources of Sediment and Nutrients in Streams

In some watersheds, streambank erosion can be the most significant process contributing to in-stream sediment loads (Stott, 1997). Eleven studies reviewed by Purvis and Fox (2016) reported that eroding streambanks contributed 17 to 92% of total sediment loads. Similarly, Palmer (2014) reported that eroded streambanks can contribute as much as 51% of the annual sediment load. Gellis and Noe (2013) found that both streambank erosion and agricultural land use were the greatest contributors to the sediment load in Linganore Creek, an agricultural watershed in Maryland. Lenhart et al. (2018), however, found that sediment loads from streambank erosion exceeded loads from field erosion in an agricultural stream.

Sediment from streambanks also can serve as a dominant source of nutrient pollution. Streambank erosion due to erosive flows and channel enlargement introduce sediments, and associated bioavailable P, to downstream water bodies. These sediment inputs can contribute between 10-40% of total phosphorus load in a watershed (Fox et al., 2016; Kronvang et al., 2012; Sekely et al., 2002). The percentage of dissolved P loads from streambank erosion can increase 20-40% during a dry year compared to a wet (Kronvang et al., 2012). As a result, studies have been conducted to understand and predict the contributions of streambank and bed erosion to phosphorus concentrations in streams. Banks are more likely to serve as a source of P due to a large percentage of fines present in the material that increase the capacity to sorb P. The coarser material of streambeds allow them to serve as sinks. It was found that the fine particles in the stream have the capacity to sorb P from sewage and industrial waste and carry that P further downstream (Inamdar et al., 2020).

In simulations of the impact of various stream restoration practices on nutrient removal, Lammers and Bledsoe (2017) reported that bank stabilization provided the greatest potential for the prevention/removal of TP (609 kg P/km/yr). Selvakumar et al. (2010) conducted pre and post-restoration monitoring of an urban stream in Virginia, finding that restoration improved bank stabilization and prevented sloughing and further incision of the channel. Multiple methods can be used for bank stabilization, including engineered in-stream structures and bank armoring; however, research has shown that protecting the bank toe-region can reduce erosion by 90% (Simon et al., 2009). Inamdar et al. (2020) suggests legacy sediments have the capacity to sorb P which could be strategically used during restoration efforts. These legacy sediments could act as a sink for P if used when recreating floodplains by maintaining oxic conditions that keeps P retained.

Identifying Streambank Erosion

Opportunities to identify, monitor and predict streambank erosion remotely are becoming possible through the technological advances that have increased the accessibility, quality and amount of high-resolution topographic data. Not only has the data collection improved but also the tools that can be used to process and store all of the data allowing for more computation power (Schaffrath et al., 2015). Boothroyd et al. (2021) indicate that past fluvial geomorphology studies have been limited spatiotemporally by traditional field methods. Adding geospatial data into the fold not only allows for expansion of the spatiotemporal scale of but also enables potential site identification of problematic areas prior to any field assessments. Palmer et al. (2014) started exploring the relationship between 1-m LiDAR data and locations of severe erosions to predict severe erosion in other watersheds.

Collecting LiDAR data is expensive and most cost effective for areas larger than 20 mi^2 (Hohenthal et al., 2011). The equipment is costly and it requires advanced expertise, especially for projects that require high resolution data (Yen et al., 2011). Extensive processing is required to transform the LiDAR data into a usable state as apparent by the methodology outlined by Schaffrath et al. (2015) and Hohenthal et al. (2011). There are multiple methods to select from when transforming the data such as analytical hill-shading, sky-view factor (SFV) and openness. The intended purpose of the data will dictate the best method to use. Hill-shading is limited by using a single light that makes it hard to depict structures parallel to the light source and is best suited for visualizing objects with sharp and well-defined edges. Openness is best at representing concave surfaces, "superficially resemble[ing] digital images of shaded relief" (Yokoyama, 2002). Positive openness represents depressions where the angles are less than 90°. Another additional benefit of positive openness is a lesser degree of sensitivity to noise in the DEMs (Yokoyama, 2002).

Because of the technical difficulty and time necessary to process DEM data, the use of USGS's positive openness pre-processed data layer will save time and reduce costs. Applying the positive openness layer in analysis and interpreting the results requires less technical capabilities than creating the initial DEM from the topography data, allowing less experienced GIS users to extract information. Moving towards a world of sharing and compiling datasets and procedures could help to create a more complete and comprehensive understanding of environmental processes. Daxer (2020) outlines steps to compute openness using QGIS from a DEM. The ability to use free software to generate positive openness makes it more accessible. Applying geospatial techniques opens the possibility to examine channel processes on larger spatial scales and longer time periods to gain a better understanding of the episodic nature of streams. It could capture both short- and long-term rates of change (erosion). If the positive openness layer proves an effective tool for evaluating channel incision and instability, it could potentially be applied by state and federal natural resource agencies for prioritizing areas for restoration intervention. Refining this data, better understanding its potential and increasing its availability and understanding about its use, could also assist city and county municipalities with their stormwater, water quality and stream restoration prioritization efforts.

Quantifying Streambank Retreat and Associated Nutrient Loads

Quantifying sediment and nutrient loads from streambank erosion can be difficult to do on a large spatial scale without the use of geospatial data. Often when these loads are computed on a large watershed scale it is done with through the generalization of characteristics along large reaches. The NC SPARROW model has one reach per catchment which excludes many of the smaller headwater streams (USGS, 2018). It is rare to find a mapped spatial distribution identifying eroding streambanks at a watershed scale (Wolter et al., 2021).

Wolter et al. (2021) estimated sediment and phosphorus loads on a watershed scale based on LiDAR coupled with field verification of locations of eroding banks. The method was only applied to larger order streams (third order and higher) since many of the first and second order streams had tree canopies and overhanging vegetation obscuring the banks.

Sediment Budgets

Urbanization increases impervious surfaces, which in turn alters the hydrology of watersheds. Higher peak flows and shorter lag times generate more energy from stormwater runoff-driven flows causing channel incision and widening (Hupp et al., 2013; Wohl et al., 2015). While sediment transport naturally occurs, the system can be knocked out of equilibrium if too much sediment moved or deposited, altering the ecosystem services provided (Florsheim et al., 2008; Hupp et al., 2013). Changes to the system can be detrimental such as the degradation of habitats (Florsheim et al., 2008; Gage et al., 2004) and increases in contaminants (i.e., sediment and nutrients) (Hopkins et al., 2018; U.S. EPA, 2017). Locating areas of severe erosion and deposition and gauging the relative impact of channel instability as a source of sediment and nutrients is vital to developing a watershed management plan to address the impacts of sedimentation and eutrophication.

One way to examine the various sources and sinks of sediment dynamics within a watershed is through a sediment budget; however, there is no standardized methodology to construct a sediment budget. In addition, sediment transport varies greatly both spatially and temporarily making it challenging to measure sediment transport for a watershed and predict sediment loads. (Walling and Collins, 2008). In recent years, there has been an increased need for quantifying erosion at a watershed scale (Hopkins et al., 2018; Palmer et al., 2014; Purvis and Fox, 2016).

One method of constructing a sediment budget is tracing sediment by tracking radionuclides. Many studies using this methodology trace measurements of Cesium-137 (^{137}Cs), produced by testing nuclear weapons in the 1950s and 60s. This isotope can be detected up to 40 years later. Soil samples are collected at various locations throughout a study area to determine sediment distribution across the watershed (Walling and Collins, 2008).

Fingerprinting sediment is another approach used to build a sediment budget (Walling and Collins, 2008). Soil samples are collected across the watershed from possible sediment sources, along with suspended sediment samples. All samples are tested for concentrations of various elements on radionuclides to identify the sediment sources (Voli et al., 2013; Walling and Collins, 2008). Voli et al. (2013) used a Monte Carlo simulation to estimate the percentage contribution from each source. Radiocarbon dating of woody materials and sediment was used for estimating the age of alluvial deposits along streambanks (Voli et al., 2013).

Allmendinger et al. (2007) and Gellis et al. (2017) constructed sediment budgets by measuring erosion and deposition rates through the watershed and extrapolating the results based on stream order. Both studies used cross-sectional surveys to measure erosion but utilized the surveys differently. Allmendinger et al. (2007) used cross-sectional surveys to measure streambank erosion while Gellis et al. (2017) used them to document changes in the channel bed and floodplain. In contrast, Gellis et al. (2017) used erosion pins to measure erosion and deposition along streambanks.

Allmendinger et al. (2007) created a sediment budget for first-order streams to determine the sediment input into the Good Hope Tributary in Montgomery County, Maryland. The sediment budget was simplified to exclude sediment storage due to a lack of floodplains along the first-order streams. Upland erosion was estimated from regression and sediment stored on floodplains was estimated using dendrochronology (Allmendinger et al., 2007). The study found that floodplain storage, upland erosion and channel erosion were similar in magnitude in their contribution to the sediment budget.

In Difficult Run, Virginia, Gellis et al (2017) used powdered white feldspar clay as a field marker to measure deposition on floodplains. Multiple measurements were taken over the monitoring period including after Tropical Storm Lee and Super Storm Sandy (A.C. Gellis et al., 2017). The Gellis et al. study captures the influence of extreme events on sediment transport within the watershed, allowing the comparison of erosion rates under different hydrologic conditions. The difference between the measured input of sediments from the bed, streambanks and bars and sediment storage subtracted from measured sediment export was assumed to equal the amount of upland erosion (A.C. Gellis et al., 2017).

Noe et al. (2022) developed a watershed budget for the Chesapeake Bay watershed using various model predictions for streambank, floodplain, suspended sediment, TN and TP loads. Watershed attributes for the model were collected from geospatial data, while reach-scale geomorphometry of channels and floodplains was gathered from LiDAR. RUSLE2 was used to estimate upland erosion delivered to streams. Dendrogeomorphology was used to measure streambank erosion rates. Extensive data collection and monitoring were needed to develop the Random Forest and SPARROW models to estimate the various pollutant loads to the Bay. (Noe et al., 2022).

Sediment budgets are constructed using various methods; however, they all have the same principle components: channel erosion, upland erosion and floodplain storage. Many variabilities within these principle components of sediment transport have yet to be fully understood or completely captured by models. There is a lot of uncertainty with identifying trends and patterns for erosion and deposition on varying temporal and spatial scales making it difficult to model (Walling and Collins, 2008). The temporal scale of the monitoring period is another important factor in capturing the dynamics of erosion (Florsheim et al., 2008; Palmer et al., 2014; Purvis and Fox, 2016). Longer monitoring periods allow a larger range of conditions to be experienced, i.e., wet and dry years, extreme storm events like tropical storms and hurricanes, and land use changes. Palmer et al. (2014) noted wet versus dry years significantly impacted the annual sediment load. Longer monitoring periods will lead to a truer annual average erosion rate (Gamble, 2021; Palmer et al., 2014). Often, a few sites with measured erosion have been used to estimate erosion rates across an entire watershed, leading to an underestimation of sediment loads as found by Purvis and Fox (2016). New methods should be based on larger samples that spatially cover the entire watershed. A wider sample range will allow stronger relationships to be developed between measured streambank erosion and explanatory factors of erosion. If the explanatory factors are pulled from GIS data layers, then sediment loads can be estimated on a larger scale with minimal effort. Recent studies like the one by Noe et. al (2022) have taken advantage of geospatial layers to extract data for reaches on a larger scale. Utilizing geospatial layers reduces time, effort and resources to collect data that can be used to predict sediment loads compared to more traditional methods of quantifying and measuring erosion in the field.

Appendix B – Flows Recorded During the Sampling Period at Five Study Watersheds

The annual peak flow data from USGS Water Data for the Nation were downloaded for the Ellerbe Creek USGS 02086849 gage, Eno River USGS 2085070 gage, and Mountain Creek USGS 208524090 gage. This data was used to determine the return interval based on the past 30 years of data. The return intervals for Horse Creek and New Light Creek were gathered from Streamstats (USGS, n.d.). The flow data during the monitoring period was plotted against the return intervals for bankfull discharge and the 2-, 5-, 10-, 25- and 100-year storms.

Horse Creek and New Light Creek did not have any events above bankfull during the monitoring period between the first and second cross-section surveys. These watersheds are adjacent to each other. Horse Creek did have one event above bankfull following the second survey. Both Mountain Creek and Eno only had one event above bankfull that occurred at the beginning of April 2023. Ellerbe had the most storms above bankfull with a total of four during the monitoring period. Two of those events were past the 2-year storm threshold. This aligns with the land use of the watersheds with Ellerbe being the most urbanized with 72% developed land.

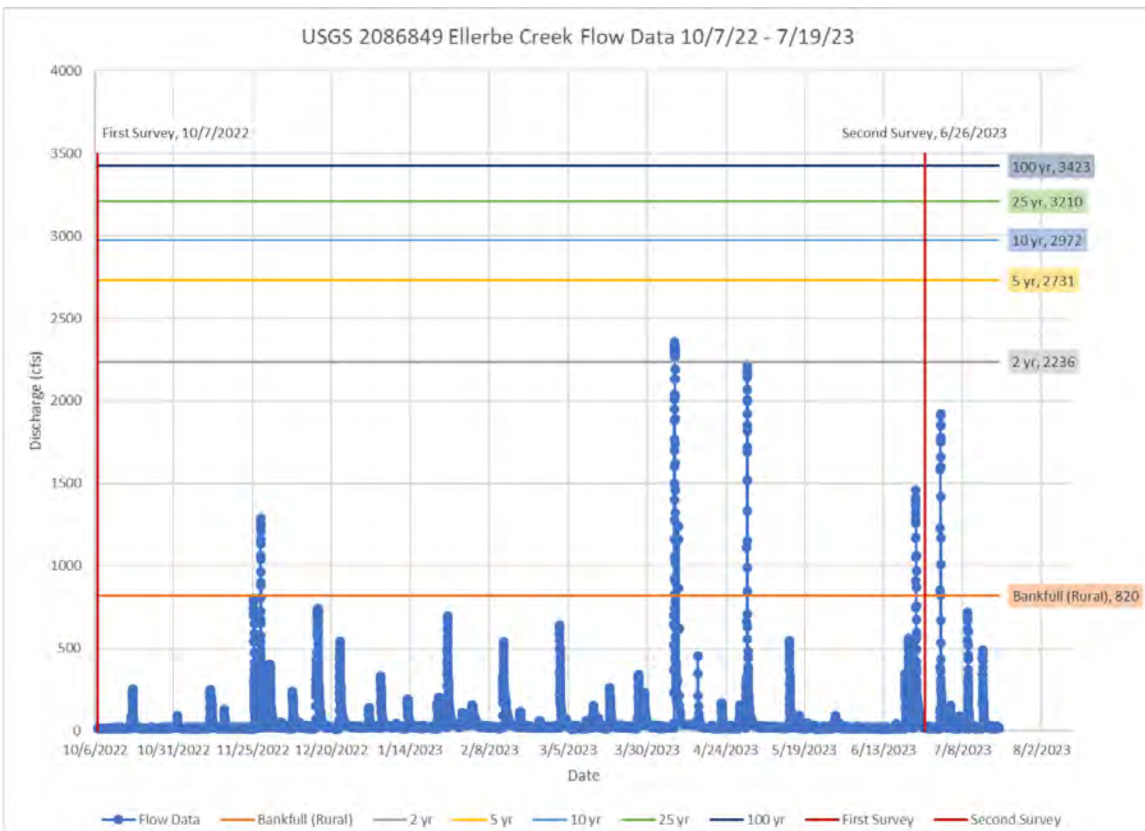

Figure 32. Flow data at Ellerbe Creek gage during monitoring period.

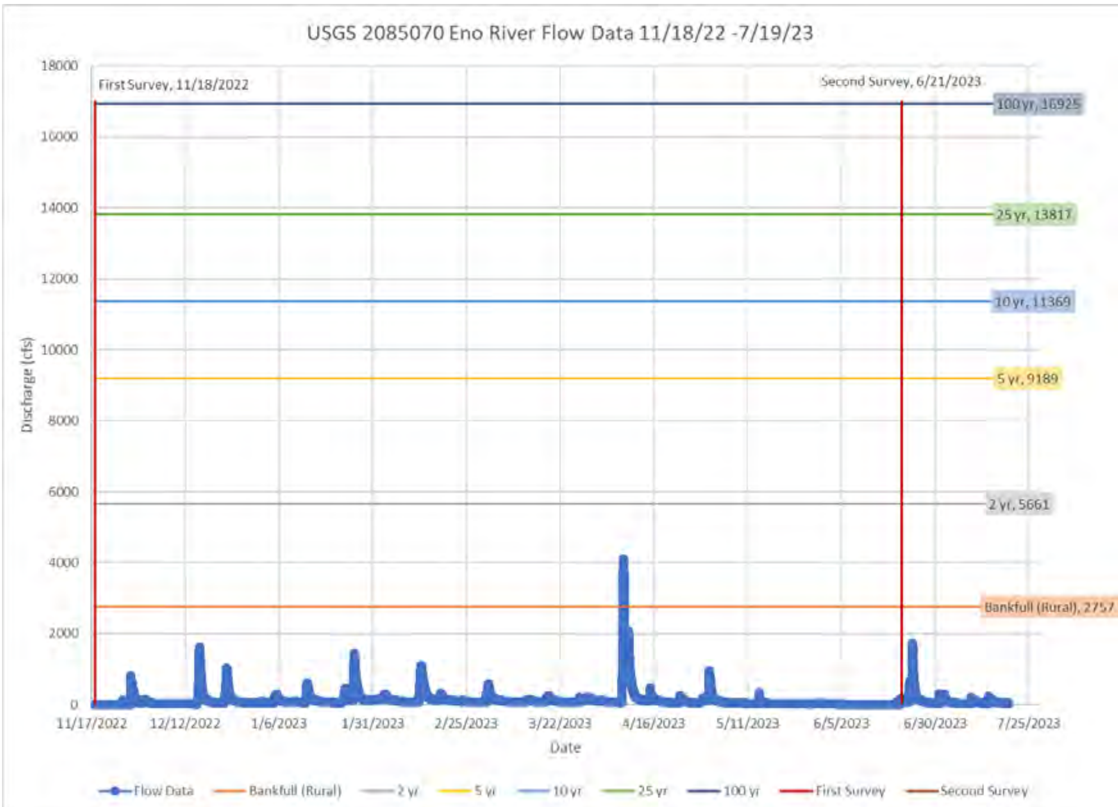

Figure 33. Flow data at Eno River gage during monitoring period.

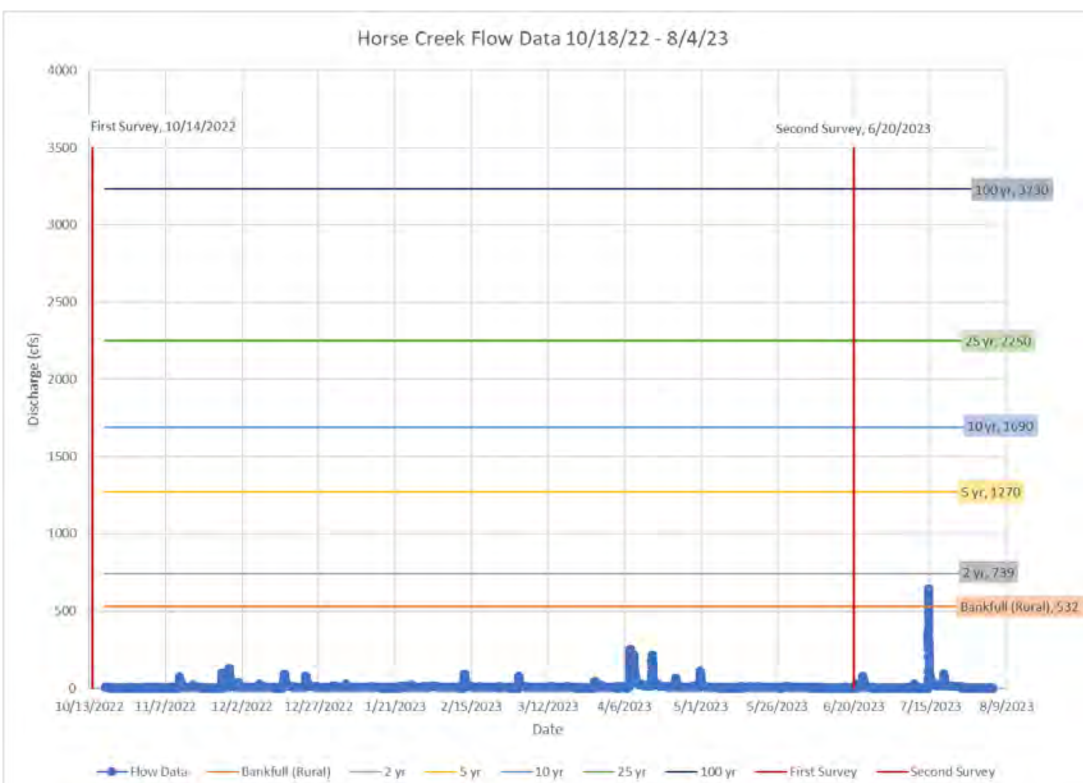

Figure 34. Flow data at Horse Creek gage during monitoring period.

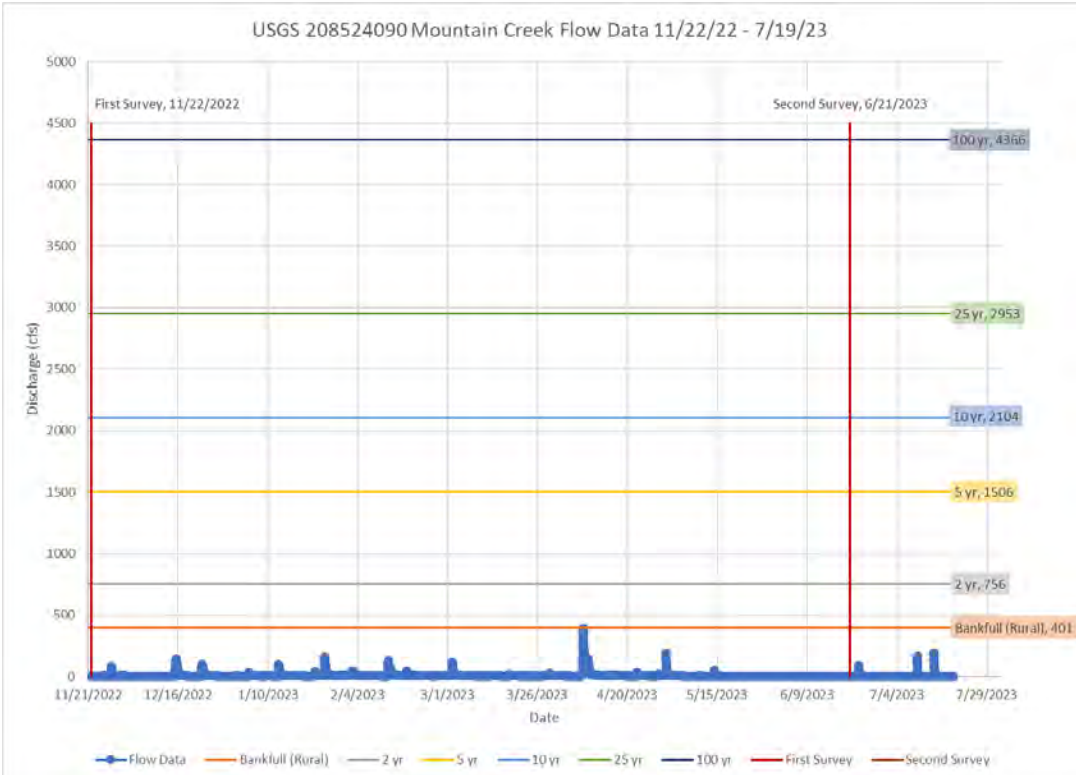

Figure 35. Flow data at Mountain Creek gage during monitoring period.

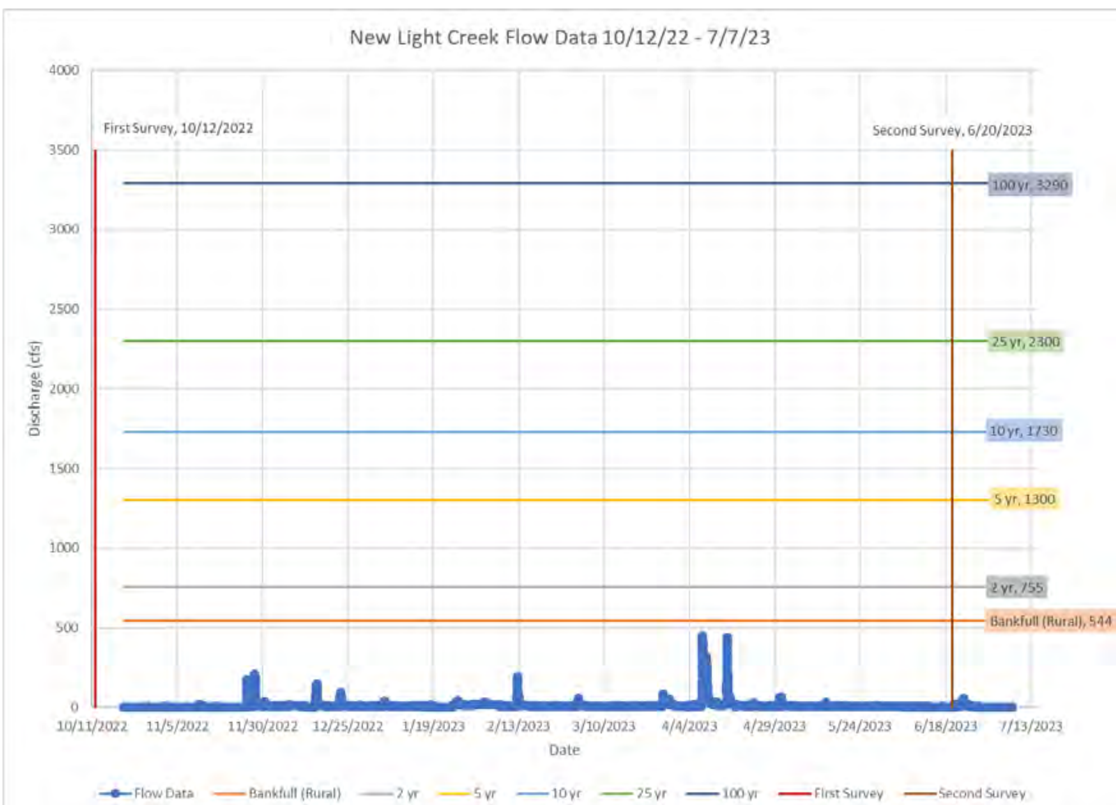

Figure 36. Flow data at New Light Creek gage during monitoring period.

Appendix C - Field Survey and Assessment Methods

Classifying Erosion

Both sides of the banks were visually assessed to classify the type of erosion for each selected 100 ft reach. The type of erosion was recorded, documenting the station value when the category changed. Figure 37 below shows an example of the types of erosion. The types of erosion were lumped into three main categories:

- Stable: non-eroding or depositing banks
- Minor Erosion: surface scour and hoof shear
- Severe Erosion: unstable undercutting and mass wasting

Figure 37. Erosion categories visually assessed in the field.

Surveying Cross-Sections

Cross-sections were selected by choosing sites that were most likely to experience the greatest amount of measurable erosion in less than a year. They were located at the point where the water hit the bank based on visual observation of the stream alignment. Cross-sections were marked with capped rebar pins and wooden stakes with flagging tape. RTK points were collected at each pin to aid in relocating pins and for GIS analyses. Survey points were taken at each point of inflection along the cross-section. More points were taken in the stream channel compared to the floodplain since the focus was on capturing the bank profile to estimate the yearly bank retreat.

Table 6. Dates of first and second surveys of all cross-sections in Falls Lake.

Site	First Survey	Second Survey	Site	First Survey	Second Survey
FL8	10/5/22	6/26/23	FL44	10/18/22	6/23/23
FL10	10/7/22	6/26/23	FL48	11/9/22	6/20/23
FL14	10/7/22	6/26/23	FL53	11/9/22	6/20/23
FL28	10/10/22	6/20/23	FL64	11/17/22	6/22/23
FL29	10/11/22	6/20/23	FL66	11/17/22	6/21/23
FL30	10/12/22	6/19/23	FL74	11/18/22	6/21/23
FL31	10/12/22	6/19/23	FL76	11/18/22	6/21/23
FL32	10/13/22	6/19/23	FL81	11/22/22	6/21/23
FL33	10/14/22	6/19/23	FL84	11/22/23	6/23/23

FL34	10/14/22	6/19/23	FL87	11/22/23	6/21/23
FL38	10/14/22	6/20/23	FL90	11/29/22	6/21/23
FL40	10/18/22	6/23/23	FL93	11/29/22	6/26/23
FL41	10/18/23	6/23/23	FL94	11/29/22	6/26/23
FL42	10/18/23	6/23/23	FL97	12/8/22	6/20/23

Two methods were used to capture undercut banks, depending on the location of the total station and the shape of the streambank. If the total station was sitting on the opposing bank, the prism was placed directly against the undercut bank using 0.00 ft for the rod height. If the total station was not positioned well to capture an undercut bank, the horizontal distance between the survey rod and the streambank was measured and used to adjust the station of the recorded point during data processing.

Figure 38. Surveying undercut banks.

A Topcon GT 505 Series total station was used to survey all cross-sections and top of banks. The total station has an accuracy of 2 mm + 2 ppm under ideal conditions (Topcon, 2016). The precision of the survey data was estimated at 0.1 feet based on the survey error determined from repeat surveys of cross-sections by two field teams at 14 cross-sections located at six streams at Virginia study sites. The NCSU team used a Topcon GT, and the Virginia team used a Trimble S5 Robotic Total Station and Trimble TSC-3 Survey Controller. The difference between the two surveys was calculated as the average of all the horizontal distances between the streambank profile for the NCSU team and the VA team. Several factors can contribute to survey error including human error (e.g. incorrectly setting the rod height, taking points when the rod is not completely vertical, collecting the survey shot before the rod is in contact with the ground, etc.) and environmental conditions (e.g. animal or human disturbance of the survey pin, freeze/thaw cycles moving the pin, etc.). The median horizontal difference was found to be 0.1 ft for total stations. Therefore, any measured bank retreat of less than 0.1 ft was excluded from the analysis.

Soil Samples

Disturbed soil samples were collected by hammering a soil core sampler into the bank. The volume of the cylinder was 288.44 cm3. The soil was removed from each cylinder and placed in labeled bags. The soil samples were analyzed for Total Nitrogen (TN), Total Phosphorus (TP) and bulk density at the BAE Environmental Analysis Laboratory. TN was measured following the APHA 4500 Norg B methodology, and TP measurements followed the APHA 4500-P F methodology. The ASTM D 2937 method was followed to measure bulk density (EAL, 2020).

Figure 39. Collecting soil samples in the field.

Turbidity Monitoring

Automated samplers with integrated flowmeters were installed at each of the five monitoring sites (Ellerbe Creek, Eno River, Horse Creek, Mountain Creek and New Light Creek) as shown in Figure 40. Five of the 24 1,000-ml bottles collected baseflow (nonstorm) samples while the remaining were designated for stormflows. Nonstorm and storm discharge were delineated by the stage of the stream. Nonstorm discharge was defined as the stage occurring at least 48 hours after the end of the most recent significant rainfall. Therefore, the nonstorm discharge stage was reset many times during the duration of monitoring. Storm discharge was defined as occurring during a 0.04 to 0.1 ft rise in the stage from the nonstorm discharge stage of the stream. The rise needed to trigger a shift to storm sampling was based on the flashiness of the stream. Each bottle was divided into two samples. Samplers were programmed to collect a 400-ml sample every 48 hours during nonstorm flows and every 4-6 hours during storm flows. More frequent sampling during storms was required to characterize the variability of total suspended solids (TSS) observed during previous studies.

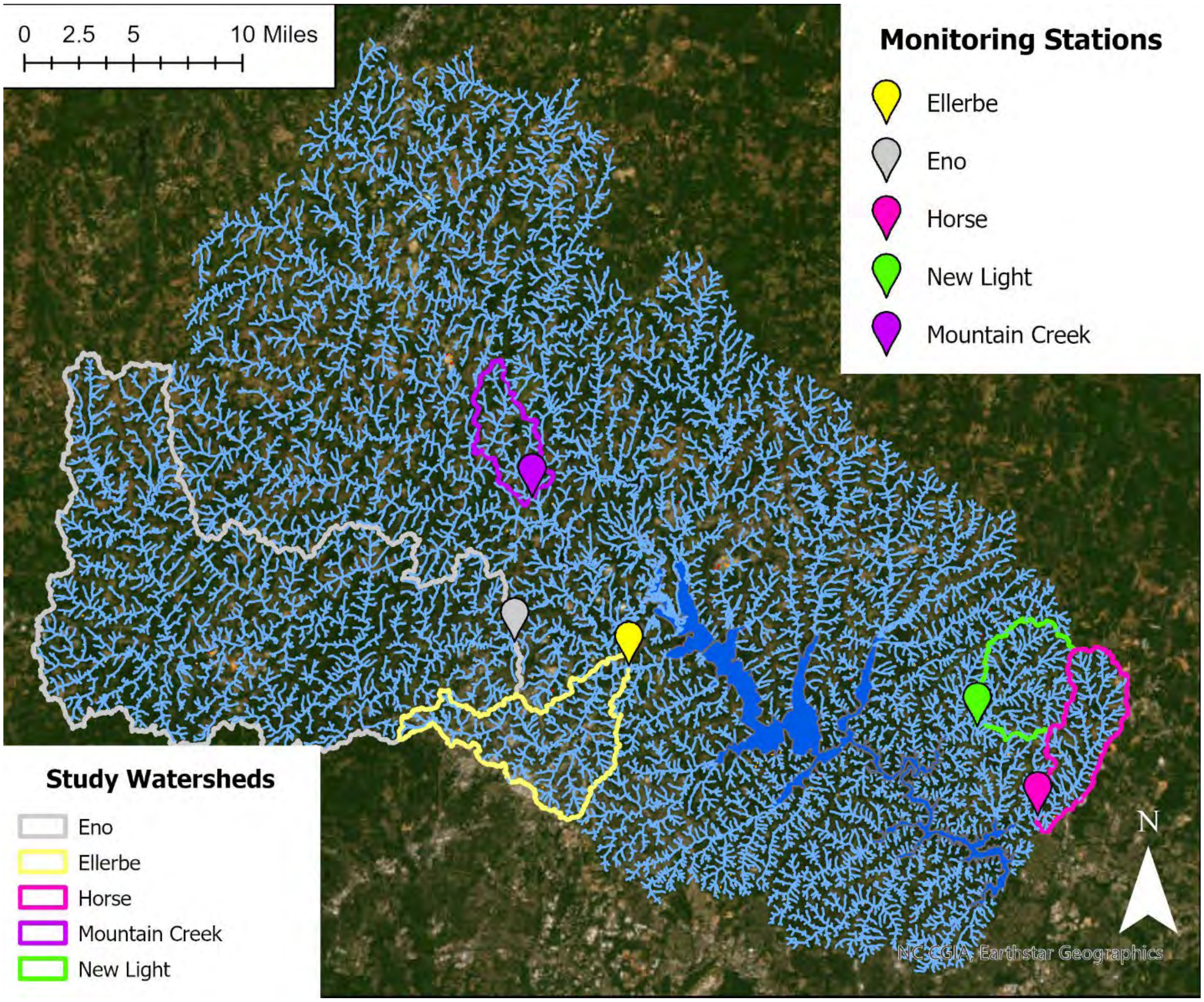

Figure 40. Location of ISCO samplers for the five study watersheds.

Figure 41 shows an example of the timing of sampling relative to storm and nonstorm discharge for Horse Creek during the period of 10/29/22 to 11/5/22. The 'plus' signs indicate time periods of storm flow sample collection, and the circles indicate the nonstorm samples. In this example, when the water level reached a stage of 0.67 feet this delineated storm from nonstorm samples, based on the stage recorded during the previous visit. The nonstorm samples were collected every 48 hours when the stage (bottom graph) was less than 0.67 feet (shown as dashed line), and every 5 hours after the stage rose above 0.67 feet. The sampler returned to collecting nonstorm samples every 48-hrs on 11/2/22 after the stage dropped below 0.67 ft.

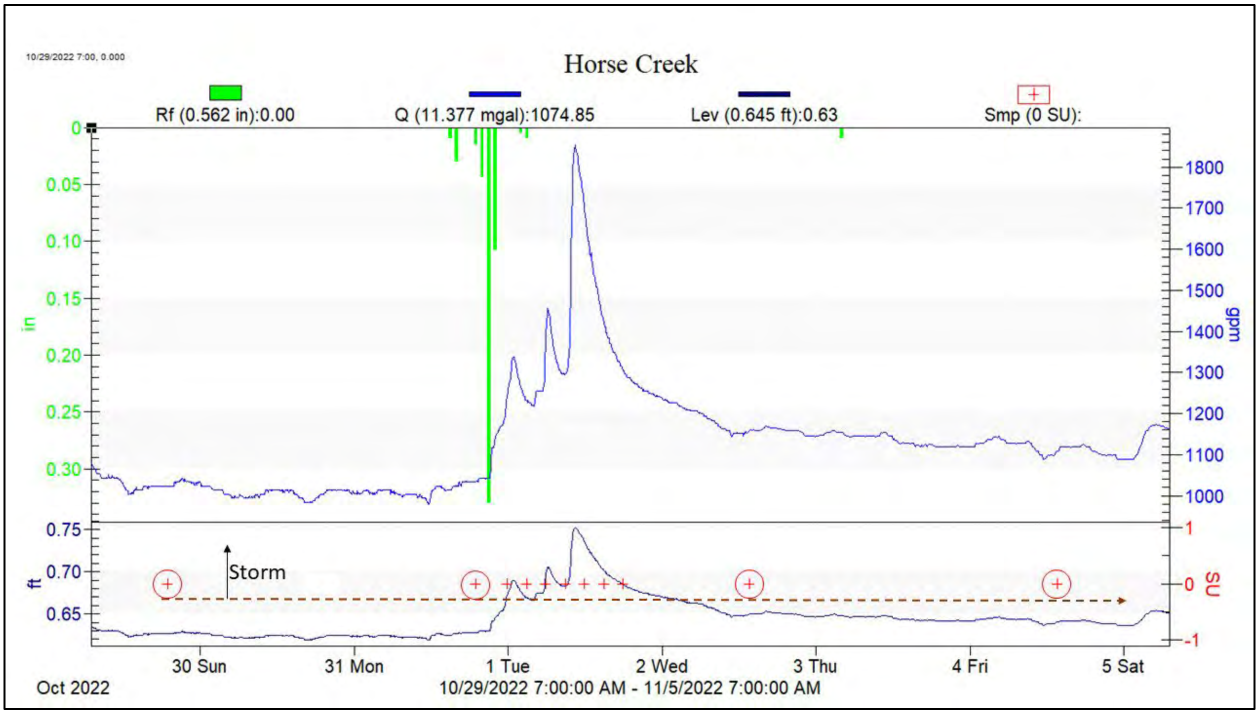

Figure 41. Example of sampling program for Horse Creek.

At least one high water event and other causes interrupted the monitoring. At Ellerbe Creek and the Eno River, heavy rains during 4/7/23 and 4/8/23 resulted in high water inundating the samplers at the two sites, which caused samples to be missed. At Ellerbe Creek there was a large plume of sediment and prolonged backwater at the sampler intake which caused several missed samples. Concentrations of TSS and TP for the missed samples were estimated from corresponding concentrations of monitored storms of similar peak and total discharge. At Horse and New Light Creeks, high water on 4/7/23 and 4/8/23 resulted in peak stages much greater than the maximum stage of measured discharge; therefore, the stage-discharge rating curve was extrapolated to provide an estimate of discharge for those stages above the maximum measured. At New Light Creek, the sampler and shelter were vandalized between 7/11/23 and 7/25/23. This along with a very high stage on 7/14/23 reshaped the stream channel; therefore, monitoring was discontinued.

Appendix D – GIS Analysis

Accuracy of Reach Data Collected

The upstream and downstream locations of every 100 ft reach were recorded in the Ersi Collector App on a phone. About halfway through inventorying streambanks, RTK points were also recorded to identify the reach start and end points. The difference in accuracy between the phone and RTK points was examined in ArcGIS Pro. Visual examination of the points revealed that the majority of the RTK points were within the channel unlike the phone points. The Near tool was used to measure and evaluate the distance between the phone upstream point and RTK upstream and downstream points at each site. The upstream points appeared to be more accurate than the downstream phone points. Therefore, the reach segments for each site were based on the upstream point and extended 100 ft downstream. The RTK unit has greater accuracy than the phone GPS, therefore RTK points were always used to establish the upstream point along the reach segment.

Appendix E – Model Development

Classification Model Development

34 data points for each type of streambank condition classification (stable, minor erosion, severe erosion) were selected as inputs for the model to maintain a balanced dataset. These data points were based on the erosion classification of the banks along stream reaches. Only the reaches marked with RTK could be used in the model due to lower accuracy of GPS points gathered with a phone. The start of the reach segment for the visited sites was established based on the upstream point for the reach taken using an RTK unit.

Two types of classification models were examined. The first was a decision tree using rpart package and the second was a random forest model using the caret and randomForest packages. The decision tree was pruned using the complexity parameter that resulted in the lowest relative error. The caret package was used to find the best mtry that results in the best accuracy for the model. Different combinations of variables were used to find the best predictors and model type to classify the presence or absence of erosion and the severity of erosion.

A total of five models were run for both classification models. The random forest model was fitted for a maximum mtry of 15. The default mtry for regression models is the square root of the number of predictors which would be 5 since there are 25 total predictors. The maximum mtry was reduced to the maximum number of variables for models 3, 4 and 5.

Table 7. All variables considered for classification model.

Individual Point Variables			**Site/Watershed Variables**		
Variable Name	**Description**	**Models**	**Variable Name**	**Description**	**Models**
PCT5_PO	PO 5^{th} percentile	1, 2	Stream_Order	Stream order	1, 2, 3
PCT75_PO	PO 75^{th} percentile	1, 2	GEOL250_ID	Geologic ID	1, 2
PCT90_PO	PO 90^{th} percentile	All	GEOCODE	Geologic Code	1, 2
MAX_Slope	Slope max percentile	All	BELT	Geologic belt	1, 2, 3
PCT75_Slope	Slope 75^{th} percentile	1, 2	BELT2		1, 2
PCT90_Slope	Slope 90^{th} percentile	1, 2	GROUP_		1, 2
REM75_REM	REM 75^{th} percentile	3, 4	TYPE	Rock type	1, 2, 3
Watershed Variables			FORMATION		1
Developed	% of developed land in watershed	1, 2, 3	EON		1
Cropland	% of cropland in watershed	1, 2, 3	ERA		1
Grass_Shrub	% of grass/shrub land in watershed	1, 2, 3	PERIOD		1
Tree	% of forested land in watershed	1, 2, 3	BankHeight	Bank height measured in the field (ft); estimate for 100 ft reach	2

Water	% of water in watershed	1, 2, 3	TOBWidth	TOB width measured in the field (ft); estimate for 100 ft reach	2
Wetland	% of wetland in watershed	1, 2, 3	W_D_Ratio	Ratio of TOB Width to bank height	2
Barren	% of barren land in watershed	1, 2, 3			
Area_sqmi	Watershed area in square miles	1, 2, 3			

Classification Model Results

Table 8 compares the accuracy and kappa results for each model run through a decision tree and random forest classification model. Kappa coefficients from 0.21-0.4 are considered to have fair agreement between observed and predicted classes, 0.41-0.6 is moderate agreement, 0.61-0.8 is substantial agreement and a strong agreement for anything greater than 0.81. The random forest models outperformed the decision tree models for each of the different combinations of variables. The best model was the random forest model 5 but model 3 was also comparable with the same accuracy and just one hundredth off for the kappa value.

Table 8. LOOCV results for erosion classification model.

set.seed(14)	**Decision Tree**		**Random Forest**	
Model	**Accuracy**	**Kappa**	**Accuracy**	**Kappa**
Model 1	0.48	0.22	0.51	0.26
Model 2	0.43	0.15	0.55	0.32
Model 3	0.43	0.15	0.57	0.35
Model 4	0.39	0.09	0.46	0.19
Model 5	0.47	0.20	0.57	0.36

Two final models were fit: one using the variables from model 3 and another using the variables in model 5. The first model (rf.mod) has a higher error rate (45.1%) than the second model (40.2%). Rf.mod2 has a higher accuracy of 0.6 compared to 0.55 and higher kappa coefficient of 0.4 compared to 0.32. The detection rate in the confusion matrix for rf.mod2 is closer to 0.333 for each class which is the ideal value if the model perfectly predicted the classification every time. The balanced accuracy in the confusion matrix is higher in rf.mod2 than in rf.mod indicated the second model is better at accurately classifying the type of erosion. The final model contains the following predictor variables: 90th percentile PO, max slope, cropland land cover %, barren land cover %, tree land cover %, 75th percentile REM, geologic belt and developed land cover %.

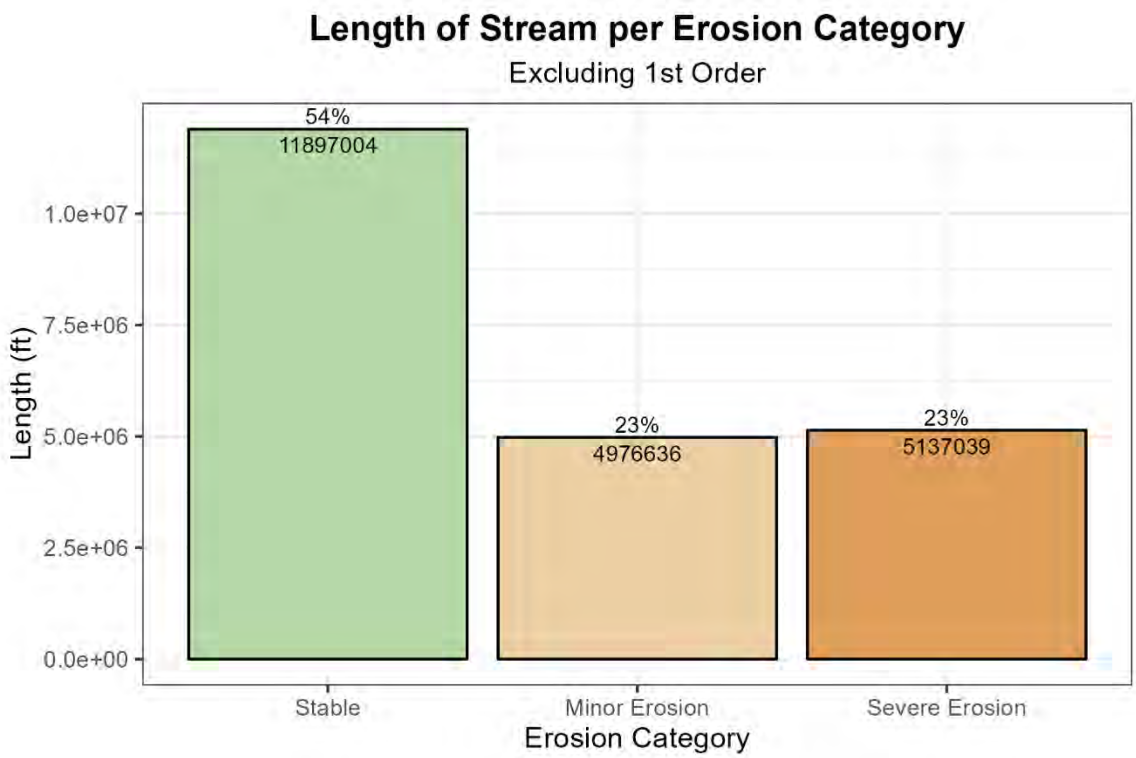

Figure 42. Length of stream per erosion category for Falls Lake watershed.

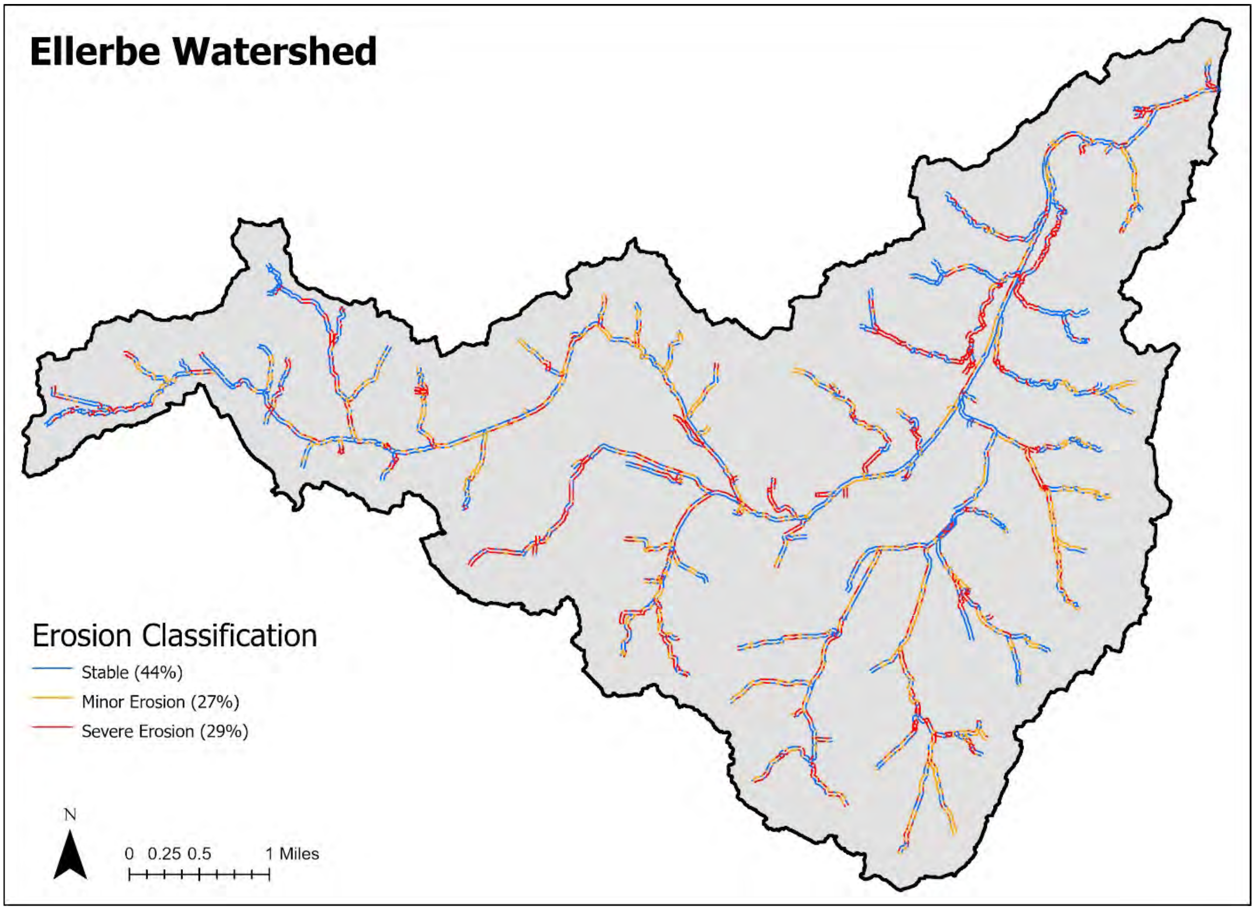

Figure 43. Model prediction of erosion classification for Ellerbe watershed.

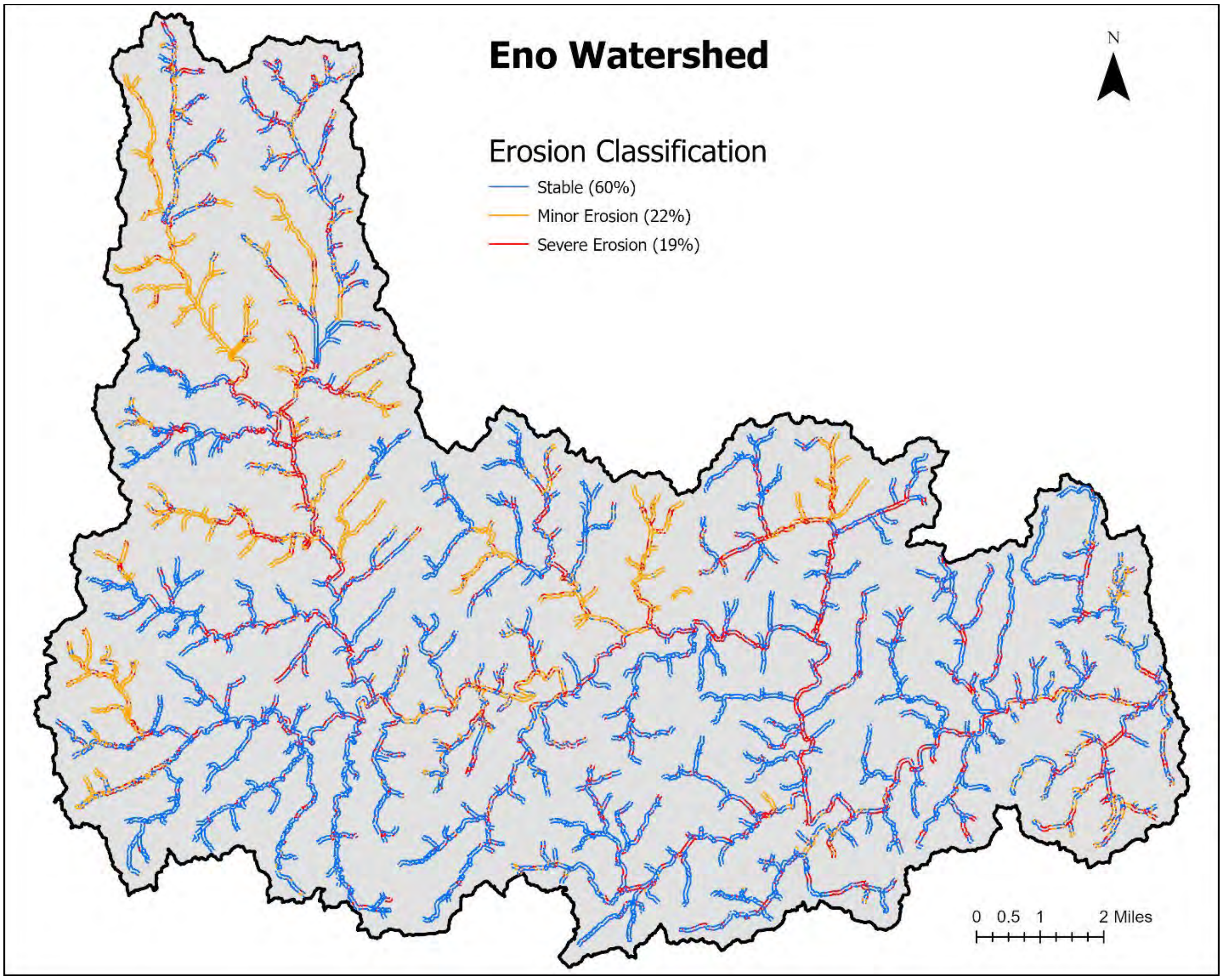

Figure 44.Model prediction of erosion classification for Eno watershed.

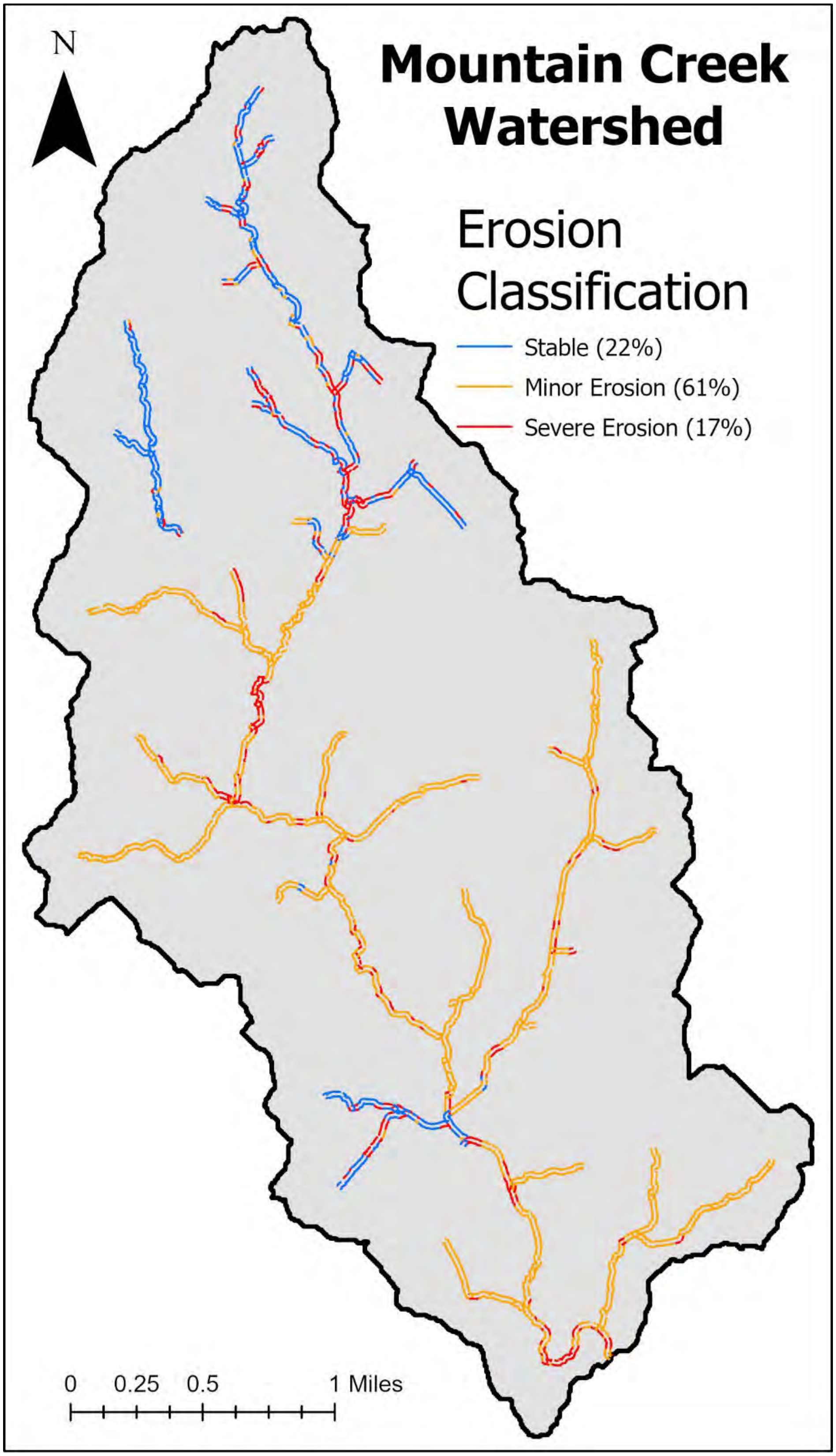

Figure 45. Model prediction of erosion classification for Mountain Creek watershed.

Bank Height Model Development

A linear regression model was trained and tested to predict bank heights using the measured bank height from all sites except FL104 where the water was too deep to measure a bank height. The dependent variable (bank height) was transformed by taking the cube root to make a more normal distribution which improved the model (Figure 46 and Figure 47).

Zonal Statistics as Table tool in ArcGIS Pro was used to extract PO, slope and REM percentiles for various sized buffers at each site. The correlations between the percentiles and transformed bank height were examined to determine which would be included in the model. A best subset selection was run on all of the data using the regsubsets function in R with the exhaustive method to reduce the number of predictors. In total six different models were tested with various combinations of predictors to find the best model.

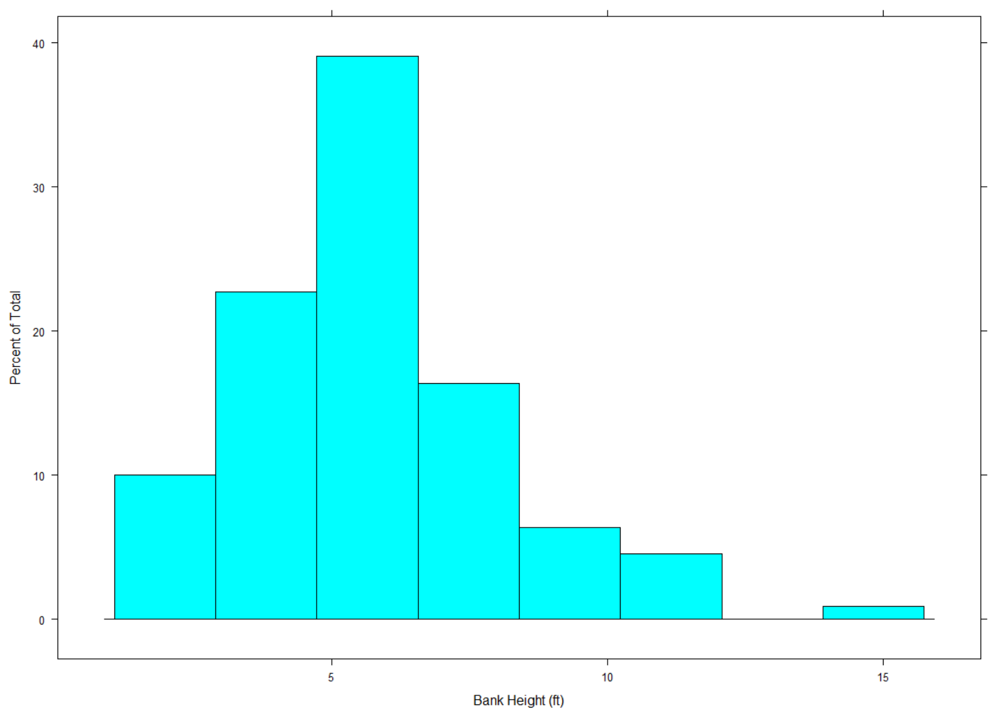

Figure 46. Histogram of measured bank height.

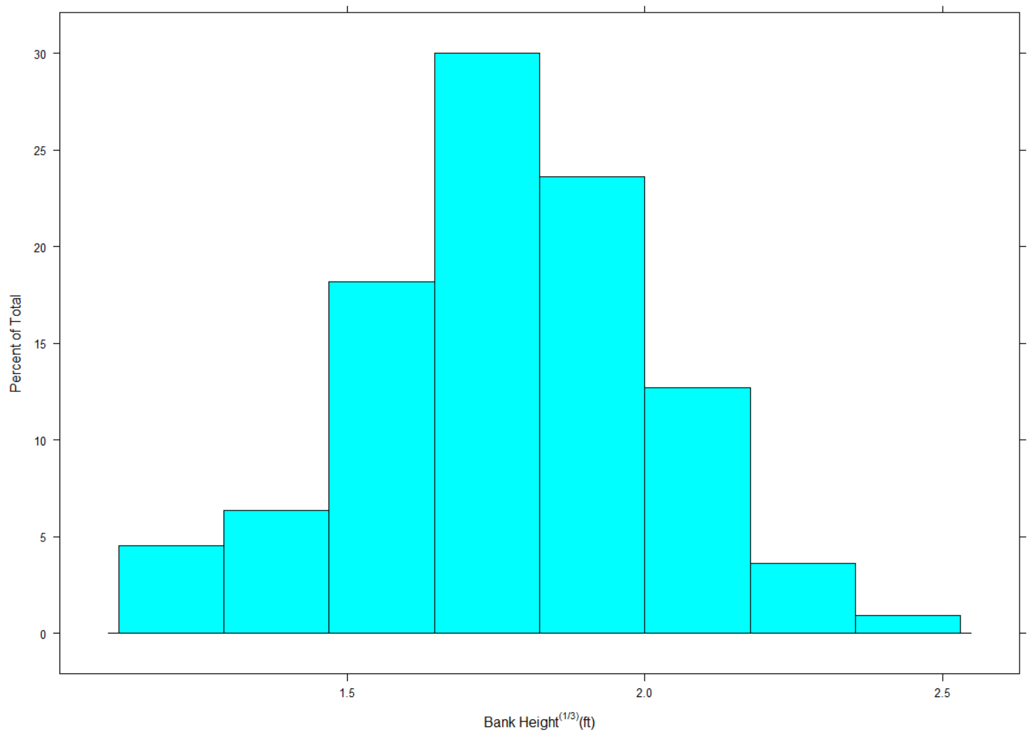

Figure 47. Histogram of the cube root of measured bank height.

The correlations for each percentile were compared to the bank height and transformed bank height to select the percentile with the strongest correlation. The percentiles with the highest correlations are shown below in Table 9, Table 10, and Table 11. A buffer width of twice the stream width showed the best correlations for PO and Slope, while a buffer that was three times the stream width had the strongest correlations for REM. The minimum percentile had the best correlation for PO, maximum for Slope and median for REM. The 90th percentile for slope was close to the maximum and had a more normal distribution so both were included and to run through best subset selection.

Table 9.Correlations between bank height, transformed bank height and PO percentiles based on varying buffer sizes. The buffer sizes are based on the widths assigned by stream order.

PO	**Width**	**2x Width**	**3x Width**
Bank Height	MIN: -0.54	MIN: -0.57	MIN: -0.52
Transformed Bank Height	MIN: -0.58	MIN: -0.61	MIN: -0.55

Table 10.Correlations between bank height, transformed bank height and Slope percentiles based on varying buffer sizes. The buffer sizes are based on the widths assigned by stream order.

Slope	**Width**	**2x Width**	**3x Width**
Bank Height	MAX: 0.60	MAX: 0.61	MAX: 0.58
Transformed Bank Height	MAX: 0.62	MAX: 0.62	MAX: 0.59

Table 11. Correlations between bank height, transformed bank height and REM percentiles based on varying buffer sizes. The buffer sizes are based on the widths assigned by stream order.

REM	Width	2x Width	3x Width
Bank Height	PCT90: 0.43	PCT75: 0.46	MEDIAN: 0.49
Transformed Bank Height	PCT90: 0.42	PCT75: 0.45	MEDIAN: 0.48

A best subset selection was run on all of the data using the regsubsets function in r with the exhaustive method. This was run after removing TOB width and forested land cover percentage from the dataset since these variables were highly correlated with others and would therefore cause issues when running the model. The best subset was run twice: once with the regular bank height and again with the transformed bank height. The coefficient of determination (R^2), squared correlation coefficient (r^2) and adjusted r^2 were used to test the fit of the model. The squared correlation coefficient examines how much of the variation in the data is explained by the model while the coefficient of determine examines the model efficiency. The root mean squared error (RMSE), mean absolute error (MAE) were used to examine the accuracy of the model, and AIC and BIC examined the model trade-off between complexity and fit (Haefner, 2005; Wallach et al., 2006).

Both selected 6 variables as the best (lowest AIC, highest adjusted r^2, and one of the lower BIC values). These variables were: watershed area, developed, water, min PO, max Slope and median REM.

Based on the LOOCV of each model, Model 5 appears to be the best with the highest R^2, Pearson r^2 and adjusted r^2. Model 5 also has the lowest RMSE, MAE, SSE, AIC and BIC when looking at the median values across all models. The maximum RMSE was 0.5 ft meaning at most the bank height would be half a foot off from the actual height.

Table 12. Adjusted r^2 LOOCV bank height model results for the various models tested.

Model	Adjusted r^2
Model 1	-0.10
Model 2	-0.09
Model 3	0.42
Model 4	0.44
Model 5	0.53
Model 6	0.52

Bank Height Model Results

The final bank height model contains five predictor variables: percentage of developed land in the watershed, minimum PO percentile, 90th slope percentile, median REM percentile, and bankfull depth estimated from the NC Rural Piedmont regional curve (Doll et al., 2002) based on drainage area. Below is the equation to predict the transformed bank height. All predicted values must be raised to the third power to transform back to measurable bank height values. All predictors were significant except for REM. From training and testing the model, the adjusted r^2 was 0.53 and the median RMSE was 0.09 ft.

Equation 2. Transformed bank height.

$$Transformed\ Bank\ Height\ (ft) = 0.00182 * Developed - 0.0134 * PO + 0.00820 * Slope + 0.00970 * REM + 0.0880 * Dbfk$$

Bank Retreat Model Development

Correlation plots of all possible predictor variables with measured bank retreat were examined to narrow down the selection of variables prior to applying best subset selection. The percentile for PO, Slope and REM raster layer that had the best correlation with the measured bank retreat was kept for a predictor variable. Three regression model types were tested: linear regression, ridge and lasso. Measured bank retreat values for all eroding banks were used to build the model for a total of 30 banks from 25 unique cross-sections. All bank retreat values of 0 ft/yr were excluded from the model which is why three cross-sections were excluded from the model.

Three approaches were taken for selecting bank retreat values to use and types of buffers used to collect PO, Slope and REM raster data. The first had bank retreat values for the entire XS (considering both banks) and the PO, Slope and REM factors were extracted from a 100 ft reach centered at the XS. The second approach extracted PO, Slope and REM factors from buffers created around a point on either bank at the XS. The third approach was the same as the second except it used bank retreat values for all eroding banks meaning that some XS had two values, one from each bank. The third approach produced better test metrics with lower RMSE, MAE, SSE, AIC and BIC values. The linear regression models performed better than the ridge or lasso regressions for average bank retreat.

The percentage of land cover per watershed was determined for the NC SPARROW catchments which were relatively small catchments. All stream segments within the catchment had the same land cover. It was determined that these catchments were small enough to be representative for all stream segments within the catchment. Since the stream was broken up into 100 ft segments, it was not feasible to develop a watershed for each individual segment and calculate the land cover within each of those watersheds.

Table 13. Coefficient of determination (R2), squared correlation coefficient (r2) and adjusted r2 values for each average bank retreat model calculated by merging all observed and predicted values from each LOOCV set.

Model	R^2	Pearson r^2	Adjusted r^2
Linear Regression 1	0.15	0.38	0.18
Linear Regression 2	0.64	0.67	0.55
Linear Regression 3	0.63	0.63	0.54
Linear Regression 4	0.60	0.62	0.50
Ridge	0.47	0.47	NA
Lasso	0.50	0.50	NA

The second linear regression model developed based on variables selected with best subset selection is the best model. It has the lowest RMSE, MAE, SSE, AIC, and BIC values and highest R^2, r^2 and adjusted r^2 values as seen in Table 13.

Bank Retreat Model Results

The final bank retreat model selected was a linear regression with variables resulting from a best subset selection (Equation 3). The test median RSME was 0.15 ft/yr and adjusted r^2 (squared correlation coefficient) was 0.55. The final average bank retreat model has an adjusted r^2 of 0.77 and p-value of less than 0.05. All of the coefficients are significant except for developed land cover percentage. This model does include two field measurements, TOB width and bankfull area. To apply this model to the entire watershed, the drainage area was used to estimate both dimensions. Bankfull area used the NC Rural Piedmont regional curve equation (Doll et al., 2002) and a new regression was developed to estimate TOB width (Figure 48). Alternatives to these channel dimensions were tried such as using just drainage area but the model performance drastically dropped with correlation coefficient around 0.2 that would be unacceptable for use.

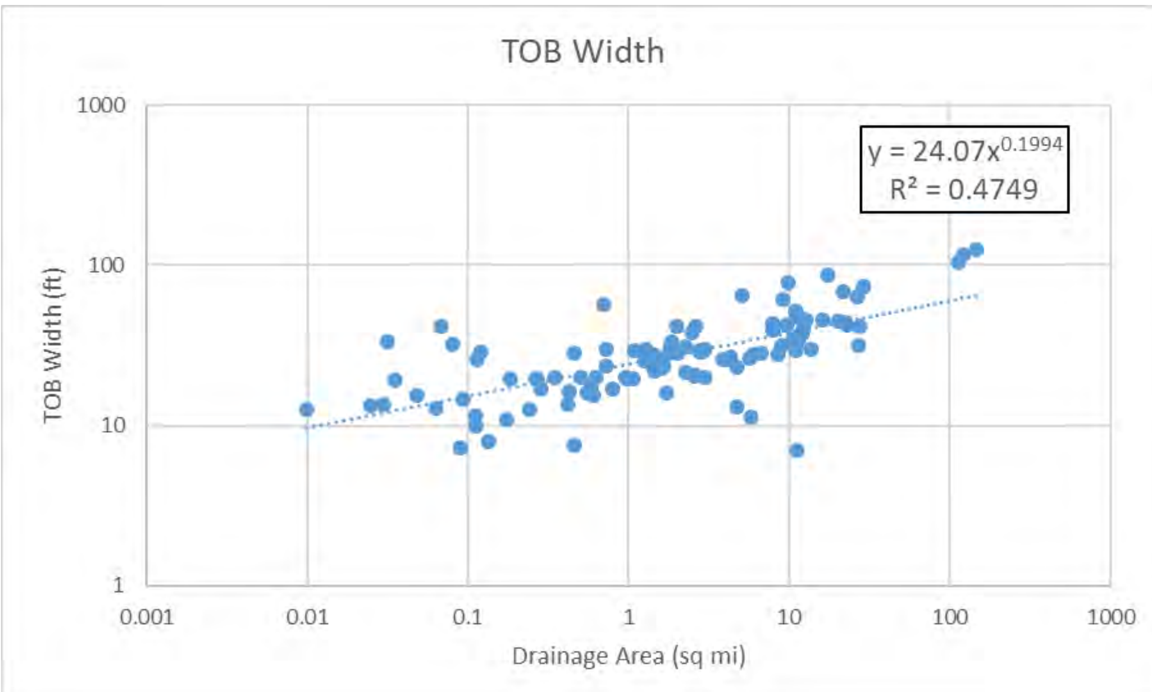

Figure 48. A power regression equation to estimate TOB width (ft) based on drainage area (sq mi).

Equation 3. Bank retreat.

$$Bank\ Retreat\ (ft/yr) = -0.012 * Abkf + 0.027 * WTOB + 0.047 * PO - 0.0037 * Developed - 0.0603 * GrassShrub + 0.122 * Barren + 0.36 * RaleighBelt - 0.224 * IntrusiveRock$$

Abkf = bankfull area (ft); WTOB = TOB width (ft); PO = median PO; Developed = % of developed land in watershed; GrassShrub = % of grass/shrub land in watershed; Barren = % of barren land in watershed; RaleighBelt = 0 not in Raleigh Belt, 1 in Raleigh Belt; Intrusive Rock = 0 not made of intrusive rock, 1 made of intrusive rock

Appendix F – Estimating Sediment and Nutrient Loads

Turbidity Monitoring

Continuous discharge measurements for Mountain Creek, Ellerbe Creek, and the Eno River were downloaded from the USGS website and plotted along with the sampling times from the corresponding automated sampler. Rainfall data measured at the Eno River site (at Roxboro Street) were downloaded from the USGS website and used for these three sites. For New Light and Horse Creeks, a stream staff gage was installed and stage-discharge relationships were developed from discharge measurements made using standard stream gaging methods. At least 6 discharge measurements were conducted at each monitoring site over a range of stages (Appendix B – Flows Recorded During the Sampling Period at Five Study Watersheds. Continuous stage measurements made by the two automated samplers' integrated flowmeters were used along with the stage-discharge relationships to computed discharge. Hourly rainfall was downloaded from the State Climate Office (SCO) website for the Horse Creek outlet location. The SCO used a combination of nearby raingage measurements and radar data to estimate the rainfall at a given location. The Horse Creek rainfall was also used for New Light Creek as the two watersheds are adjacent.

Total discharge for each period between visits was divided into nonstorm and storm discharge based on the stage used to delineate between the two types of discharge and best professional judgement. In general, storm discharge ended when the stage/discharge descended to the pre-storm stage or to less than 80% of the difference between the peak and pre-storm discharge for storm. Composite turbidity for nonstorm discharge was computed as the average of the turbidities of the nonstorm sample in each of the sampler bottles. Because the turbidity and discharge rate of nonstorm samples was relatively consistent, the average was considered an adequate representation of the composite turbidity over the entire 2-week duration. Corresponding regression equations (figures 49-53) were then used to estimate TP and TSS concentrations from the average/composite turbidity. These concentrations were multiplied by the nonstorm discharge and a conversion factor to obtain the nonstorm load. Composite turbidity for storm discharge, which often varied greatly between storm samples, was computed as a flow-weighted turbidity for most storms. This involved computing the total discharge corresponding to the time over which each sampler bottle was filled. Then this discharge was multiplied by the turbidity for the bottle, the products were then summed and divided by the total discharge for the storm. The estimated TP and TSS from the regression equations were combined with the discharge to obtain the storm load.

Monitoring duration, rainfall, discharge, and TP and TSS export rates for the 5 monitoring stations are shown in Table 14. The rainfall, discharge and export rates were divided by the duration to obtain the annual values even though none of the stations were monitored for a complete year. Rainfall totals varied slightly depending on the start date of monitoring, but were generally greater for the two streams in Wake County (New Light and Horse Creeks) compared to the other three in Durham County. Discharge was greatest for Ellerbe Creek, which was expected as its watershed was primarily developed/urban with nearly 22% of the land covered with impervious surfaces (Table 15). Discharge from the other three streams and the Eno River were similar. Mountain Creek was slightly greater likely due to the greater area of cultivated land.

Table 14. Rainfall, Discharge, and TP and TSS Export from Sites.

Site	**Start**	**End**	**Duration**	**Rain**	**Discharge**	**TP**	**TSS**
			yr	**in/yr**	**in/yr**	**** kg/ha/yr ****	
New Light Creek	10/18/22	7/11/23	0.73	51.54	10.60	0.41	185
Horse Creek	10/18/22	10/3/23	0.96	52.19	10.26	0.59	392
Ellerbe Creek	10/20/22	10/2/23	0.95	43.83	26.82	1.18	301
Eno River	12/5/22	10/2/23	0.82	44.30	9.44	0.23	104
Mountain Creek	11/21/22	10/2/23	0.86	47.91	11.38	0.53	231
Other studies							
New Light Creek[1]	7/29/08	10/14/09	1.21	45.03	6.22	0.48	316
Horse Creek[1]	7/29/08	10/14/09	1.21	45.03	9.80	0.61	416
Mountain Creek[2]	1995	2009	15.0	46.50	11.63	0.60	655

[1] From Line, 2013.

[2] From Fine et al., 2013.

Table 15. Land Use/cover in drainage areas to monitoring stations as of 2011.

Station	**Cultivated**	**Forest**	**Herb/grass**	**Developed**	**Impervious**	**Wetland**
	%	**%**	**%**	**%**	**%**	**%**
Horse Creek	10.2	55.3	3.9	26.2	3.8	1.6
New Light Creek	15.4	65.7	3.2	9.5	1.0	1.5
Ellerbe Creek	1.9	15.4	3.9	74.6	21.8	3.8
Eno River	17.1	57.9	5.6	18.1	3.0	0.5
Mountain Creek	31.8	52.3	5.8	9.3	1.3	0.3

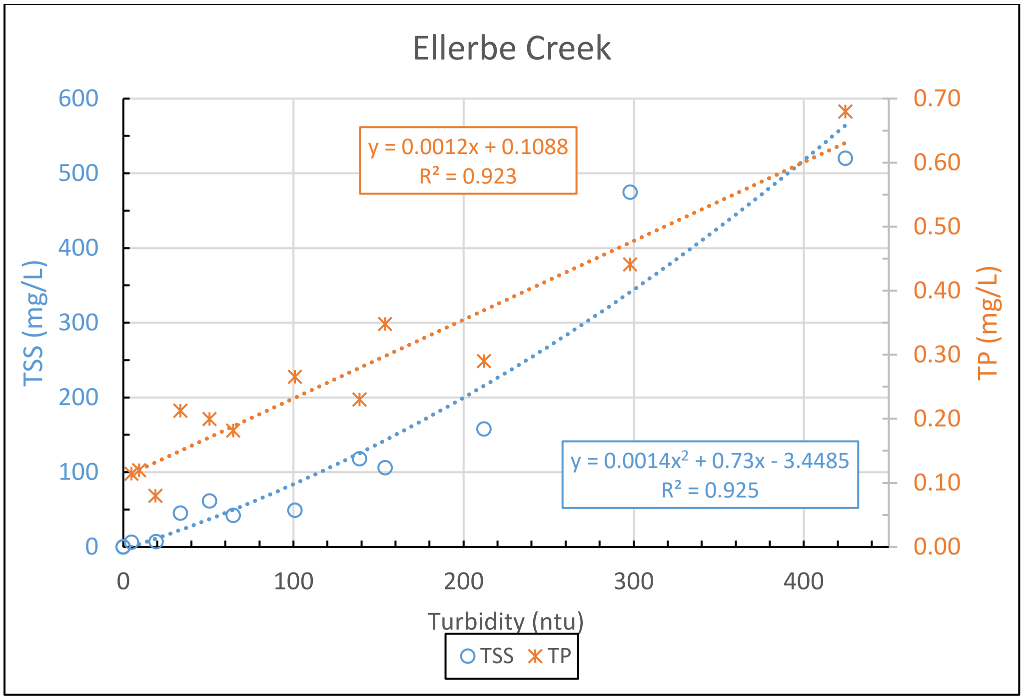

Figure 49. TSS and TP versus turbidity for Ellerbe Creek.

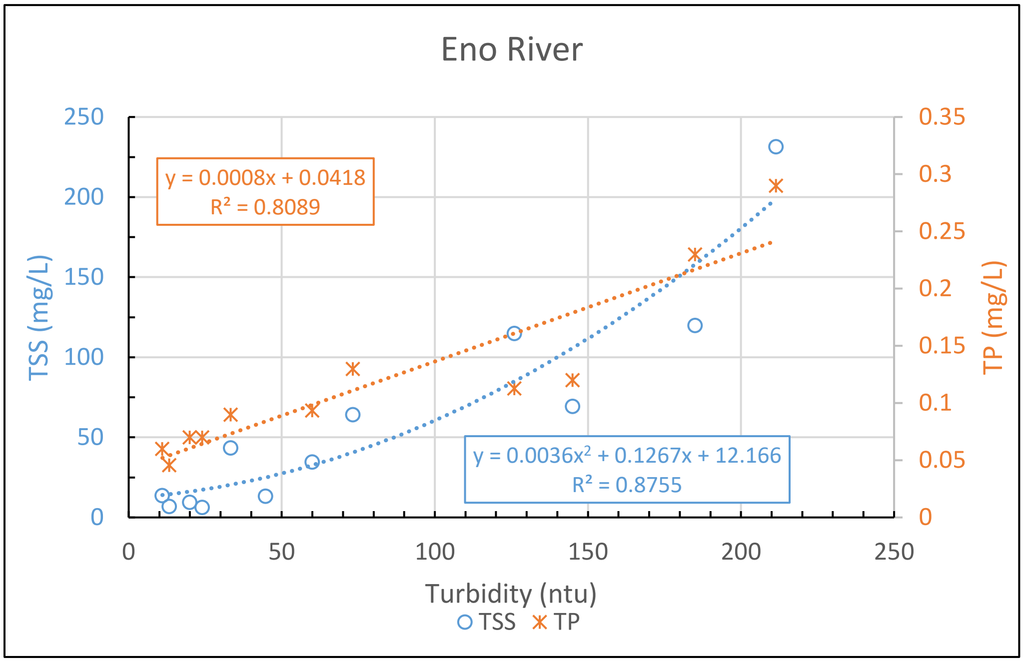

Figure 50. TSS and TP versus turbidity for Eno River.

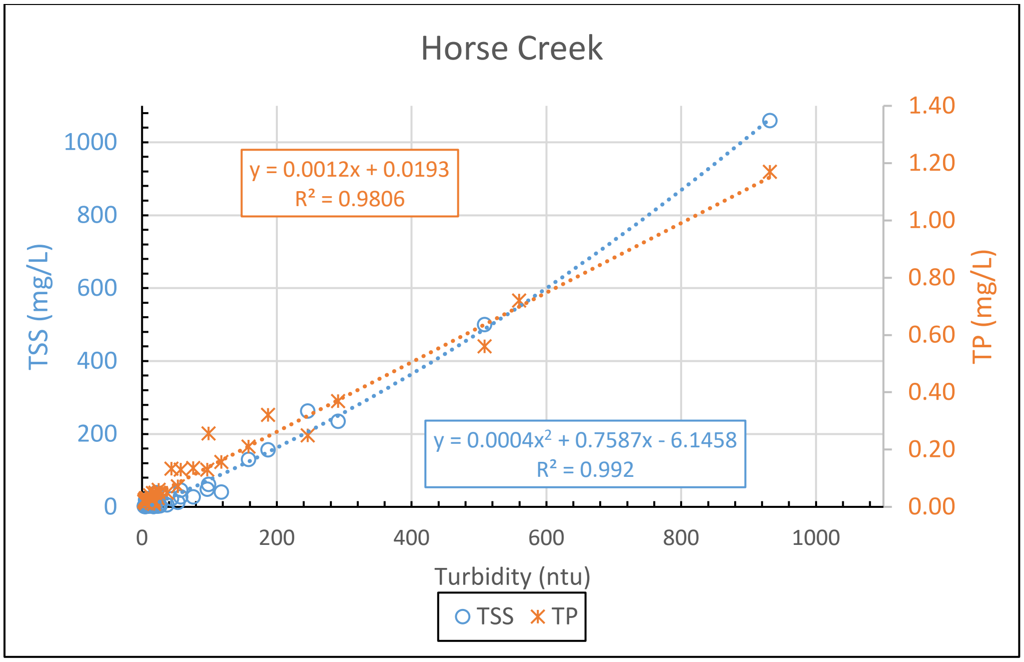

Figure 51.TSS and TP versus turbidity for Horse Creek.

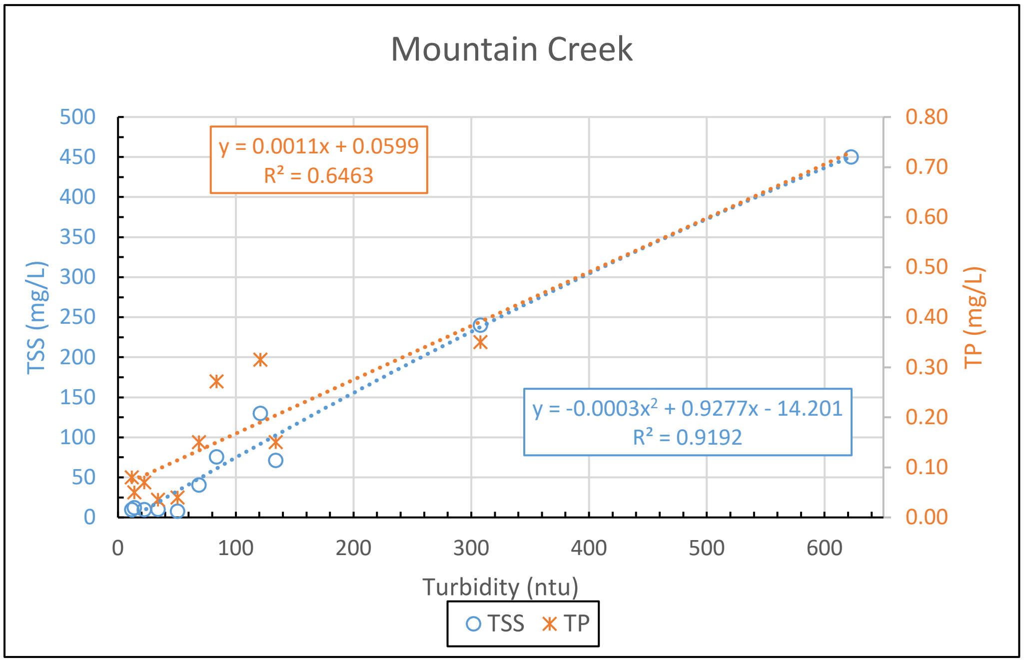

Figure 52. TSS and TP versus turbidity for Mountain Creek.

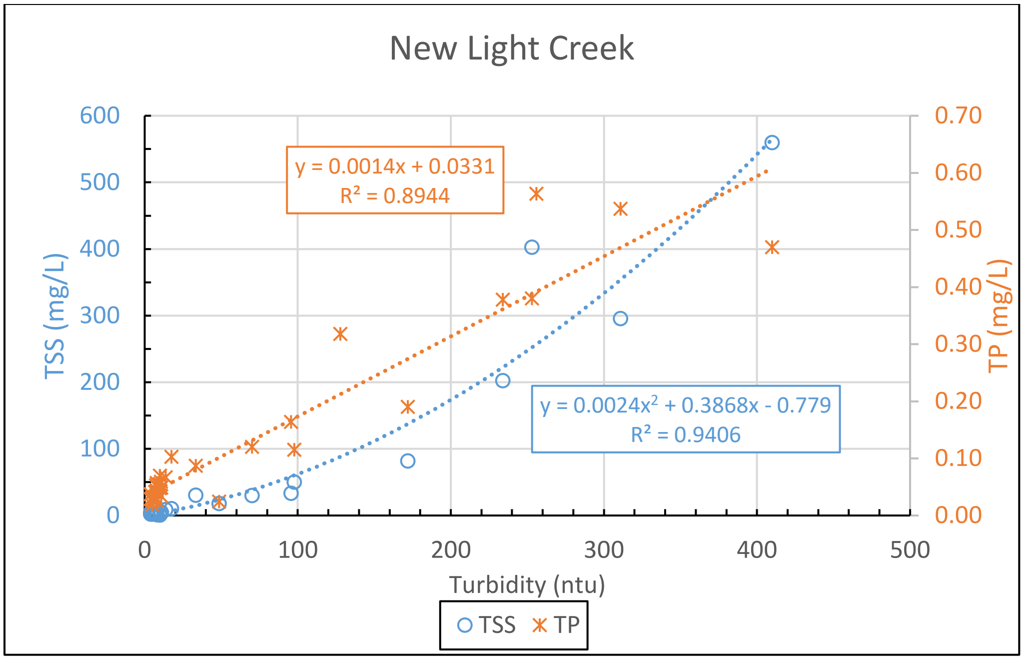

Figure 53. TSS and TP versus turbidity for New Light Creek.

Appendix G – Land Use Characterization

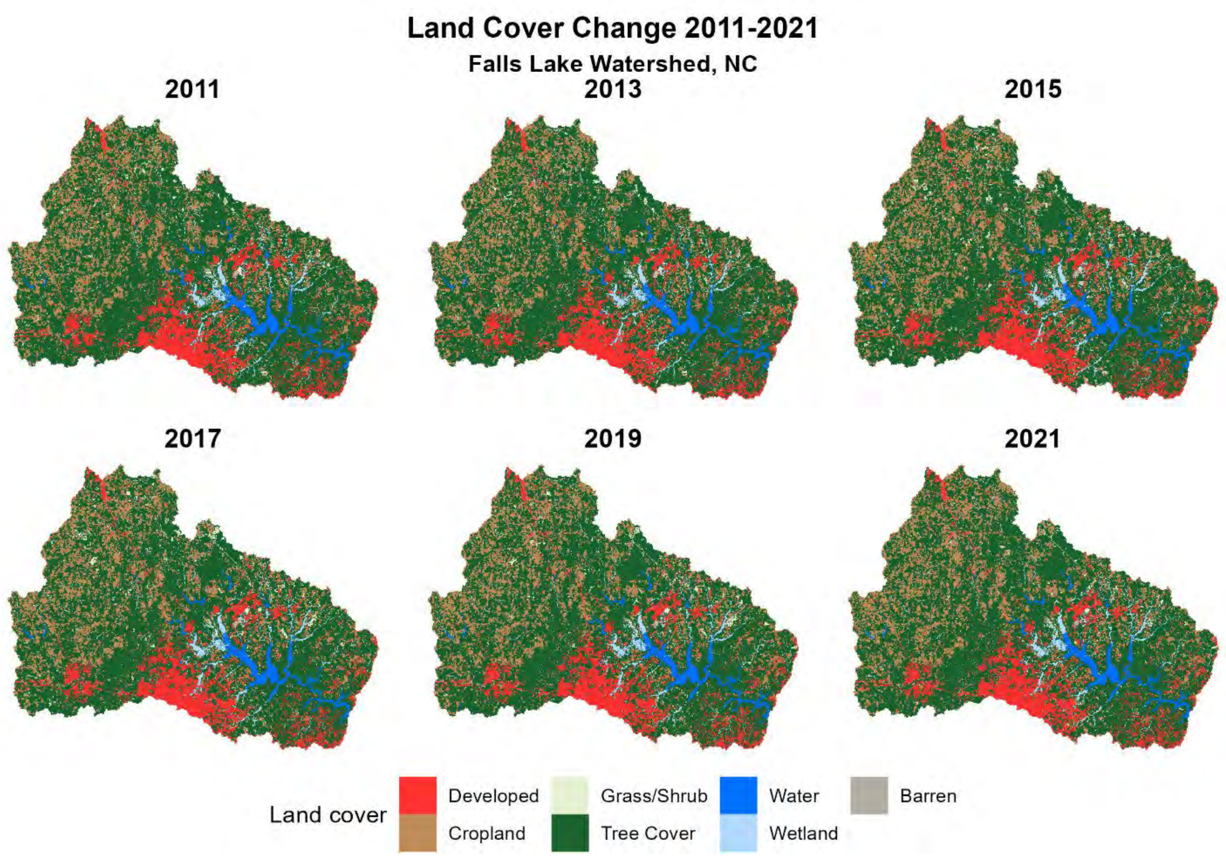

Figure 54. Map of land use change from 2011 to 2021 for the Falls Lake watershed.

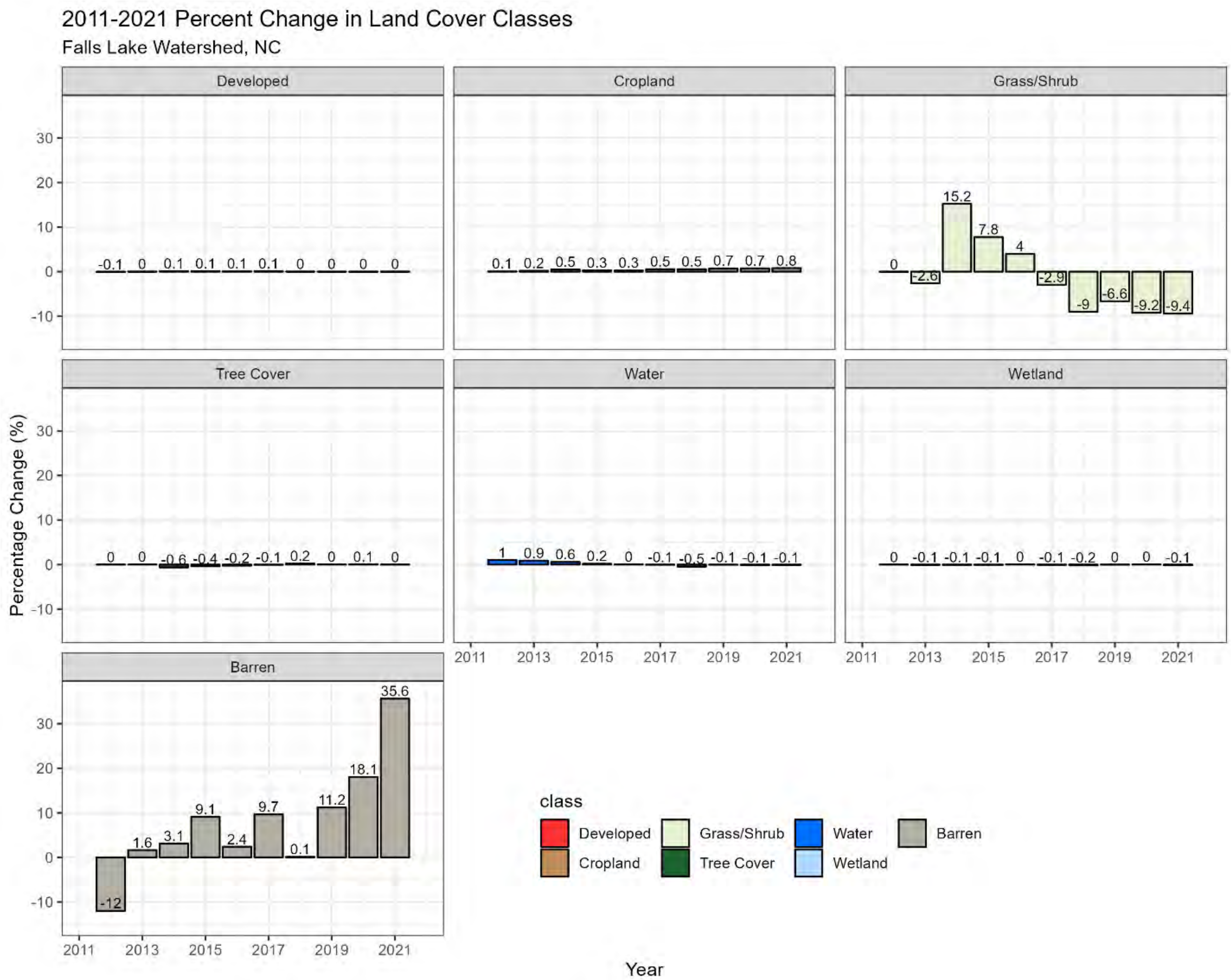

Figure 55. Percentage change in land use for the entire Falls Lake watershed.

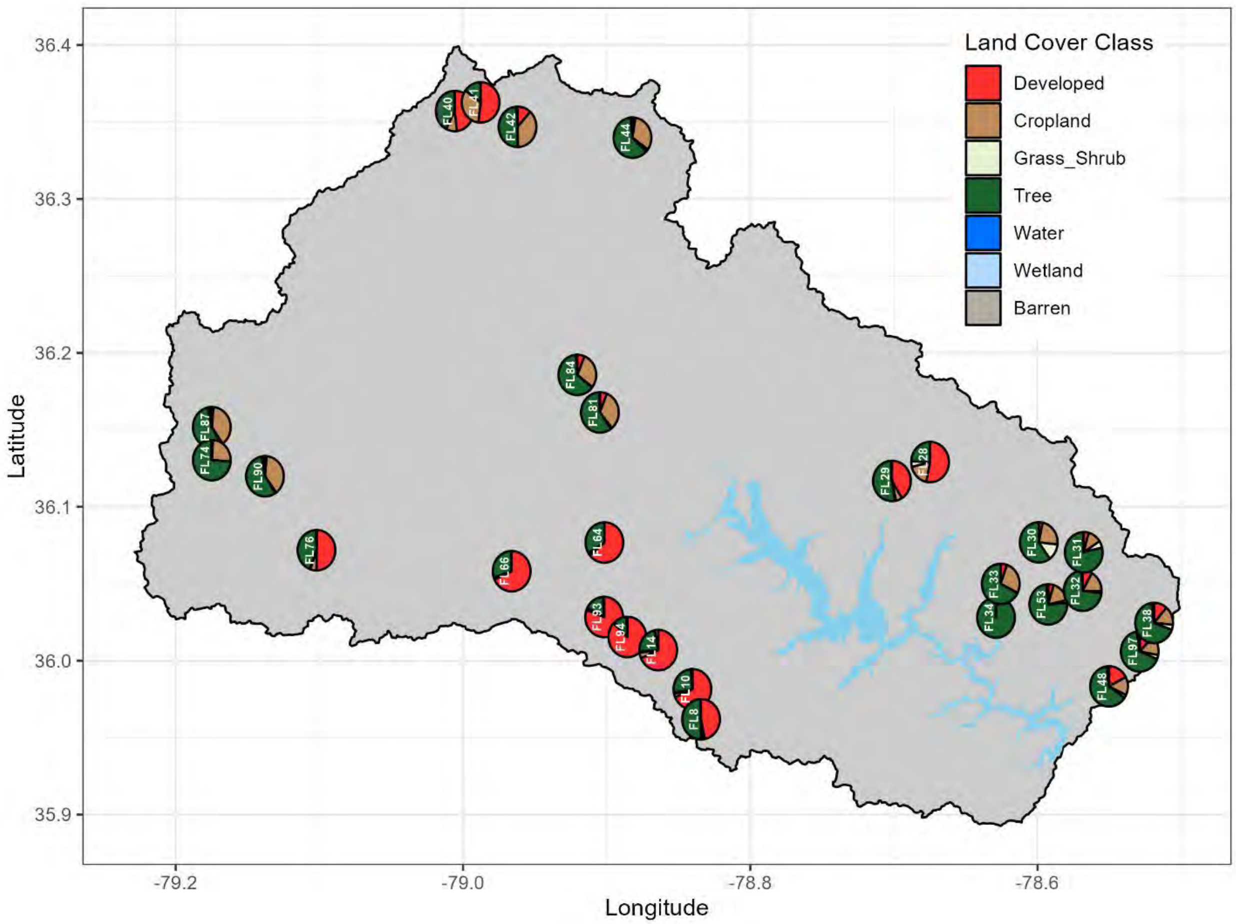

Figure 56. Pie charts of land use for each cross-section.

Figure 57 presents the percent change in developed land from 2011 to 2021 for the five watersheds. New Light watershed in Wake County had the largest change in developed land cover. Overall, there was minimal change in developed land cover in most subwatersheds, with the greatest annual change of around 2%

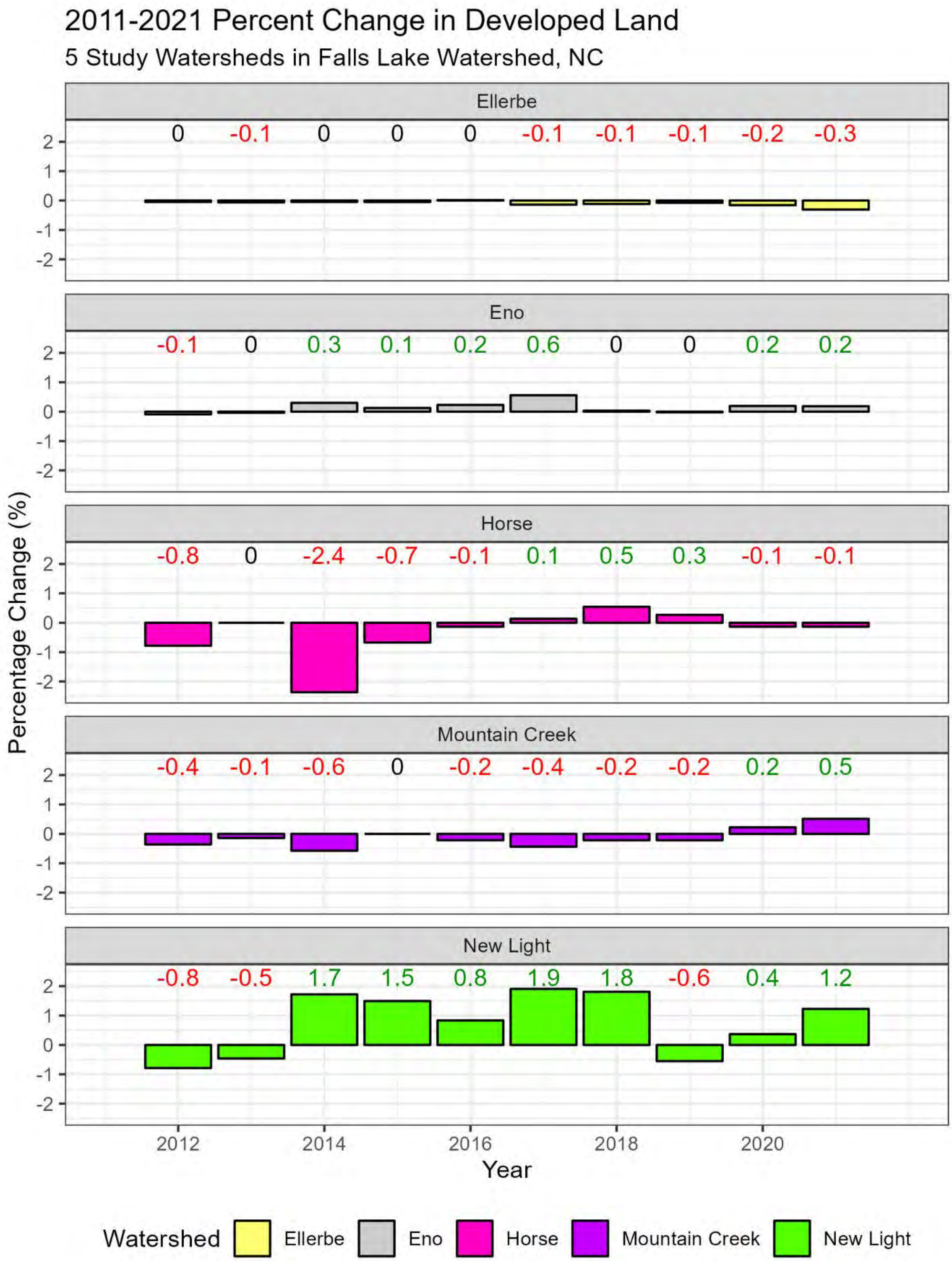

Figure 57. Percent change in developed land from 2011-2021 for the five study watersheds.

Appendix H - Soil Samples Results

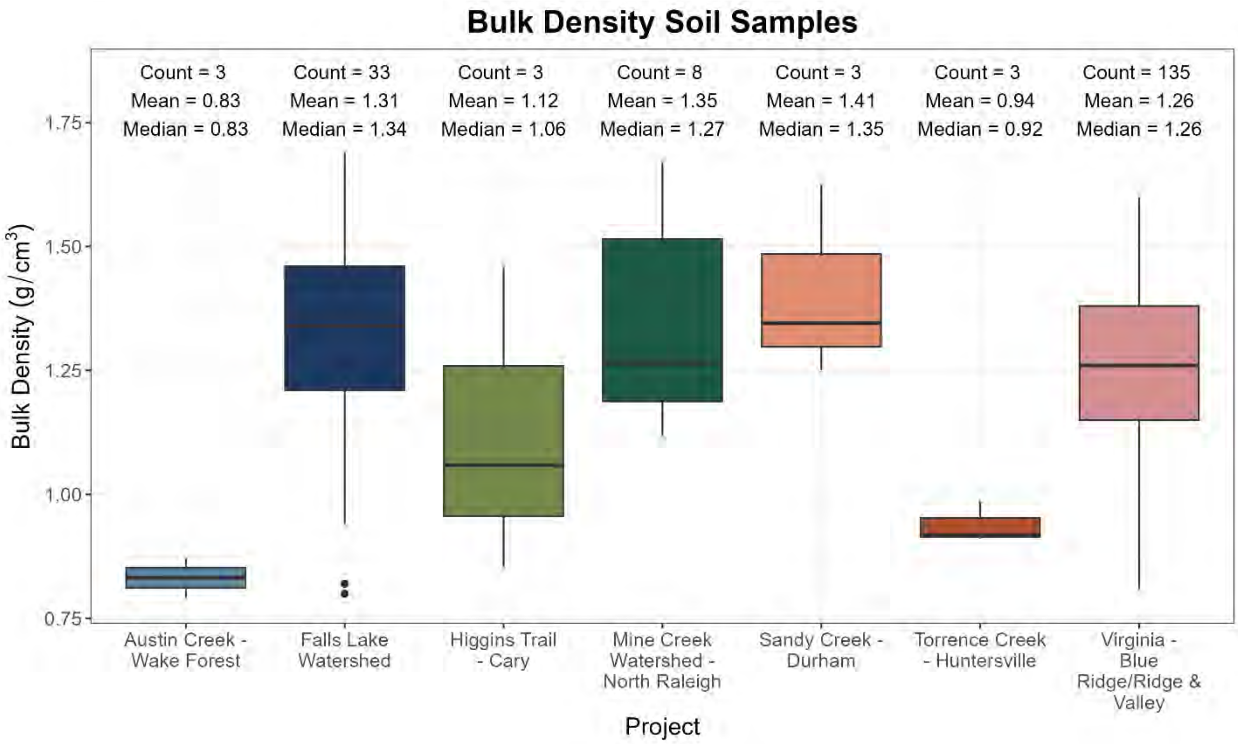

Figure 58. Boxplot of measured bulk density from this study and other studies in North Carolina.

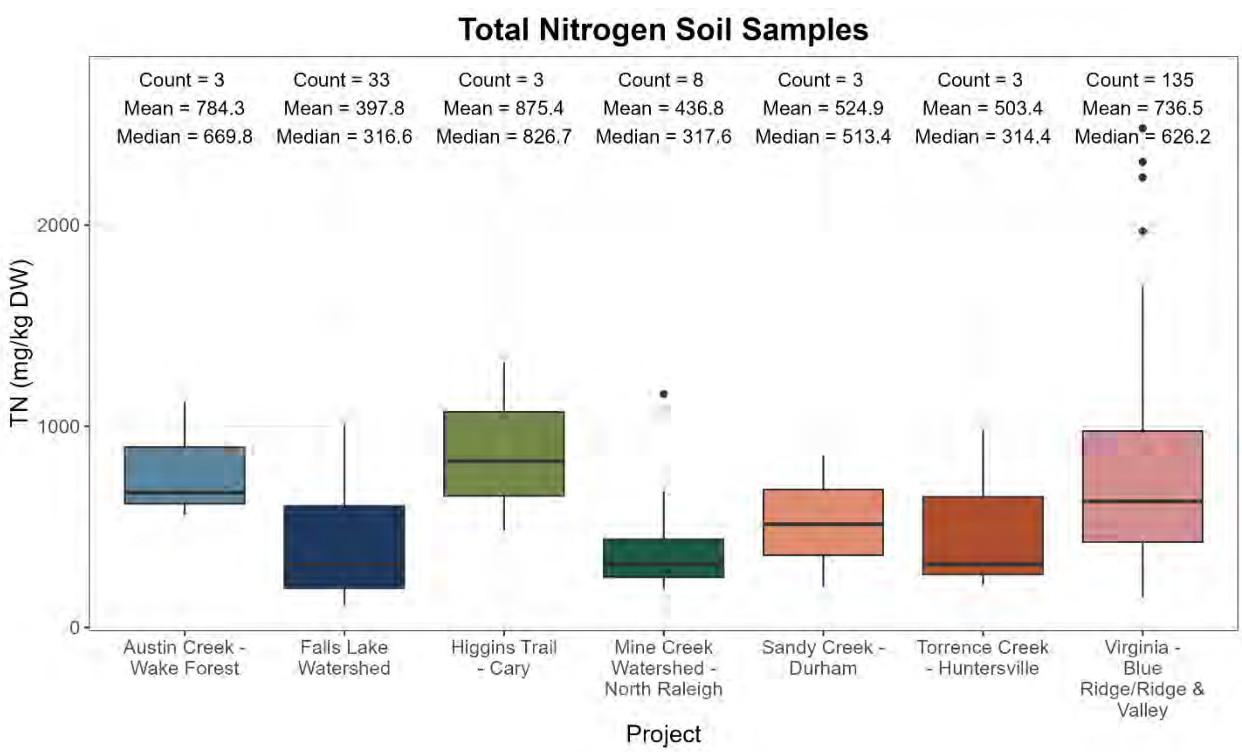

Figure 59. Boxplot of measured TN from this study and other studies in North Carolina.

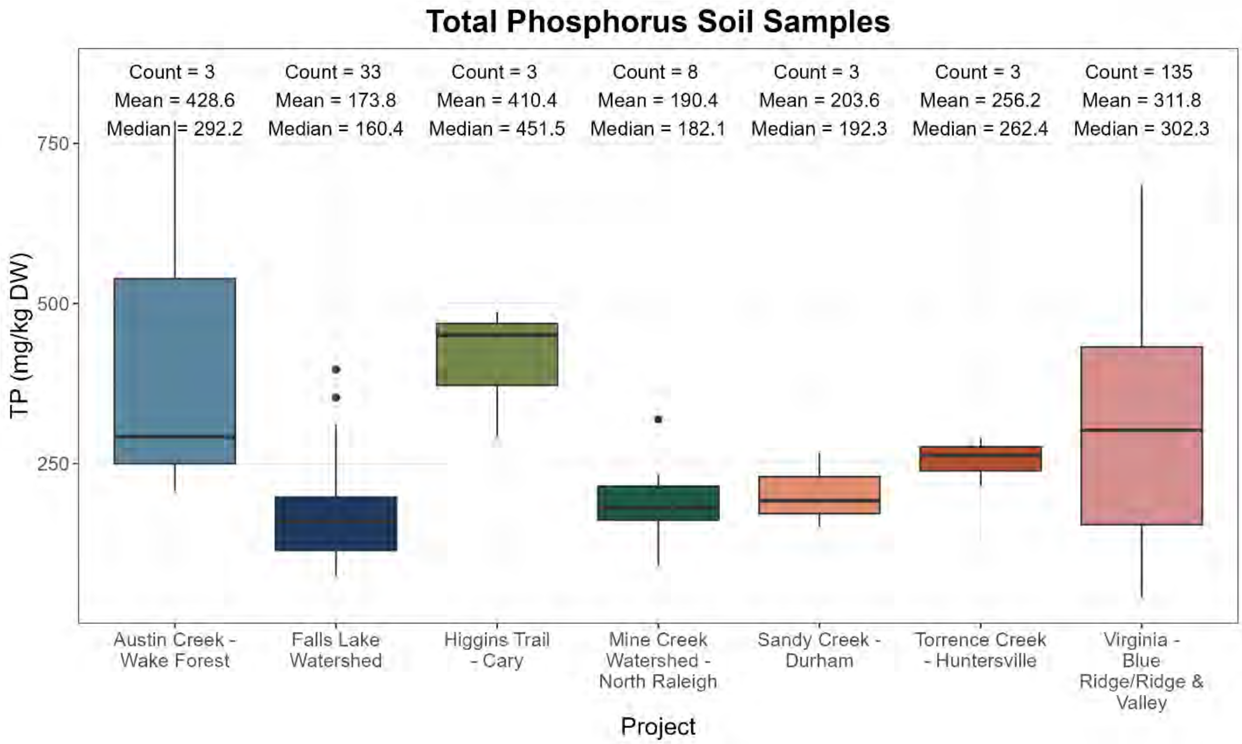

Figure 60. Boxplot of measured TP from this study and other studies in North Carolina.